國立臺灣大學機械工程學系

博士論文

Department of Mechanical Engineering
National Taiwan University

Ph.D. Dissertation

上肢阻力訓練裝置之設計及評估

Design and Evaluation of a Spring-loaded Upper Limb Exoskeleton for Resistance Training

吳宗明

Tzong-Ming Wu

指導教授：陳達仁 博士

Advisor: Dar-Zen Chen, Ph.D.

中華民國 101 年 7 月

July, 2012

誌謝

博士學位的歷程總算告一個段落，很高興最終還是完成了這一年輕時訂下的自我實踐目標，雖然距計畫於 1994 年在美國取得學位，已經過了 18 年！這個漫長的理想追求歷程中，得感謝許許多多的人！

首先，感謝指導教授陳達仁老師這段期間包括選課與修課的建議、論文題目的訂定、研究內容的討論及學術期刊投稿等各方面的指導；國際學術會議的參與以開拓研究視野，研究與實驗經費的充分支持，讓整個研究得以逐步展開；彈性且寬廣的研究空間給予，讓這段歷程得以在工作與學業的雙重壓力中求得平衡點，這些都是這段研究歷程得以完成的主要關鍵因素。黃漢邦老師、黃文敏老師、劉霆老師及蔡穎堅老師口試時對於論文內容的悉心指教與建議，讓論文內容更趨堅實與完善，未來做研究時思考更加縝密與嚴謹。

IAID 實驗室的夥伴在這段學習期間的相處愉快，博揚、宗勳、Molly、Tracy、Iris 一起修課及研究的討論；桓豪、佳穎、明輝協助實驗的進行，讓實驗得已完成測試；政彥在電腦網路資源的搜尋，在此一併致謝。另外，若齊總是能夠精準的依照我的想法繪製生動的人體上肢動作圖畫，讓論文內容的文字說明更能完整的表達，這該是一種美麗機緣，更勾起少年時成為科學家以外的漫畫家夢想。

謝謝姐姐與大嫂二次於台大醫院急診室扮演守護天使，大哥於手術房外的守候，在生命承受最大苦難時得以安然度過；侄兒、侄女與外甥女的成長歷程與親情豐富了人生的色彩；工研院 SMIF 計畫團隊的夥伴們，在那沒有高鐵的時代，隨著高速公路上南征北討的里程累積，所培養出的深厚革命情感及一起創造的成果與獲得的榮譽，不僅在工作場域創造亮點，那份拚勁與精神依舊延續。

還有 Sandra 在星巴克尚未進入台灣的年代，帶我走入的美式咖啡的世界，那份濃濃咖啡飄香至今，更伴我度過數不清的深夜；最後還是謝謝 Mermaid 一路曾經相陪，共同品嘗這些年攻讀博士學位的辛苦與快樂！

最後，僅將此一份喜悅，與一直相信我、支持我的親人及朋友分享！

中文摘要

在本論文中，我們提出一種創新的上肢阻力訓練裝置設計，此裝置具有三個肩關節與一肘關節自由度，可依據肌力訓練處方需求，連續性的調整阻力訓練所需的荷重大小，並透過在人體不同活動平面的動作，包括肩關節的外展/內收，肩關節的屈曲/伸展與肘關節的屈曲/伸展，訓練包括三角肌、胸大肌、上斜方肌、棘上肌、肱二頭肌與肱三頭肌等人體上肢主要肌肉群。研究的目的主要是希望能研究開發出一種設計簡潔、容易操作與安全的上肢阻力訓練裝置。適合於年長與慢性疾病醫療健康需求族群，可以在復健或健康照護人員低度參與的情況下，居家進行和緩到溫和程度速度的自主性上肢阻力運動，以維持與強化上肢肌肉群肌力。透過運動學與動力學分析建立自由重量訓練與本阻力訓練裝置數學模型，並以類比於相同人體動作的自由重量訓練的概念，求得阻力訓練裝置各個桿件與彈簧剛性值的設計方程式或準則。依據上述求得的設計方程式與準則，在給定的最大需求荷重規格下，進行了阻力訓練裝置的具體化設計與雛型實驗載台的製作。並透過男女受試者以三個等級的荷重搭配兩種運動速度實際操作啞鈴與阻力訓練裝置，執行肩關節的外展/內收，肩關節的屈曲/伸展與肘關節的屈曲/伸展的動作。運用動作分析方法與肌電值量測，進行肩關節與肘關節扭矩及選定之相關肌肉群的肌肉肌電圖之實驗量測與評估。經由實驗資料的收集與分析，提供測試數據驗證我們以零自由長度彈簧作為阻力訓練裝置阻力源，配合外甲式機構設計之阻力訓練裝置，可以有效減少關節與肌肉在高荷重與速度之啞鈴運動中所承受的慣性矩負面影響的想法，並可提供未來進行相類似裝置設計與驗證時的參考。

關鍵詞：阻力運動，上肢訓練裝置，自由重量訓練，動作分析，肌電圖

Abstract

Regular physical activity reduces the risk of adverse health outcomes for people of all ages. Research has demonstrated that most individuals can benefit from regular physical activity, regardless of whether they participate in vigorous exercise or moderate physical activity. Habitual physical activity and exercise also reduce the risk of chronic disease. For young, healthy people, many aspects of physical fitness can easily be realized by performing exercises that do not require special equipment. Various exercise devices have been developed to enable individuals who require assistance to achieve their physical fitness goals efficiently and consistently. However, concerns have been raised over the possible negative effects and safety of these exercise devices for elderly and clinical populations. Here, an unpowered spring-loaded upper limb exoskeleton designed for strengthening the muscles of the upper limbs at single and multiple joints in different planes is proposed. The upper limb exoskeleton consists of a shoulder joint with three degrees of freedom and an elbow joint with one degree of freedom, and it can perform internal-external, abduction-adduction, and flexion-extension movements of the shoulder, as well as flexion-extension motions of the elbow. Our aim was to provide an upper limb resistance training device that is compact, cost-effective, easy to operate, and safe for elderly and clinical populations who exercise at low and moderate speeds and that can be used for home-based rehabilitation in the absence of a fitness instructor or therapist. Kinematic and dynamic models have been formulated to develop design criteria to analyze free-weight and spring-loaded exoskeletons for upper limb resistance training. Embodiment design was performed and a prototype was constructed for evaluation. Motion analysis methods and electromyography measurements were chosen for evaluation of the joint torques and the neuromuscular response of major upper limb muscles when male and female subjects performed the designated resistance training. The collected data, along with kinematic and dynamic joint torque analysis, not only verifies our hypothesis that, with zero-free-length springs, this spring-loaded upper limb exoskeleton is capable of reducing unfavorable lengthening of the muscles during high-intensity free-weight exercises but also provides important general principles for designing appropriate spring-loaded exoskeletons for upper limb resistance training.

Keywords: resistance exercise, upper limb exoskeleton, free-weight exercise, motion analysis, electromyography

Table of contents

List of Tables

List of Figures

List of Symbols

F_h external load applied in the center of the palm

$\boldsymbol{g}$ vector of gravitational acceleration, pointing downwards

G_u the center of gravity of the upper arm

G_f the center of gravity of the forearm arm

G_F the center of gravity of the external load

$I_{u,Si}$ the $\boldsymbol{s_i}$ component for the mass moment of inertia about point G_u in $\mathbf{s_1}$, $\mathbf{s_2}$, and $\mathbf{s_3}$ coordinate system, where i=1, 2, 3

$I_{f,Si}$ the $\boldsymbol{s_i}$ component for the mass moment of inertia about point G_f in $\mathbf{s_1}$, $\mathbf{s_2}$, and $\mathbf{s_3}$ coordinate system, where i=1, 2, 3

$I_{Gj,Si}$ the $\boldsymbol{s_i}$ component for the mass moment of inertia about point the center of mass for link j (point G_j) in the $\mathbf{s_1}$, $\mathbf{s_2}$, and $\mathbf{s_3}$ coordinate system, where i=1, 2, 3 and where j=2, 3, 4

$I_{u,ei}$ the $\boldsymbol{e_i}$ component for the mass moment of inertia about point G_u in the $\mathbf{e_1}$, $\mathbf{e_2}$, and $\mathbf{e_3}$ coordinate system, where i=1, 2, 3

$I_{f,ei}$ the $\boldsymbol{e_i}$ component for the mass moment of inertia about point G_f in the $\mathbf{e_1}$, $\mathbf{e_2}$, and $\mathbf{e_3}$ coordinate system, where i=1, 2, 3

$I_{Gj,ei}$ the $\boldsymbol{e_i}$ component for the mass moment of inertia about point the center of mass for link j (point G_j) in the $\mathbf{e_1}$, $\mathbf{e_2}$, and $\mathbf{e_3}$ coordinate system, where i=1, 2, 3 and where j=2, 3, 4

$I_{u/S,Si}$ the mass moment of inertia for the upper arm with respect to the shoulder joint using the parallel axis theorem from Si to S

$I_{f/S,Si}$ the mass moment of inertia for the forearm with respect to the shoulder joint using the parallel axis theorem from Si to S

$I_{F/S,Si}$ the mass moment of inertia for the external load with respect to the shoulder

joint using the parallel axis theorem from Si to S

$I_{u/E,ei}$ the mass moment of inertia for the upper arm with respect to the elbow joint using the parallel axis theorem from e_i to point E

$I_{f/E,ei}$ the mass moment of inertia for the forearm with respect to the elbow joint using the parallel axis theorem from e_i to point E

$I_{F/E,ei}$ the mass moment of inertia for the external load with respect to the elbow joint using the parallel axis theorem from e_i to point E

K_i spring stiffness of spring *i*

$\boldsymbol{l}_{A_iB_i}$ vector of spring *i*

l_{A1C} adjustable length from point *S* to point *A1*

l_{SAi} adjustable length from point *S* to point *Ai*, *i*=2, 3

l_{PBi} link length from point *P* to point *B1* on link 1

l_{EBi} link length from point *Bi* on link 4 to elbow joint *E, i*=2, 3

l_{CP} link length from point *C* on link 2 to point *P*

l_i link length between the two joints of link *i*, where *i*=1, 2, 3, 4

$l_{i,Gi/S}$ the link length between point G_i and the shoulder joint of link *i*, where *i*=2

m_f mass of forearm

m_i mass of link *i*

m_u mass of upper arm

R_f the ratios of the weights of the forearm segment

R_u the ratios of the weights of the upper arm segment

$\boldsymbol{r_f}$ vector of forearm from elbow joint *E* to middle of hand *H*

$\boldsymbol{r_u}$ vector of upper arm from shoulder joint *S* to elbow joint *E*

$\tilde{\mathbf{r}}_f$ vector of mass center of forearm referenced in CS 4

$\boldsymbol{r_i}$ vector of mass center of link *i* referenced in CS *i*

$\tilde{\mathbf{r}}_{\boldsymbol{u}}$ vector of mass center of upper arm referenced in CS 3

${}^{i-1}T_i$ D-H transformation matrix between link *i* and *i-1*

T_u the upper arm kinetic energy

T_f the forearm kinetic energy

T_F the applied load kinetic energy

T_{Li} kinetic energy of link i, where i=1, 2, 3, 4

V_{total} total potential energy of the upper limb exoskeleton

V_g gravitational potential energy of free-weight exercise

$V_{L\,i}$ gravitational potential energy of link *i*

$V_{S\,i}$ elastic potential energy of spring *i*

V_u the upper arm potential energy

V_f the forearm potential energy

V_F the applied load potential energy

V_{Li} potential energy of link i, where i=1, 2, 3, 4

V_{Si} potential energy of spring K_i, where i=1, 2, 3

$\bar{M}_S$ simulated joint torques

M_i joint torque of axis-z_i for exercise with the exoskeleton

$M_{i,dc}$ joint torque of axis-z_i for exercise with the exoskeleton to emulate dumbbell curl motion

$M_{i,fr}$ joint torque of axis-z_i for exercise with the exoskeleton to emulate frontal raise motion

$M_{i,lr}$ joint torque of axis-z_i for exercise with the exoskeleton to emulate lateral raise motion

$M_{i,tri}$ joint torque of axis-z_i for exercise with the exoskeleton to emulate overhead

triceps extension

$\widetilde{M}_{i,dc}$ dynamic joint torque of axis-z_i for exercise with the exoskeleton to emulate dumbbell curl motion

$\widetilde{M}_{i,fr}$ dynamic joint torque of axis-z_i for exercise with the exoskeleton to emulate frontal raise motion

$\widetilde{M}_{i,lr}$ dynamic joint torque of axis-z_i for exercise with the exoskeleton to emulate lateral raise motion

M_u moment at the upper arm (with the exoskeleton)

M_f moment at the forearm (with the exoskeleton)

θ_i angle rotates about axis-z_i

θ_u the generalized coordinates for the two-segment system, upper arm

θ_f the generalized coordinates for the two-segment system, forearm

$\dot{\theta}_u$ the first derivatives of θ_u with respect to time

$\dot{\theta}_f$ the first derivatives of θ_f with respect to time

$\ddot{\theta}_u$ the second derivatives of θ_u with respect to time

$\ddot{\theta}_f$ the second derivatives of θ_f with respect to time

$\bar{\Gamma}$ theoretical joint torques

τ_i joint torque of axis-z_i of objective free-weight exercise

$\tau_{i,dc}$ joint torque of axis-z_i of dumbbell curl motion

$\tau_{i,fr}$ joint torque of axis-z_i of frontal raise motion

$\tau_{i,lr}$ joint torque of axis-z_i of lateral raise motion

$\tau_{i,tri}$ joint torque of axis-z_i of overhead triceps extension

$\tilde{\tau}_{i,dc}$ dynamic joint torque of axis-z_i of dumbbell curl motion

$\tilde{\tau}_{i,fr}$ dynamic joint torque of axis-z_i of frontal raise motion

$\tilde{\tau}_{i,lr}$ dynamic joint torque of axis-z_i of lateral raise motion

τ_u the moment at the upper arm

τ_f the moment at the forearm

τ_f the moment at the forearm

ζ the ratio of the longitudinal position of the center of the mass for the upper arm, defined as percentage of the upper arm segment length

ξ the ratio of the longitudinal position of the center of the mass for the forearm, defined as percentage of the forearm segment length

Chapter 1
Introduction

1.1 Background

Physical activity is usually defined as any bodily movement produced by skeletal muscles that requires energy expenditure above resting levels. This broad definition includes physical activity in all contexts and can be categorized in various ways. A commonly used approach is to segment physical activity on the basis of the identifiable portions of daily life during which the activity occurs, i.e., sleeping, leisure-time physical activity (LTPA), and occupational physical activity (OPA). LTPA has been defined as all forms of physical activity that, through casual participation, aim at expressing or improving physical fitness and mental well-being, forming social relationships or competing at all levels. OPA is associated with the performance of a job, usually within the time of an eight-hour workday. Exercise, or training, is a subcategory of LTPA that is planned, structured, repetitive, and purposeful, in the sense that the improvement or maintenance of one or more components of physical fitness is the objective. Physical fitness is a set of attributes (i.e., cardiorespiratory endurance, skeletal muscle endurance, flexibility, agility, balance, reaction time, and body composition) that people have or achieve

that relates to the ability to perform physical activity. Proper and regular physical activity is fundamental to the maintenance of health. International public health and health promotion organizations have identified health risks across the lifespan associated with physical inactivity. Physical inactivity is a modifiable risk factor for chronic diseases including cardiovascular disease, diabetes mellitus, certain types of cancer, obesity, hypertension, osteoporosis, osteoarthritis, and depression. Despite this evidence of the benefits of physical activity, the uptake and involvement in regular activity by older people is relatively low and declines with age.

An appropriate amount of regular physical activity provides people of all ages with physical and mental health benefits. Different types and amounts of physical activity are required for different outcomes. For example, experts recommend that adults get 30-60 minutes of moderate-intensity physical activity on a regular basis. Moderate-intensity physical activity refers to a level of effort in which a person experiences some increase in breathing or heart rate. At least 30 minutes of regular, moderate-intensity physical activity on most days reduces the risk of cardiovascular disease, diabetes, colon cancer and breast cancer. Muscle strengthening and balance training can reduce falls and increase functional status among older adults. More activity may be required for weight control. Therefore, the promotion of physical

activity is an essential public health and health promotion strategy to improve the health of individuals and populations [1-4].

Exercise for physical fitness is generally grouped into three types depending on the overall effect on the human body: flexibility (stretching, range of motion) exercise, aerobic (cardiovascular) exercise, and resistance (strengthening) exercise. Flexibility is defined as a joint's ability to move freely through a normal range of motion. Flexibility exercises improve the range of motion of muscles and joints. Stretching and bending are common flexibility training exercises, as is yoga. Aerobic exercise involves large muscle groups in dynamic activities that result in substantial increases in heart rate and energy expenditure. Regular participation results in improvements in the function of the cardiovascular system and the skeletal muscles, which leads to an increase in endurance. Examples include walking, running, jogging, swimming, and aerobic dancing, where the focus is on increasing cardiovascular endurance. Resistance exercise such as weight lifting, is designed to specifically increase muscular strength, power, and endurance by varying the resistance, the number of times that the resistance is moved in a single set of exercises, the number of sets performed, and the rest interval between sets. Strength training plays a more important role in improving muscle quality and body mass density (BMD), whereas aerobic exercise can improve cardiovascular

function more effectively. Flexibility exercises are performed to enhance the movements of muscles and joints. [5-8].

In the mid-1980s, the medical community began to recognize the potential health value of resistance training on functional capacity and other health-related factors such as bone mineral density, basal metabolism and weight control. At present, resistance training has become the preferred mode of exercise because of its profound health benefits. Major national health organizations, including the American College of Sports Medicine (ACSM), the National Strength and Conditioning Association (NSCA), the American Heart Association (AHA), the American Association of Cardiovascular and Pulmonary Rehabilitation (AACVPR), and the American Diabetes Association (ADA), have published science-based guidelines for resistance exercise appropriate for healthy nonathletic populations, including patients with chronic disease and other clinical populations ranging in age from prepubescent to elderly [9-13]. Patients can reduce risk factors associated with chronic disease by participating in individualized, progressive resistance training programs (Table 1.1) [14].

Free weights and weight machines are the most familiar forms of resistance that can be used for muscle loading. The user's needs or patient's disability level will generally influence the type of resistance chosen. Generally speaking, free

Table 1.1 Comparison of the effects of aerobic training and resistance on health and fitness variables [14]

Variable	Aerobatic Exercise	Resistance exercise
Bone mineral density	↑↑	↑↑
Body composition		
% fat	↓↓	↓
LBM	→	↑↑
Strength	→	↑↑↑
Glucose metabolism		
Insulin response to glucose challenge	↓↓	↓↓
Basal insulin levels	↓	↓
Insulin sensitivity	↑↑	↑↑
Serum lipid		
HDL	↑↑	↑→
LDL	↓↓	↓→
Resting heart rate	↓↓	→
Stroke volume	↑↑	→
Blood pressure at rest		
Systolic	↓↓	→
Diastolic	↓↓	↓→
VO_2max	↑↑↑	↑
Endurance time	↑↑↑	↑↑
Physical function	↑↑	↑↑↑
Basal metabolism	↑	↑↑

HDL: high-density lipoprotein; LBM: lean body mass; LDL: low-density lipoprotein

VO_2max: maximal oxygen uptake; % fat: percentage body fat

↑: increase; ↑↑: marked increase; ↑↑↑: very marked increase

↓: decrease; ↓↓: marked decrease; →: no change

weights may be more difficult to master and are more likely to cause injury. However, they are more versatile and functional and can offer a wider variety of possible motions than weight machines. Weight machines only target specific muscle groups; several machines are required for a full-body workout. Current

evidence indicates that for most activities, training with complex, multi-joint exercises using free weight can produce superior results to training with machines. Nevertheless, free weights and weight machines were both designed to be used by athletes and body builders, who are healthy enough to obtain effects on athletic performance or body fitness. Although an entire rack of dumbbells takes up less space than weight machines, dumbbells and weight machines are both bulky, cumbersome, and difficult to move. They are usually used in gym- or studio-based exercise. Concerns have been raised over the negative effects and safety of resistance exercise as a physical therapy intervention, as well as over the usage and appropriateness of the relevant equipment for the elderly and populations with chronic diseases [15].

1.2 Related works

According to the World Health Organization, by 2050, the number of elderly persons over 65 years of age will increase by 73 percent in developed countries and 20.7 percent worldwide. This age group is particularly prone to stroke. Stroke is the leading cause of physical disability and death in most countries around the world; an estimated 64.5 million stroke survivors live with some level of disability that requires long-term rehabilitation and assistance in the activities of daily living (ADLs) [16-18]. Recent studies estimate that 795,000 people in the U. S.

experience a new or recurrent stroke each year; approximately 610,000 are first attacks, and 185,000 are recurrent. On average, every 40 seconds, someone in the United States has a stroke. From 1998 to 2008, the stroke death rate decreased by 34.8%, and the actual number of stroke deaths declined by 19.4%. The direct and indirect cost of strokes in 2008 was $34.3 billion US dollars [19]. High stroke incidence, in combination with an increasingly aged population, presages future increases in incidence that will greatly strain national healthcare services and related expenditures. Therapeutic rehabilitation and health care devices associated with stroke-related disability are thus in great demand.

Acute hemiparesis that affects the upper limbs is one of the major symptoms of stroke survivors that makes ADLs difficult to perform. ADLs are a defined set of activities necessary for normal self-care. ADLs involving bilateral arm or hand use, such as fastening buttons, self-feeding, dressing, grooming, bathing and toileting, are especially difficult for individuals with hemiparesis to complete. Conventional multi-disciplinary stroke rehabilitation, which employs one-on-one manual interactions with therapists, is labor-intensive and usually costly, and these costs often lead to insufficient training sessions, lack of repeatability, and a lack of objective measures of patient performance and progress. Timely and adequate rehabilitation is crucial to maximizing recovery, especially in the first six months

after a stroke. This situation can worsen after patients are discharged from the hospital where they received initial rehabilitation. Robotic devices are a potential route to increasing treatment access by aiding therapists in providing post-stroke rehabilitation. By employing robotic-assisted rehabilitation devices, training sessions, the number of repetitions, and performance and progress can be increased and measured.

Many research groups have developed innovative robotic devices for upper limb rehabilitation. Efforts toward developing robot-assisted treatments are motivated by the need to improve clinical outcomes and the public health burden associated with stroke-related disability as well as a desire to improve effectiveness, accessibility, and cost savings in health care. Early research into robotic therapy for upper limbs was based on end-effector robotics. End-effector robots hold the patient's hand or forearm at a single point and generate forces only at the interface. The joints of end-effector robots do not match with those of the human limb. This type of robot is simple, easy to fabricate or commercially available, and easily adjusted to fit different human limb lengths. However, it is difficult to generate isolated movements at a single joint; movement of the end-effector can cause unwanted combinations of movements at the wrist, elbow, and shoulder joint. In addition, the range of motion (ROM) that this type of robot can generate in the

upper limb tends to be limited. Examples of end-effector robots include the MIT-Manus [20], the mirror image movement enhancer [21], and the Gentle/s [22].

The work of Krebs *et al*. at MIT on the MIT-Manus is shown in Fig. 1-1 (a) and has been commercialized as InMotion2 (Interactive Motion Technologies, MA, US). The device allows patients to execute reaching movements in the horizontal plane. It is a planar SCARA (Selective Compliance Assembly Robot Arm) module two-degrees-of-freedom (DOF) robot that enables unrestricted movement of the shoulder and elbow joints. The assisted rehabilitation and measure (ARM) guide [23] (Fig. 1-1(b)) is a trombone-like device that has four controlled DOF. A DC servo motor can assist or resist the movement of a subject's arm in the reaching direction along a linear track. The track can be oriented at different yaw and pitch angles to allow reaching to different workspace regions. The device is statically counterbalanced so that it does not gravitationally load the arm. Optical encoders record the position in the reach, elevation, and yaw axes. The mirror image movement enhancer (MIME) system (Fig. 1-1(c)) consists of a six-DOF industrial robot manipulator (PUMA 560 robot, Staubli Unimation Inc, CA, US). The robot enables bilateral practice of a three-DOF shoulder-elbow movement where the nonparetic arm guides the paretic arm. The GENTLE/s system uses a three-DOF

(a)

(b)

(c)

(d)

Fig. 1.1 (a) InMotion2, the commercially available version of the MIT-Manus robot system [20]; (b) The ARM guide [23]; (c) The MIMI [21]; (d) The Gentle/s [22]

force control haptic robot (HapticMaster, Moog Inc., Netherland) in a virtual reality (VR) environment to motivate patients to engage in the therapy (Fig. 1.1 (d)). The HapticMaster measures the force exerted by the user with a sensitive force sensor. Software manages data collection, controls the robot, and simulates VR. The patient's hand is placed in an elbow orthosis with a wire suspending it from an overhead frame to eliminate the effects of gravity and address the problem of shoulder subluxation. Patients using this system can exercise "reach-and-grasp"-type movements through interaction with the VR display. There

are three modes: patient passive mode, where the haptic device teaches the correct movements; active-assisted mode, where the patient initiates movement and the robot assists in the same direction; and active mode, where the patient moves the device and, if there are deviations from the predetermined path, the robot provides only correction of movement by creating resistance to help the patient return to the pathway [24-27].

Recently, robotic therapy research has shifted toward exoskeleton robots. Research on powered human exoskeleton devices has primarily been focused on developing technologies to augment the abilities of able-bodied humans, often for military purposes, and on developing assistive technologies for physically challenged persons. The most visible exoskeleton technology has been the Berkeley Lower Extremity Exoskeleton (BLEEX) [28]. One of the distinguishing features of the Exoskeletons for Human Performance Augmentation (EHPA) program, sponsored by the U.S. Defense Advanced Research Projects Agency (DARPA), is that it is energetically autonomous because it carries its own power source. Hybrid Assistive Leg (HAL), developed at the University of Tsukuba, Japan, by Yoshikuyi Sankai and Kawamoto H, represents an exoskeleton concept that is designed for both performance-augmenting and rehabilitative purposes [29]. In contrast with the load-carrying BLEEX exoskeletons, the HAL system does not transfer a load to the

ground surface but simply augments joint torques at the hip, knee, and ankle.

Exoskeletons have configurations that resemble the human upper and lower limb, with robot joint axes that are in alignment with the upper and lower limb joint axes of the patients or operators. This feature makes it more difficult for the exoskeleton to adapt to different arm lengths but may allow the exoskeleton to fully comply with the upper and lower limb posture and torques to be applied to each joint separately to train specific muscles. A larger ROM becomes possible, which enables a wider variety of movements to be used in rehabilitation training compared with end-effector robots. The advantages of exoskeleton robots compared with end-effector robots are that the arm posture is statically fully determined and overstretching can be prevented by adding mechanical stops [24-27]. Examples of exoskeleton robots for upper limb rehabilitation include T-WREX, Pneu-WREX, ARMin, RUPERT, CADEN-7, and BONES [30-35].

The Therapy-Wilmington Robotic Exoskeleton (T-WREX) is an antigravity arm orthosis that is designed to enable individuals with arm weakness to achieve intense movement training without a supervising therapist. It is a passive, five-DOF, body-powered device that contains no robotic actuators. It provides a large 3-D workspace that enables naturalistic movement across approximately 66% of the normal workspace of the arm in the vertical plane and 72% in the horizontal plane.

In addition, because it counterbalances the weight of the arm, it potentially allows even a severely weakened stroke patient to practice functional arm movements at home, without the safety concerns raised by an active robotic device. A modified T-WREX has been commercialized by Hocoma AG, Switzerland as the Armeo Spring [38] (Fig. 1-2(a)). T-WREX can only apply a fixed pattern of assistive forces to the arm. In addition, its gravity balance function does not restore a full range of motion. Therefore, the same research team is developing a robotic version of WREX named Pneu-WREX that can apply a wide range of forces to the arm during naturalistic movements. Pneu-WREX uses mechanically grounded pneumatic actuators, non-linear force control, and passive counter-balancing to generate a wide range of forces during naturalistic, three-DOF, upper extremity movements.

The ARMin III robot, or its commercialized version Armeo Power (Hocoma AG, Switzerland) (Fig. 1-2(b)), provides three actuated degrees of freedom for the shoulder including flx-ext, add-add, and internal-external rotations (int-ext) as well as one degree of freedom for the elbow joint (flx-ext). An additional module provides actuated forearm pro/supination and wrist flexion/extension that allow it to move the human arm in all possible directions. To accommodate patients of different sizes, the shoulder height can be adjusted through an electric lifting column, and the lengths of the upper arm and forearm are adjustable. Laser pointers

indicating the center of the glenohumeral (GH) joint help the therapist to position the patient in the ARMin III device. The ARMin III robot can be configured to accommodate either the left or the right arm very quickly. A spring in the uppermost horizontal robotic link compensates for part of the weight of the exoskeleton. This design not only lessens the load of the actuators but also balances the robot arm when the power is off. The robotic shoulder actuation compensates for scapula elevation movement, which results in comfortable, ergonomic shoulder motion.

A wearable robotic-assisted upper extremity repetitive therapy (RUPERT) targeted for clinical and home-based rehabilitation has been developed to provide a low-cost, safe, and easy-to-use robotic device to assist patients and therapists in achieving more systematic therapy (Fig. 1-2(c)). The RUPERT has four actuated DOF driven by compliant, safe pneumatic muscle actuators (PMA) for shoulder elevation (flexion), elbow extension, forearm pronation and wrist/hand extension. The current design (RUPERT IV) has added shoulder external rotation to expand the space available for performing assisted tasks. Assistance and measurement of the following joint motions is provided in RUPERT IV: hand/wrist extension, forearm supination, elbow extension, humeral external rotation and shoulder elevation. RUPERT IV is programmed to actuate the device to extend the arm and

move it in the 3-D space. Notably, gravity is not compensated and daily tasks are practiced in a natural setting. Because the device is wearable, lightweight, and portable, it can be worn standing or sitting to perform therapeutic tasks that better mimic ADLs.

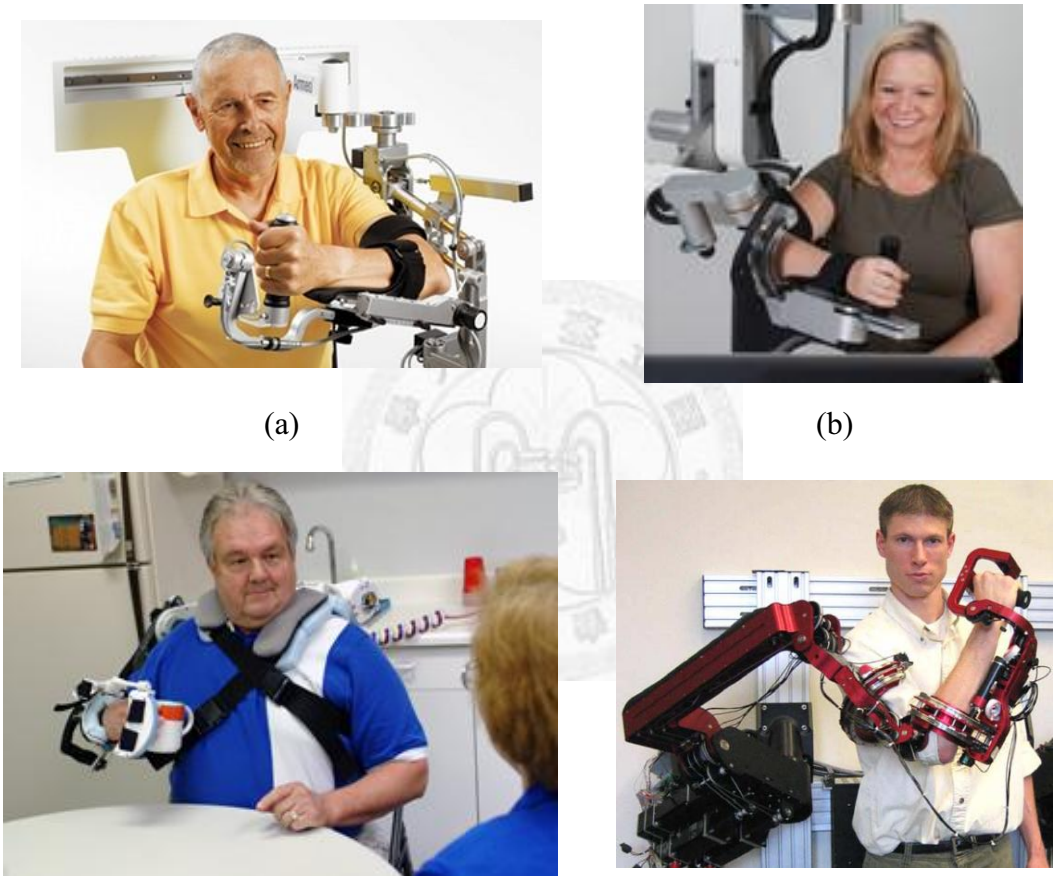

(a) (b)

(c) (d)

Fig. 1.2 (a) The Armeo Spring, which is the commercial version of the T-WREX robot system [38]; (b) The Armeo Power, which is the commercial version of the ARMin robot system [32]; (c) The RUPERT [33]; (d) The CADEN-7 [34]

A seven-DOF cable-actuated dexterous exoskeleton for neurorehabilitation, (CADEN)-7, has a design that is based on a database that defines the kinematics

and dynamics of the upper limb during daily living activities, as well as joint physiological and upper limb anatomical considerations, workspace analyses, and joint ROM (Fig. 1-2(d)). The proximal placement of the motors and the distal placement of pulley reductions are incorporated into the design of a cable-driven wearable robotic arm. This design has low inertia, stiff links, and back-drivable transmissions with zero backlash. Articulation of the exoskeleton is achieved at seven single-axis revolute joints: one for each shoulder abd-add, shoulder flx-ext, shoulder int-ext rotation, elbow flx-ext, forearm pronation-supination (pron-sup), wrist flx-ext, and wrist radial-ulnar (rad-uln) deviation. Potential applications of the exoskeleton as a wearable robot include use as a therapeutic and diagnostic device for physiotherapy, an assistive device for human power amplification, a haptic device in virtual reality simulation, and a master device for teleoperation.

The biomimetic orthosis for neurorehabilitation of the elbow and shoulder (BONES) uses a simple parallel mechanism with mechanically grounded actuators to achieve three-DOF shoulder movement, including shoulder int-ext rotation, which is perceived as very important for stroke rehabilitation. The robot incorporates a serially placed actuator for elbow flx-ext, but uses a pneumatic actuator for this DOF to achieve high force output with little weight. BONES is aimed to assist, resist, and perturb naturalistic arm movements in the clinic for the

purpose of retraining movement ability after stroke.

The devices described in Table 1.2 are reviewed because they attracted our attention the most, but the table does not include all of the upper limb rehabilitation robots in the literature. Nine devices were selected based on their clinical testing, their focus on the proximal upper limb, or their status as the most representative designs of their type.

Over the past two decades, several arm rehabilitation robots have been developed to assist neurological patients during therapy. Early devices were limited in DOF and ROM, whereas newer robots such as ARMin III, RUPRET IV, and CADEN-7 can support the entire arm but do not include additional DOF for finger movements. A high DOF allows a wide variety of movements, with many anatomical joint axes involved. However, this can make the device complex, inconvenient and expensive. The number of DOF that is optimal for upper limb rehabilitation remains unclear. Actuation has become more diverse, and most existing upper limb rehabilitation robots are actuated by electric motors. Recently, there has been increased interest in the use of pneumatic muscle actuators [33, 36], pneumatic actuators [35], hydraulic disk brakes [37], and linear springs [38].

Table 1.2 Rehabilitation robots/exoskeletons in use for clinical research or therapy and their status as the most representative design of their type

Device	Institution	DOF	Joints	Clinical/Personal intended Use	Movement characteristics	Actuation
MIT-Manus	MIT/ Interactive Motion Technologies	2	S/E	Clinical	Passive Active Resistive Unilateral Planar movement	Electric motors
ARM Guide	U of California at Irvine	4	S/E	Clinical	Passive Active Resistive Unilateral	Electric motors
MIMI	Rehab Research & Development Center, Palo Alto, CA	6	S/E	Clinical	Passive Active Resistive Unilateral/bilateral	Electric motors
Gentle/s	U of Reading	3	S/E	Clinical	Passive Active Resistive Trajectory fork Unilateral	Electric motors
T-WREX	UCI/RCI Armeo AG	5	S/E	Clinical	Passive	Elastic bands
ARMin III	ETH Zurich	6	S/E/W	Clinical	Passive Active Assistive	Electric motors
RUPERT IV	Arizona State	5	S/E/W	Clinical/Personal	Passive Active Assistive	Pneumatic muscle actuator
CADEN-7	U of Washington	7	S/E/W	Clinical	Passive Active Assistive VR Teleoperation	Electric motors
BONES	U of California at Irvine	4	S/E	Clinical	Assistive Resistive	Pneumatic actuators

S: Shoulder; E: Elbow; W: Wrist

The studies cited above indicate that the medical advances resulting from research on stroke and the resources invested in the rehabilitation of stroke victims have been focused on the acute and subacute recovery phases and that less attention has been directed at the more chronic recovery phases. This situation has resulted in substantial health disparities in the later phases of stroke care. These circumstances clearly reflect the state of the art. There is a need for robotic devices that can be used to support rehabilitation in the later or more chronic phases of stroke care, in chronic diseases, and in other conditions to which the technology can be extended, such as multiple sclerosis [38], tremor assessment and suppression [39], and neurological disease [40]. Broadening the medical uses of exoskeleton robots can stimulate development of other branches of the technology to applications such as exercise training, as well as geriatric therapy and care.

Most rehabilitation and health care robotic devices are primarily designed to actively assist patients with motion. In contrast, most exercise training devices are body-power oriented. The users are expected to perform the motion by themselves to gain strength and power from the exercise. For instance, resistance exercises for fitness are often performed using fitness equipment [41-46]. However, the inertial forces increase as the resistance increases during the use of equipment or devices of this type. As a result, the muscles must produce a greater force to overcome the

inertia of the heavier weights. This situation may cause a sports injury if the user operates the training devices improperly. The minimum resistance for this type of training device is also excessively high, and these devices are more suitable for athletes than for patients with muscle degeneration. A patient's training goals might not be achieved with this type of training device, or the use of this type of training device may cause an injury. The devices are also bulky, and the user must travel to a gym or other location that can offer this type of training device. The training program could be difficult to pursue if travel to a training facility is required.

In a recent investigation, clinical practices and design requirements were identified through a survey of therapists. Many features are desired in a future robotic rehabilitation device. The device should be able to facilitate many arm movements, be adaptable to different types of movement, be able to adjust its resistance or assistance based on the stroke survivor's performance and rehabilitation program, and have virtual ADL-specific activities. The necessity of biofeedback for these applications therefore requires further investigation [47].

The results of this investigation suggest that therapists would prefer to have a rehabilitation device that can be used both with the therapist in a clinical setting and by patients in their homes. It was also suggested that current treatment modalities struggle to provide the needed exercise intensity and frequency. A rehabilitation

robotic device in the clinic or at home could augment current treatment by providing more intense and frequent rehabilitation sessions, but the cost may be a strong limiting factor. Another problem of interest is the evaluation of robotic rehabilitation. In this field of research, a study is not widely accepted until validated clinical measures are provided, but the required mechanical assessment techniques for devices in clinical tests are rarely reported. New technologies for upper-limb rehabilitation are currently experiencing a boom; increased DOF, virtual reality, and telerehabilitation for neurorehabilitation of the upper limb are popular new trends. There is an increasing emphasis on studies in patients requiring rehabilitation from injuries or disease other than stroke, such as multiple sclerosis, traumatic brain injury, cerebral palsy and arm pain, as well as shoulder and elbow lesions. Robotic devices are also increasingly used as evaluation tools. Finally, many of the most effective robots are currently research prototypes and not yet commercially available. These devices remain relatively large and cumbersome. The affordability and portability of most of the devices will need to be improved by orders of magnitude before they can be regularly used at home by patients [47-49].

1.3 Motivation and objectives

Increases in elderly populations and sedentary lifestyles have led to an increase in age-related health problems other than stroke, such as chronic disease.

Science-based guidance of resistance training has been endorsed by major national health organizations for its potential health value on functional capacity and other health-related factors. Healthcare services and home-based rehabilitation are demanding; however, due to a decrease in the youth and labor populations, professional physical therapists face increasing job burdens. For this reason, healthcare and rehabilitation training devices must keep pace with the standard of care and cost-effectiveness requirements of today's rehabilitation trends. However, healthcare and exercise training devices targeted to these populations are rarely proposed. Most exercise machines or devices are designed for healthy young people and athletes to improve their fitness and muscular performance, and are usually used in gym- or studio-based fitness exercise. Cost-effective, safe, and accessible physical fitness for all are the prime motivations for the creation of devices based on the evidence-based science of resistance training.

The objectives of this research are to:

1. Determine the factors that contribute to design of a usable, compact, cost-effective, easy-to-operate, safe upper-limb resistance-training device for elderly and clinical populations to practice moderate exercise and which of these factors can be used for home-based exercise training or rehabilitation in the absence of a fitness instructor or therapist;

2. Formulate kinematic and dynamic models to develop design criteria for analyzing free-weight and spring-loaded exoskeletons for upper-limb resistance training;
3. Design and construct a prototype device aimed at upper-limb resistance training based on the results of objectives one and two;
4. Establish appropriate evaluation methods to evaluate joint torques and the neuromuscular response of major upper limb muscles while performing the designated resistance training; and
5. Evaluate the resulting prototype device with male and female subjects.

1.4 Overview of the dissertation

In Chapter 2, an unpowered spring-loaded upper limb exoskeleton conceptual design for use in strengthening the muscles of the upper limbs at single and multiple joints in different planes is presented. The upper limb exoskeleton consists of a 3-DOF shoulder joint and a 1-DOF elbow joint. The upper arm can perform internal-external (int-ext), abduction-adduction (abd-add), and flexion-extension (flx-ext) motions. The forearm is also able to perform a flx-ext motion. The motion joint torques of the shoulder and elbow joints in the upper limb exoskeleton are equivalent to the objective joint torques obtained from models of free-weight exercises, such as the dumbbell lateral raise motion, dumbbell frontal raise motion,

dumbbell curl motion, and overhead triceps extension. This design methodology is based on the concept of conservation of potential energy. The Denavit-Hertenberg (D-H) parameters are used to model the kinematic motion of the upper limb with free weights and exoskeleton. The zero-free-length springs installed on the link of the exoskeleton were designed to equalize the joint torques for the shoulder and elbow joints with the joint torques obtained from free-weight exercises. The installation configuration and spring design constrains are obtained from the joint torque of shoulder and elbow for different motions.

In Chapter 3, dynamic models for different movements of the upper limb at single and multiple joints in different planes are established. The Lagrange approach is used to derive the equations of motion for the upper limb motion and the spring-loaded upper limb exoskeleton because it uses fewer parameters to describe a given system and determine that these motions are mechanically analogous to the free-weight exercises. Because the exoskeleton can progressively increase the resistance as spring length changes to intensify the training of muscle groups with a lower inertia effect, the potential risk of muscle injury in the upper limb generated by free weights and training equipment is lowered. The objectives of this chapter are to develop a dynamic model of the spring-loaded upper limb exoskeleton, to prove our hypothesis that with zero-free-length springs, the

spring-loaded upper limb exoskeleton is capable of reducing unfavorable lengthening of the muscles during high-intensity free-weight exercises and to determine the additional design constraints to which the mass moment of inertia of the linkages should conform.

In Chapter 4, the preliminary embodiment design of the spring-loaded upper limb exoskeleton is performed using 3D computer-aided design (CAD) software. The maximum resistance force and the adjustable range of the zero-free-length spring are defined. We demonstrate that link length can be measured based on the anthropometric database and introduce a body segment parameter data estimation. The material characteristics of the links are defined in the CAD software to determine the inertia parameters of the upper limb exoskeleton, and the range of spring stiffness for installed springs is determined. A prototype is fabricated for evaluation of the proposed design overall and an experiment is designed to measure the static and dynamic joint torques of the shoulder and elbow. An experiment is then conducted to collect joint torque data for two healthy subjects for the upper limb dumbbell lateral raise, the dumbbell frontal raise, and the dumbbell curl, and these data are compared to measurements obtained from the shoulder abd-add flx-ext, and elbow flx-ext movements with the exoskeleton prototype. The joint torques are thus calculated using a 3D generic inverse dynamic method. The results

of the preliminary evaluation are analyzed and discussed. The purpose of this study is to establish appropriate evaluation procedures for continuing performance evaluations and determining the effect of the spring-loaded upper limb exoskeleton for strengthening the upper limb muscle. Ultimately, this chapter provides a design and prototype for an upper limb exoskeleton.

Chapter 5 describes a motion analysis study of an improved spring-loaded upper limb exoskeleton prototype, which is manufactured on the basis of the experience and preliminary evaluation of the first-generation prototype. To assess the functionality of the design and the design principle, we measured kinematic data for six young healthy subjects performing the designated movements using a motion capture system to verify our mechanism. A verification test is conducted according to the refined experiment design to collect data from six healthy subjects for the upper limb dumbbell lateral raise, the dumbbell frontal raise, and the dumbbell curl exercises and compare them to measurements obtained from the shoulder abd-add, flx-ext, and elbow flx-ext exercises with the novel exoskeleton prototype at two different moving speeds. The collected data along with the kinematic and dynamic joint torque analysis may not only verify our hypotheses but also provide a foundation for designing appropriate spring-loaded exoskeletons for upper limb resistance training.

In Chapter 6, an electromyography study of free-weight exercise and the designated motion of an improved spring-loaded upper limb exoskeleton prototype is presented. To assess the performance and functionality of the design from another perspective, an experiment is designed for measuring the electromyography (EMG) of muscles related to shoulder and elbow motion. We investigate EMG electrodes to record the muscle activity of eight upper limb muscles to resistance exercises through surface EMG. The surface EMG signals acquired from eight upper limb muscle groups of interest during the shoulder lateral raise, front raise, and elbow curl motion of free-weight exercise are analyzed and compared with measurements obtained from shoulder abd-add, flx-ext, and elbow flx-ext movement at different moving speeds. The collected surface EMG signal of the selected muscles along with the analysis may provide insight into the muscle performance of the free-weight exercise and upper limb resistance training using spring-loaded exoskeletons and may provide valuable feedback or inspiration for novel designs in the future or for the establishment of a new design principle for upper limb spring-loaded exoskeletons.

Chapter 2
Kinematic and static analysis

2.1 Introduction

The mechanical behavior of skeletal muscle contributes to the function and/or dysfunction of the human musculoskeletal system [50]. The muscle strength in an individual's limbs is crucial for physical independence. For example, in the upper limbs, impaired arm and hand function may cause serious limitations in daily living activities for the majority of stroke patients. In addition, whether older individuals have adequate muscle strength has a great influence on their daily living activities. Hisamoto and Higuchi [51] demonstrated that the extremity joint torque (EJT) values measured in 1,000 healthy Japanese men and women aged between 20 and 70 showed that women in their 20s had significantly lower EJT values than women in their 40s or 50s in the upper limbs (i.e., wrist palmar flexion, wrist dorsiflexion, elbow flexion, elbow extension, and shoulder extension). One EJT value in the lower limbs (hip flexion) also differed. The results were attributed to the use of excessive automation and labor-saving equipment, which has diminished opportunities for muscle use in daily life

Appropriate muscle training can not only enhance muscular strength, power,

and endurance but also improve health and fitness by reinforcing cardiopulmonary function, reducing body fat, improving bone mineral density, and providing other benefits [52]. Resistance exercise leads to muscle hypertrophy and increased strength in both men and women, regardless of age. Decreased activity, on the other hand, produces a decrease in the cross-sectional area of muscle fibers and a loss of strength [50]. Resistance exercise has been widely adopted to help patients recover normal physiological functions after impairing motor activity and to improve dynamic stability [53, 54]. The MIT-Manus, a robot designed for clinical neurological application, was the first device to be evaluated extensively in clinical trials to examine whether robot-aided therapy was an acceptable form of exercise therapy for stroke patients and whether it could improve the arm function of stroke patients [20]. Several studies on robotic devices have reported positive outcomes using various approaches, such as the MIME [21] and the Arm guide [23].

Resistance exercises for fitness are often performed using fitness equipment. However, most conventional training devices use weights such as weight stacks combined with a training structure to provide resistance and accomplish training goals. For example, see U.S. patent 6394937 [41], U.S. patent 7601187 [42], and U.S. patent 7670269 [43]. A pulley system described in U.S. patent 6394937 couples a handle and weights in a single system. When the user exercises by

manipulating the handle, the weight stack provides resistance and magnifies the effect of the exercise. U.S. patent 7235038 [44] is designed specifically for the elbow. However, the design is intended for exercising a single muscle group. Some machines use springs as a source of resistance (e.g., U.S. patent 5613928 [45] and U.S. patent 7060012 [46]). Most machines permit movements in a single plane to isolate specific muscle groups. These compare with free-weight exercises, where movement is allowed on different planes, training more muscle groups [15, 50, 52]. However, as the resistance increases, the inertial forces also increase, and the muscles have to produce more force to overcome the inertia of the heavier weights. This may cause a sports injury if the user operates the training devices improperly. The minimum resistance for this kind of training device is high, and these devices are more suitable for athletes than patients with muscle degeneration. A patient's training goals might not be accomplished using this type of training device, or the use of this kind of training device may cause an injury. The devices are also bulky, and the user has to travel to a gym or other location that has this type of training device, which could make the training more difficult to perform.

For these reasons, an upper limb training device that is able to perform arm exercises with multiple degrees of freedom would be beneficial to patients. In addition, it would be useful for the device to allow an individual to exercise or

complete their physical therapy at a convenient time and to prevent injuries that could be caused by inertial forces. Such a device should be easy to adjust and carry, such that its use is not limited by space or location constraints.

In this chapter, we propose an unpowered upper limb exoskeleton design for use in strengthening the muscles of the upper limbs. The upper limb exoskeleton consists of a 3-DOF shoulder joint and a 1-DOF elbow joint. The upper arm can perform int-ext, abd-add, and flx-ext motions. The forearm is also able to carry out a flx-ext motion. The motion joint torques of the shoulder and elbow joints in the upper limb exoskeleton are equivalent to the objective joint torques obtained from models of free-weight exercise, such as the dumbbell lateral raise motion, dumbbell frontal raise motion, dumbbell curl motion, and overhead triceps extension. By altering the arrangement of low-inertia springs, the locations of the springs can be adjusted for higher intensity training, and the gravitational potential energies for the upper limb and the exoskeleton remain constant, which differs from free-weight exercises, where external weights are increased to induce large inertial changes for greater muscle strengthening. As such, the exoskeleton should be capable of preventing injuries that arise as the result of large inertial changes. The upper limb exoskeleton could be used for muscle strengthening or muscle strength recovery as it has the advantages of a compact and cost-effective design that is easy to operate

and prevents injuries. These advantages make the exoskeleton very suitable for people or patients who can manipulate the resistive mode movement of the robotic devices for moderate exercise, and it can be used for home-based rehabilitation in the absence of a fitness instructor or therapist.

2.2 Kinematic model and joint torque analysis

2.2.1 Kinematic model of the upper limb

An upper limb includes the upper arm and forearm. The upper arm in Fig. 2.1 is pictured from the glenohumeral (GH) joint *S* to the elbow joint *E,* and the forearm extends from the elbow joint *E* to the middle of the palm of the hand *H*. The segmental lengths of the upper arm and the forearm are r_u and r_f, respectively. The hand is usually held in a neutral position during forearm movements. Therefore, the gravitational variation due to the wrist motion is negligible. Hence, the upper limb can be modeled as a two-link linkage. The geometries of the upper arm and the forearm were assumed to be axially symmetric, and the positions of the centers of mass, m_u and m_f, were assumed to be fixed and located at the center lines with respect to the upper arm and forearm. The mass of the human hand was ignored here as it is relatively light compared to the upper limb as a whole. The kinematic model for the arm linkage is shown in Fig. 2.1, and the GH joint in the human skeleton, which connects the scapular and the humerus, was modeled using a

3-DOF ball joint at point *S*. Kinematically, any Euler angle sequence of three orthogonal rotation axes can be used to model three pure rotations of the GH center point, including the shoulder int-ext rotation, abd-add, and flx-ext. The elbow joint is regarded as a revolute joint at point *E*, which provides only elbow flx-ext.

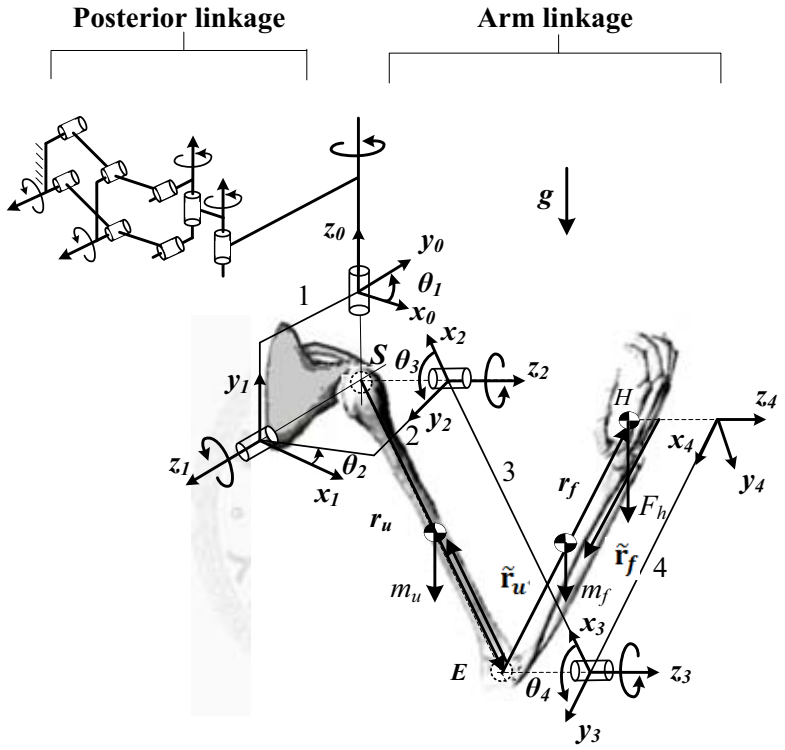

Fig. 2.1 Kinematic model and coordinate system of the right upper limb**.**

When modeling the kinematic motion of the upper limb, we used the Denavit-Hertenberg (D-H) parameters for kinematic modeling of the upper limb [55]. Following the conventions established by Denavit-Hertenberg and presented in Fig. 2.1, four Cartesian coordinate systems (CSs), CS 1, 2, 3, and 4, were attached to each link, and CS 0 was attached to the ground. The link parameters established between links *i* and *i-1* are described based on the definition of D-H

notation, and the 4 × 4 D-H transformation matrix is represented as

$$ {}^{i-1}\boldsymbol{T}_{\boldsymbol{i}} = \begin{bmatrix} \cos\theta_i & -\cos\alpha_i \sin\theta_i & \sin\alpha_i \sin\theta_i & a_i \cos\theta_i \\ \sin\theta_i & \cos\alpha_i \cos\theta_i & -\sin\alpha_i \cos\theta_i & a_i \sin\theta_i \\ 0 & \sin\alpha_i & \cos\alpha_i & d_i \\ 0 & 0 & 0 & 1 \end{bmatrix} \tag{2.1} $$

where d_i is the distance along z_{i-1} from the x_i-axis to the x_{i-1}-axis, and a_i is the distance along x_i from the z_i-axis and the z_{i-1}-axis. The value α_i is the angle measured from the z_{i-1}-axis to the z_i-axis near the x_i-axis, and θ_i is the joint angle from axis x_{i-1} to x_i near the z_{i-1} axis

From Fig. 2.1, the origins of CSs 0, 1 and 2 are coincident at GH joint *S*, and their corresponding values of d_i and a_i are zero. The axes z_2 and z_3 are parallel and their distance is the length of the upper arm. Additionally, the z_3-axis and z_4-axis are parallel and the distance is length of the forearm. θ_1, θ_2, θ_3 and θ_4 represent the rotation angles near the axes of the shoulder during int-ext, abd-add, flx-ext and elbow flx-ext motion, respectively. The D-H parameters are listed in Table 2.1.

Table 2.1 D-H parameters for the upper limb

Frame *i*	d_i	θ_i	a_i	α_i
1	0	θ_1	0	90°
2	0	θ_2	0	90°
3	0	θ_3	$-r_u$	0
4	0	θ_4	$-r_f$	0

The inside portion of the human shoulder is called the shoulder girdle, and consists of a clavicle and scapular. Klopcar and Lenarcic [57] indicate that the girdle motion can be modeled using two degrees of freedom. In our study, the motion of the girdle was modeled using two parallelogram linkages and two serially connected links. The assembly is shown in the posterior linkage from Fig. 2.1. The parallelogram linkages provide the elevation-depression movement of the scapular, and the two serially connected links allowed the GH center to be free on the horizontal plane.

2.2.2 Static joint torques during free-weight exercise

Free-weight exercises are muscular exercises that use an external weight as a resistant force on a freely moving body. The muscle force is strengthened by increasing the free-weight load gradually. In Fig. 2.1, an objective model is constructed as a free-weight exercise using an external load F_h grasped in the middle of the palm H as well as the segmental masses of the upper arm and forearm. The values for m_u and m_f are located at the mass centers of the upper arm and the forearm, respectively. During exercise, the gravitational potential energy of the kinematic model can be expressed as

$$V_g = -m_u\mathbf{g}\cdot(\boldsymbol{r_u} + \mathbf{r_f}) - m_f\mathbf{g}\cdot(\boldsymbol{r}_u + \mathbf{r}_f + \tilde{\boldsymbol{r}}_f) - F_h\mathbf{g}\cdot(\boldsymbol{r}_u + \mathbf{r}_f)$$

$$= -m_u(-\mathbf{g}\boldsymbol{k}_o)\cdot(-r_u\boldsymbol{i_3} + \tilde{r}_{u,x}\boldsymbol{i_3}) - m_f(-\mathbf{g}\boldsymbol{k}_o)\cdot(-r_u\boldsymbol{i_3} - r_f\boldsymbol{i_4} + \tilde{r}_{f,x}\boldsymbol{i_4})$$

$$-F_h(-\mathbf{g}\boldsymbol{k}_o)\cdot(-r_u\boldsymbol{i_3} + r_f\boldsymbol{i_4}) \qquad (2.2)$$

where $\tilde{\mathbf{r}}_{\boldsymbol{u}}$ and $\tilde{\mathbf{r}}_{\boldsymbol{f}}$ are the mass center position vectors of m_u and m_f referenced for each corresponding CS, and the quantities $\tilde{\mathrm{r}}_{u,x}$, $\tilde{\mathrm{r}}_{u,y}$, $\tilde{\mathrm{r}}_{u,z}$, $\tilde{\mathrm{r}}_{f,x}$ $\tilde{\mathrm{r}}_{f,y}$, and $\tilde{\mathrm{r}}_{f,z}$ are the corresponding local coordinates. Note that quantities $\tilde{\mathrm{r}}_{u,y}$ and $\tilde{\mathrm{r}}_{f,y}$ are omitted in Eq. (2.2). For CS 0, the quantities $\tilde{\mathrm{r}}_{u,z}$ and $\tilde{\mathrm{r}}_{f,z}$are zero. The mass center of F_h was assumed to be located at point *H*.

Derived from the D-H transformation matrix and the parameters, Eq. (2.2) yields the following equation for the total gravitational potential energy of an objective model of free-weight exercise

$$\begin{aligned} V_g = {} & [-m_u g(r_u - \tilde{r}_{u,x}) - (m_f + F_h)gr_u]\sin\theta_2\cos\theta_3 \\ & -[m_f g(r_f - \tilde{r}_{f,x}) + F_h g r_f]\sin\theta_2\cos(\theta_3 + \theta_4) \end{aligned} \qquad (2.3)$$

In muscular exercise, external loads can produce points around the pivot joint where there is a tendency for the muscle to resist the opposite torques from external loads. Therefore, whether the muscle exercises or not can be learned from the changes in joint torques. The gravitational joint torque τi on the joint i is calculated as

$$\tau_i = \frac{\partial V}{\partial \theta_i} \qquad i = 1,2,3,4 \tag{2.4}$$

Equation (2.4) suggests that the joint torque of θ_1 is zero and the joint torques of θ_2 , θ_3 and θ_4 are τ_2 , τ_3 and τ_4. The gravitational joint torques of the upper limb for the free-weight exercise are derived as

$$\begin{aligned}\tau_2 = {} & [-m_u g(r_u - \tilde{r}_{u,x}) - (m_f + F_h) g r_u] \cos\theta_2 \cos\theta_3 \\ & - [m_f g(r_f - \tilde{r}_{f,x}) + F_h g r_f] \cos\theta_2 \cos(\theta_3 + \theta_4)\end{aligned} \tag{2.5}$$

$$\begin{aligned}\tau_3 = {} & [m_u g(r_u - \tilde{r}_{u,x}) + (m_f + F_h) g r_u] \sin\theta_2 \sin\theta_3 \\ & + [m_f g(r_f - \tilde{r}_{f,x}) + F_h g r_f] \sin\theta_2 \sin(\theta_3 + \theta_4)\end{aligned} \tag{2.6}$$

$$\tau_4 = [m_f g(r_f - \tilde{r}_{f,x}) + F_h g r_f] \sin\theta_2 \sin(\theta_3 + \theta_4) \tag{2.7}$$

2.3 Preliminary design of the spring-loaded exoskeleton

2.3.1 Upper limb exoskeleton

In Fig. 2.1, the upper limb exoskeleton was separated from the arm linkage and posterior linkage. The posterior linkage was achieved through parallelogram linkages for girdle motions. In this study, only the arm linkage was taken into account in the design. In practice, using the exoskeleton configuration shown in Fig. 2.1, Links 1 and 2 interfere with the posterior side of the human body when the upper limb is rotated outward horizontally. The GH joint is comprised of the three

revolute joint axes z_0, z_1 and z_2 , which are arranged to be orthogonal to each other. However, this design is difficult to produce due to the difficulty of designing the human GH joint center. As such, we present a modified design in Fig. 2.2 that avoids these drawbacks, and the exoskeleton becomes wearable using a band on the upper arm and a handle for gripping.

The modified exoskeleton configuration shown in Fig. 2.2 was constructed using four links, and the 4-DOF kinematic chain contains four links, where Link 1 and the posterior linkage are connected by a revolute joint at axis z_0*. Links 1 and 2 are connected by the other revolute joint at axis z_1*. The axes z_0* and z_1* are parallel to axes z_0 and z_1, respectively, and the rotational joint angles for the z_0* and z_1* axes are the same as the rotational angles for the shoulder int-ext and abd-add exercises (θ_1 and θ_2). Links 2 and 3 pivot using a revolute joint at axis z_2, and the rotational joint angle near axis z_2 is θ_3. The interference problem arising between Link 1 and the human body was resolved by parallel shifting the axis of the shoulder int-ext, and the 3-DOF shoulder joint yielded three revolute joints near axes z_0*, z_1* and z_2, where only the alignment of the z_2-axis and the human GH joint center is required. The point P is the intersection of axes z_1* and z_2, and the measurements taken near point P are the same as those at the human shoulder joint S. For the 1-DOF elbow joint, Links 3 and 4 pivot using a revolute joint at axis z_3 to

accomplish the elbow flx-ext exercise. CSs 0, 1, 2, 3, and 4 are used in the modified exoskeleton configuration, and the relationships between the four CSs are the same as those shown in the previous analysis (Fig. 2.1).

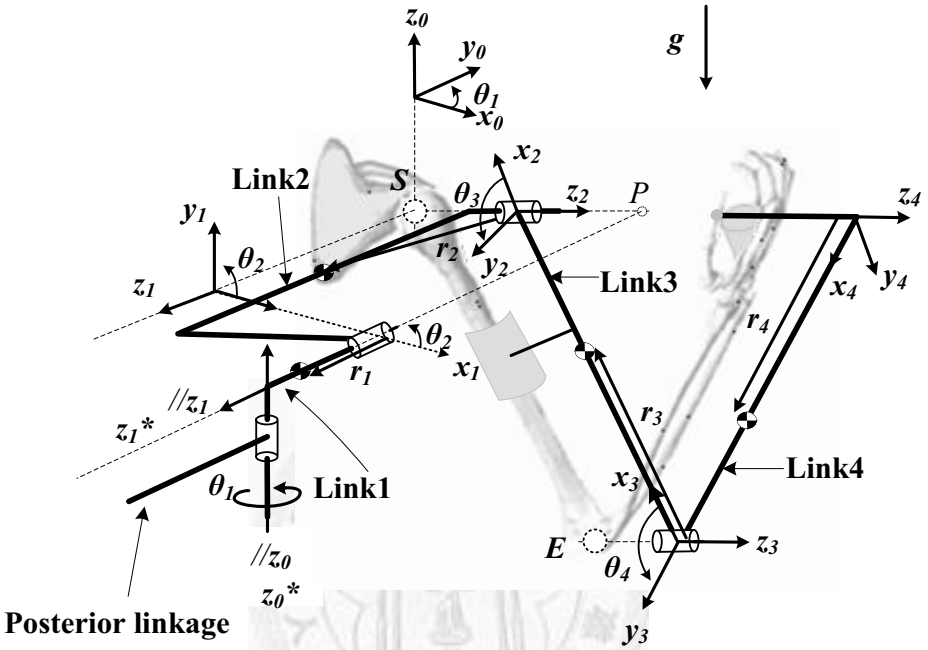

Fig. 2.2 A modified exoskeleton configuration.

By taking the link masses of the exoskeleton into account, the gravitational potential energy of Links 1, 2, 3, and 4 can be derived using the following equations:

$$V_{L1} = -m_1 \mathbf{g} \cdot \mathbf{r_1} = const. \tag{2.8}$$

$$V_{L2} = -m_2 \mathbf{g} \cdot \mathbf{r_2} = m_2 g r_{2,x} \sin\theta_2 - m_2 g r_{2,z} \cos\theta_2 + const. \tag{2.9}$$

$$V_{L3} = -m_3 \mathbf{g} \cdot \mathbf{r_3} = m_3 g (r_{3,x} - r_u) \sin\theta_2 \cos\theta_3 - m_3 g r_{3,z} \cos\theta_2 + const. \tag{2.10}$$

$$V_{L4} = -m_4 \mathbf{g} \cdot \mathbf{r_4} = -m_4 g r_u \sin\theta_2 \cos\theta_3 + m_4 g (r_{4,x} - r_f) \sin\theta_2 \cos(\theta_3 + \theta_4) - m_4 g r_{4,z} \cos\theta_2 + const. \quad (2.11)$$

Here, m_i is the mass of link i of the exoskeleton; $r_{i,x}$, $r_{i,y,}$ and $r_{i,z}$ describe their corresponding coordinates for the mass center of the link i on local coordinate x_i-y_i-z_i; and i is 1, 2, 3, and 4. It is assumed that Links 3 and 4 are axis-symmetrical links. Therefore, $r_{3,y}$ and $r_{4,y}$ are negligible.

Instead of using external loads, an increase in the amount of resistant force from the upper limb exoskeleton is achieved by changing the elastic force of the loaded spring. The resistance can be changed by adjusting the locations of the spring connections. On the spring-loaded exoskeleton, spring K_1 was attached to Point *A1* on Link 2 and Point *B1* on Link 1; Spring K_2 was attached to Point *A2* on Link 2 and Point *B2* on Link 4; and Spring K_3 was attached to Point *A3* on Link 2 and Point *B3* on Link 4. The location of the connected Points *A1*, *A2*, and *A3* for Springs K_1, K_2, and K_3 were adjusted for increased spring resistance, whereas Points *B1*, *B2*, and *B3* were fixed to connected points. The schematic diagram of the spring-loaded exoskeleton is shown in Fig. 2.3.

The concept of employing elastic force as a resistance force originated from the reverse idea behind the gravity-balance mechanism. The zero-free-length spring is used to make the spring stiffness independent of the rotational angles of the links.

Therefore, the resistance force can be changed only by adjusting the locations of the spring connections. The design of zero-free-length springs was adopted in the spring-loaded exoskeleton, and this was accomplished by combining the use of standard springs with cables, and pulleys or alignment shafts [58-59].

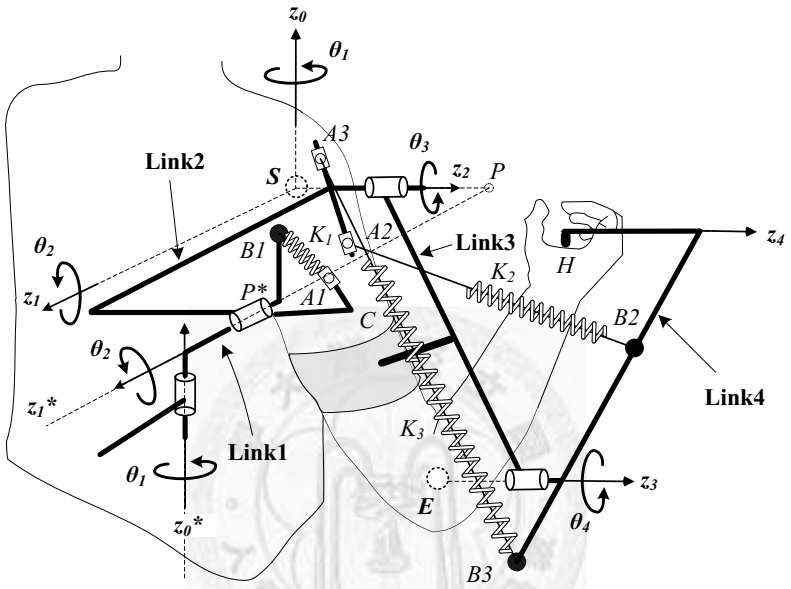

Fig. 2.3 A schematic diagram of the spring-loaded exoskeleton.

The corresponding elastic potential energies, V_{S1}, V_{S2}, and V_{S3} of Springs K_1, K_2, and K_3 are derived as

$$\begin{aligned} V_{S1} &= \frac{1}{2} K_1 \left(\boldsymbol{l}_{A1B1} \cdot \boldsymbol{l}_{A1B1} \right) \\ &= \left(-K_1 l_{CA1} l_{PB1} \right) \sin\theta_2 - \left(K_1 l_{CP} l_{PB1} \right) \cos\theta_2 + const. \end{aligned} \tag{2.12}$$

$$\begin{aligned} V_{S2} &= \frac{1}{2} K_2 (\boldsymbol{l}_{A2B2} \cdot \boldsymbol{l}_{A2B2}) \\ &= (-K_2 l_{SA2} r_u) \cos\theta_3 + (-K_2 l_{EB2} l_{SA2}) \cos(\theta_3 + \theta_4) \\ &\quad + (K_2 r_u l_{EB2}) \cos\theta_4 + const. \end{aligned} \tag{2.13}$$

$$
\begin{aligned}
V_{S3} &= \frac{1}{2} K_3 (\boldsymbol{l}_{A3B3} \cdot \boldsymbol{l}_{A3B3}) \\
&= (K_3 l_{SA3} r_u) \cos\theta_3 - (K_3 l_{EB3} l_{SA3}) \cos(\theta_3 + \theta_4) \\
&\quad - (K_3 l_{EB3} r_u) \cos\theta_4 + const.
\end{aligned} \tag{2.14}
$$

The total potential energy of the upper limb exoskeleton is the sum of the gravitational energies of the upper limb and the four links with the elastic potential energies of the three springs.

Thus, using Eq. (2.4), the joint torques of θ_2, θ_3 and θ_4 from the use of the exoskeleton are M_2, M_3 and M_4, and the torques are derived as

$$
\begin{aligned}
M_2 &= [-m_u g(r_{\boldsymbol{u}} - \tilde{r}_{u,x}) + m_f g r_u - m_3 g(r_{3,x} - r_u) - m_4 g r_u] \sin\theta_2 \sin\theta_3 \\
&\quad + [-m_f g(r_f - \tilde{r}_{f,x}) + m_4 g(r_{4,x} - r_f)] \sin\theta_2 \sin(\theta_3 + \theta_4) \\
&\quad + [-K_1 l_{CA1} l_{PB1} + m_2 g r_{2,x}] \cos\theta_2 \\
&\quad + [K_1 l_{CP} l_{PB1} + m_u g \tilde{r}_{u,z} + m_f g \tilde{r}_{f,z} + m_2 g r_{2,z} + m_3 g r_{3,z} + m_4 g r_{4,z}] \sin\theta_2
\end{aligned} \tag{2.15}
$$

$$
\begin{aligned}
M_3 &= [m_u g(r_{\boldsymbol{u}} - \tilde{r}_{u,x}) + m_f g r_u - m_3 g(r_{3,x} - r_u) + m_4 g r_u] \sin\theta_2 \sin\theta_3 \\
&\quad + [m_f g(r_f - \tilde{r}_{f,x}) - m_4 g(r_{4,x} - r_f)] \sin\theta_2 \sin(\theta_3 + \theta_4) \\
&\quad + [K_2 l_{SA2} r_u - K_3 l_{SA3} r_u] \sin\theta_3 \\
&\quad + [K_2 l_{EB2} l_{SA2} + K_3 l_{EB3} l_{SA3}] \sin(\theta_3 + \theta_4)
\end{aligned} \tag{2.16}
$$

$$
\begin{aligned}
M_4 &= [m_f g(r_f - \tilde{r}_{f,x}) - m_4 g(r_{4,x} - r_f)] \sin\theta_2 \sin(\theta_3 + \theta_4) \\
&\quad + [K_2 l_{EB2} l_{SA2} + K_3 l_{EB3} l_{SA3}] \sin(\theta_3 + \theta_4) - [K_2 l_{EB2} r_u - K_3 l_{EB3} r_u] \sin\theta_4
\end{aligned} \tag{2.17}
$$

2.3.2 Spring design constrains for upper limb muscular exercise

The 3 DOF motions of the shoulder: shoulder int-ext, shoulder abd-add, and shoulder flx-ext have a similar range of movement as the dumbbell bench fly, the

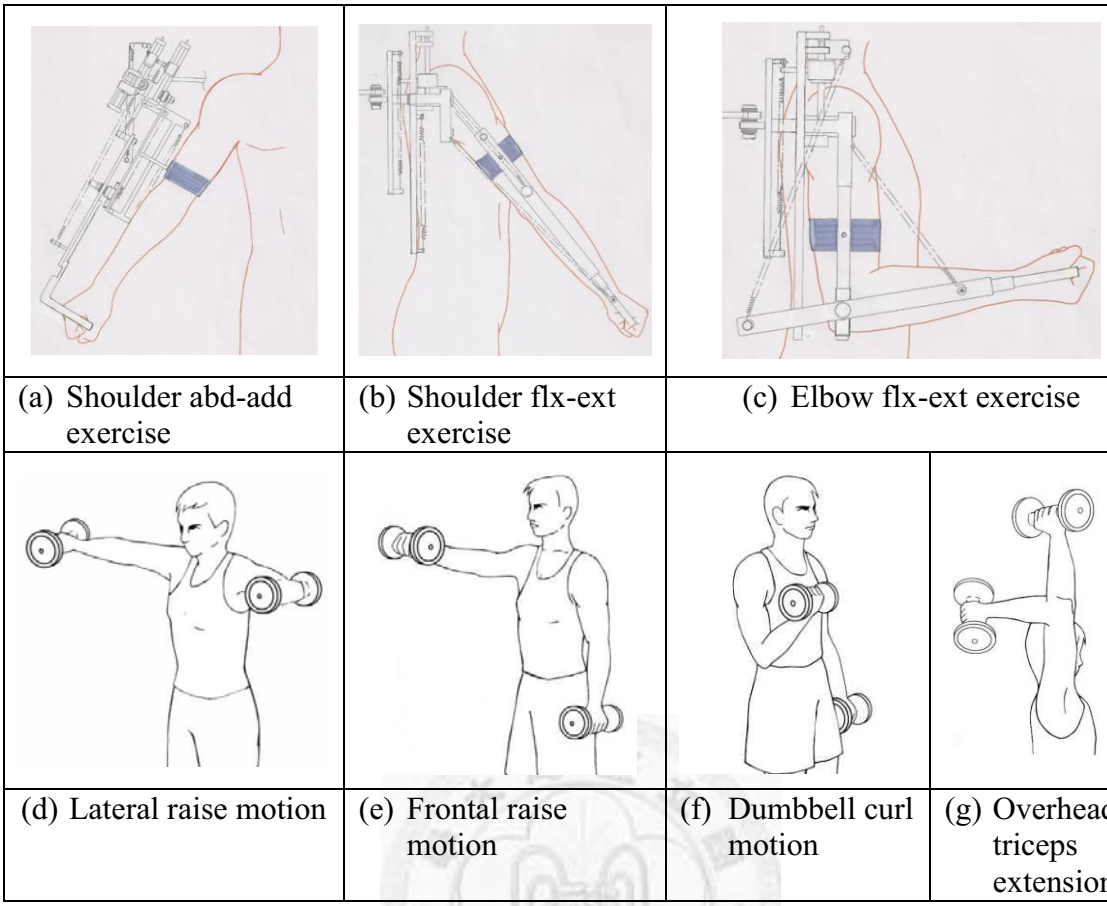

Fig. 2.4 Upper limb exoskeleton muscular exercise and dumbbell motions.

dumbbell lateral, and the frontal raise motions of free-weight exercises. The dumbbell bench fly is an exercise where the user lies on a bench and gravity acts in the direction of negative y_0 for CS 0 to provide torque on the shoulder joint near the axis of the shoulder int-ext motion. However, in this study, the stand posture was the position where gravity acts in the direction of negative *ko* for CS 0. This makes the torque of shoulder int-ext motion zero. Therefore, only the dumbbell lateral and frontal raise motions for shoulder abd-add and flx-ext exercises for the shoulder joint, and dumbbell curl motion and overhead triceps extension for elbow flx-ext

exercises for the elbow joint were taken into account for the upper limb exoskeleton, as shown in Fig. 2.4.

2.3.2.1 Training upper limb muscles with shoulder abd-add

As an example of shoulder abd-add resistance exercise, the lateral raise motion was used for strengthening the deltoid, latissimus dorsi, pectoralis major, supraspinatus, and trapezius muscles [60]. In the kinematic model, the angles θ_3 and θ_4 were fixed at 0 degrees. As such, the upper arm and forearm can be considered a single link, and the rotation about axis z_1 applies for θ_2 alone. By substituting the 0 degree condition for Angles θ_3 and θ_4 into Eqs. (2.5)-(2.7), the joint torques of θ_3 and θ_4 equal zero, and the joint torque of θ_2 is expressed as

$$\tau_{2,lr} = [-m_u g(r_u - \tilde{r}_{u,x}) - m_f g(r_u + r_f - \tilde{r}_{f,x}) - F_h g(r_u + r_f)]\cos\theta_2 \qquad (2.18)$$

In Fig. 2.3, Spring K_1 connects Link 1 and Link 2 to generate torques near the axis of shoulder abd-add. In this exercise, the upper limb maintains the same posture as the lateral raise motion with exoskeleton, except that the resistance from the external load is replaced using springs. The joint torques of a shoulder with the exoskeleton are obtained by substituting the same angles for the lateral raise motion (θ_3 and θ_4) into Eqs. (2.14)-(2.16). The joint torques of θ_3 and θ_4 are zero, the same values as those for the lateral raise motion. The joint torque of θ_2 can be calculated

as

$$M_{2,lr}$$

$$= \left[-m_u g\left(r_u - \tilde{r}_{u,x}\right) - m_f g\left(r_u + r_f - \tilde{r}_{f,x}\right) + m_2 g r_{2,x} + m_3 g\left(r_{3,x} - r_u\right)\right.$$

$$\left. + m_4 g\left(r_{4,x} - r_f - r_u\right) - K_1 l_{CA1} l_{PB1}\right] cos\theta_2$$

$$+\left[K_1 l_{CP} l_{PB1} + m_u g \tilde{r}_{u,z} + m_f g \tilde{r}_{f,z} + m_2 g r_{2,z} + m_3 g r_{3,z} + m_4 g r_{4,z}\right] sin\theta_2 \quad (2.19)$$

For emulating free-weight exercise, the joint torques in the lateral raise motion and the upper limb exoskeleton should be equivalent to each other. As a result, the coefficients of $\cos\theta_2$ in Eq. (2.18) have to be equal to those in Eq. (2.19), and the coefficients $\sin\theta_2$ of Eq. (2.19) are zero. The design constrain of Spring K_1 obtained from the equation of coefficients with $\cos\theta_2$ as expressed as

$$l_{CA1} = F_h \left[\frac{g(r_u - r_f)}{K_1 l_{PB1}}\right] + \frac{m_2 g r_{2,x} + m_3 g(r_{3,x} - r_u) + m_4 g(r_{4,x} - r_f - r_u)}{K_1 l_{PB1}} \quad (2.20)$$

Equation (2.20) represents the linear proportion relationship between the weight of an external load F_h and the length of the connected points for Spring K_1, with an adjustment of l_{CA1} to increase the resistance for training intensity.

The weights of the upper limb and the exoskeleton generated momentum about axis z_1* due to the effect of gravity, and Spring K_1 also compensated for the gravitational potential energy of the upper limb and the links. The spring design constrain of Spring K_1 is expressed as

$$l_{CP} = -\frac{m_u g\tilde{r}_{u,z} + m_f g\tilde{r}_{f,z} + m_2 g r_{2,z} + m_3 g r_{3,z} + m_4 g r_{4,z}}{K_1 l_{PB1}} \quad (2.21)$$

2.3.2.2 Training upper limb muscles with shoulder flexion/extension

As an example of shoulder flx-ext resistance exercise, the frontal raise motion can be used for strengthening deltoid, pectoralis major, latissimus dorsi, and trapezius muscles [60]. In the kinematic model, the angles θ_2 and θ_4 are fixed at 90 and 0 degrees, respectively. The upper arm and forearm are considered as a single rigid body rotating about axis z_2 with the angle θ_3. By substituting the conditions for θ_2 and θ_4 into Eqs. (2.5)-(2.7), the joint torque of θ_2 is equal to zero, and the joint torques of θ_3 and θ_4 can be expressed as

$$\tau_{3,fr} = [m_u g(r_u - \tilde{r}_{u,x}) + m_f g(r_u + r_f - \tilde{r}_{f,x}) + F_h g(r_u + r_f)]\sin\theta_3 \quad (2.22)$$

$$\tau_{4,fr} = \left[m_f g\left(r_u - \tilde{r}_{f,x}\right) + F_h g r_f\right] sin\theta_3 \quad (2.23)$$

In the frontal raise motion, the shoulder and elbow joints generate torques. Fig. 2.3 demonstrates that Spring K_2 connects Links 2 and 4, which produced torques that had the same strength as the same muscles using a free-weight exercise. For shoulder flx-ext exercise using the upper limb exoskeleton, a user would have the same movement as for the frontal raise motion. By substituting the same angles, θ_2 and θ_4, for frontal raise motion in Eqs. (2.15)-(2.17), the joint torques of the

shoulder with the exoskeleton are obtained using the equations:

$$M_{2,fr} = K_1 l_{CP} l_{PB1} + m_u g \tilde{r}_{u,z} + m_f g \tilde{r}_{f,z} + m_2 g r_{2,z} + m_3 g r_{3,z} + m_4 g r_{4,z} \quad (2.24)$$

$$\begin{aligned} M_{3,fr} = [&m_u g(r_u - \tilde{r}_{u,x}) + m_f g(r_u + r_f - \tilde{r}_{f,x}) - m_3 g(r_{3,x} - r_u) \\ &- m_4 g(r_{4,x} - r_f - r_u) + K_2 l_{SA2}(r_u + l_{EB_2}) + K_3 l_{SA3}(l_{EB3} - r_{SE})] \sin\theta_3 \end{aligned} \quad (2.25)$$

$$M_{4,fr} = [m_f g(r_f - \tilde{r}_{f,x}) - m_4 g(r_{4,x} - r_f) + K_2 l_{EB2} l_{SA2} + K_3 l_{EB3} l_{SA2}] \sin\theta_3 \quad (2.26)$$

To achieve the effects of frontal raise motion, the joint torques with the upper limb exoskeleton had to be the same as the joint torques for frontal raise motion. The design constrains for Springs K_2 and K_3 are calculated as

$$l_{EB3} = 0 \quad (2.27)$$

$$l_{EB2} = r_f \quad (2.28)$$

$$l_{SA3} = \frac{-m_3 g r_f (r_{3,x} - r_u) + m_4 g r_u r_{4,x}}{K_3 r_u r_f} \quad (2.29)$$

$$l_{SA2} = F_h(\frac{g}{K_2}) + \frac{m_4 g(r_{4,x} - r_f)}{K_2 r_f} \quad (2.30)$$

During shoulder flx-ext exercise, Spring K_1 could be installed in any position, and the spring position did not affect the results of the muscle strengthening

exercises. The momentum about the axis z_1* due to the weights of the upper limb and the links in the exoskeleton was the same as the momentum in shoulder abd-add exercise. Therefore, the design for Spring K_1 could be modelled using the same equations as presented in Eq. (2.20). Eq. (2.29) also represents a linear proportion between the weight of external load mw and the length of the connected points of Spring K_2 with an adjustment l_{SA2} to increase the resistance for training intensity.

2.3.2.3 Training upper limb muscles with elbow flx-ext

As an example of elbow flx-ext resistance exercise, the dumbbell curl motion is used for strengthening the biceps brachii, brachialis, and brachioradialis muscles. In addition, the overhead triceps extension is used for strengthening the triceps brachii [60]. In the kinematic model, the angles θ_2 and θ_3 were fixed at 90 and 0 degrees, respectively. The forearm rotates about axis z_3 with θ_4. Substituting the angles θ_2 and θ_3 into Eqs. (2.5)-(2.7) produced a joint torque for θ_2 of zero, whereas the joint torques for θ_3 and θ_4 were equalized and expressed as

$$\tau_{3,dc} = \tau_{4,dc} = \left\lfloor m_f g(r_f - \tilde{r}_{f,x}) + F_h g r_f \right\rfloor \sin\theta_4 \tag{2.31}$$

In the dumbbell curl motion, the joint torques were generated on the joints of Axes z_3 and z_4, and the installation of Spring K_3 connected Link 2 and Link 4 to

produce the same joint torques as for free-weight exercise (Fig. 2.3). For training the upper limb exoskeleton for the elbow flx-ext exercise, substituting the angles θ_2 and θ_3 for the dumbbell curl motion into Eqs. (2.5)-(2.7) and (2.15)-(2.17) yielded the joint torques for the upper limb exoskeleton. The joint torque of θ_2 are the same as the shoulder flx-ext exercise expressed using Eq. (2.31), whereas the joint torques for θ_3 and θ_4 are

$$M_{3,dc} = [m_f g(r_{EH} - \tilde{r}_{f,x}) - m_4 g(r_{4,x} - r_f) + K_2 l_{EB2} l_{SA2} + K_3 l_{EB3} l_{SA3}] \sin\theta_4 \quad (2.32)$$

$$\begin{aligned} M_{4,dc} = [&m_f g(r_f - \tilde{r}_{f,x}) - m_4 g(r_{4,x} - r_f) + K_2 l_{EB2} l_{SA2} \\ &+ K_3 l_{EB3} l_{SA3} - K_2 l_{EA2} r_u + K_3 l_{EB3} r_u] \sin\theta_4 \end{aligned} \quad (2.33)$$

The joint torques for θ_3 and θ_4 for the upper limb exoskeleton have to be to the same as for the dumbbell curl motion. As such, the design constrains for Springs K_2 and K_3 are expressed as

$$l_{EB2} = \frac{K_3 l_{EB3}}{K_2} \quad (2.34)$$

$$l_{SA2} = 0 \quad (2.35)$$

$$l_{SA3} = F_h\left(\frac{g r_f}{K_3 l_{EB3}}\right) + \frac{m_4 g(r_{4,x} - r_f)}{K_3 l_{EB3}} \quad (2.36)$$

For the dumbbell curl motion, the increase in resistance is produced by

increasing the weight of external load, F_h. However, due to the linear proportion relationship between mw and K_3, the adjustment for Spring K_3, l_{SA3}, was used to increase the resistant force from Eq. (2.36) for training with the exoskeleton. The spring design constrain for Spring K_1 was the same as that for the lateral raise motion (see Eq. (2.21)).

The overhead triceps extension is a free-weight exercise that can be used to strengthen the triceps. In exercising with the upper limb exoskeleton, the motion can also be performed with the elbow flx-ext exercise. In the kinematic model, the angles θ_2 and θ_3 were fixed at 90 and 180 degrees, respectively, and the forearm was rotated about Axis z_3 with θ_4. By substituting the angles θ_2 and θ_3 into Eqs. (2.11)-(2.13) and (2.15)-(2.17), the joint torques can be calculated. The momentums for the free-weight exercise has to be the same as that for the upper limb exoskeleton. Therefore, the design constrains for Springs K_2 and K_3 were the same as those for the elbow flx-ext exercise for training biceps, as shown in Eqs. (2.34)-(2.36). In the elbow flx-ext exercise for training the biceps and triceps, Spring K_1 could be set to any position because it would not affect muscle strengthening.

2.3.3 Evaluation of the preliminary design

2.3.3.1 Joint torque calculations of free-weight exercise

The objective joint torques for the shoulder and elbow joints were derived from a free-weight exercise model. As such, the values for the joint torques were calculated for shoulder abd-add, flx-ext, and elbow flx-ext exercise using Eqs. (2.18), (2.22), (2.23), and (2.31). Table 2.2 shows the anthropometric parameters of two healthy subjects (male and female).

Table 2.2 Anthropometric parameters of the subjects used in the preliminary design evaluation

Subjects	TBW	Upper arm (r_u)	Forearm (r_f)	Segmental weight (m_u)	Segmental weight (m_f)
Male	82 kg	280 mm	352 mm	2.24 kg	1.90 kg
Female	59 kg	263 mm	335 mm	1.61 kg	1.36 kg

TBW: Total body weight

The resistant force had levels that increased from 1 kg to 7 kg of weight for the free-weight exercise. The segmental weights for the upper arms and forearms are based on Clauser et al. [61], who proposed the following regression model for the estimation of these parameters:

$$m_u = 0.0274 \times (\mathrm{TBW}) - 0.01 \tag{2.37}$$

$$m_f = 0.0233 \times (\mathrm{TBW}) - 0.01 \tag{2.38}$$

2.3.3.2 Simulation of the preliminary exoskeleton design

The preliminary design was carried out using 3D CAD software, and the materials for the links were made of aluminum in this study. The material characteristics of the links were defined in the CAD software to determine the inertia parameters of the upper limb exoskeleton. The masses and the corresponding coordinates of the mass centers for each link are listed in Table 2.3.

Table 2.3 Inertial parameters of the upper limb exoskeleton

Links (i)	mass(kg)	$r_{i,X}$ (mm)	$r_{i,Y}$ (mm)	$r_{i,Z}$ (mm)
1	0.502	-45	82	25
2	1.233	-13	29	-18
3	0.202	143	0	-75.4
4	0.418	94	0	-50.6

Based on the anthropometric parameters of the male and female subjects in the evaluation, the exact values of l_{CA1}, l_{SA2}, and l_{SA3} for 1 kg, 4 kg, and 7 kg weight resistances for the upper limb exoskeleton are listed in Table 2.4.

Table 2.4 The adjustable length of springs for 1, 4, and 7 kg weight resistances

Subjects	Resistance (kg)	Adjustments of springs for muscle strengthening exercise (mm)		
		Shoulder abd/add (l_{CA1})	Shoulder flx/ext (l_{SA2})	Elbow flx/ext (l_{SA3})
Male	1	7	6	11
	4	46	33	61
	7	86	59	111
Female	1	6	6	10
	4	42	33	54
	7	78	59	97

The resistance in the design is generated by adjusting the locations of the springs rather than changing the stiffness of the springs. This design was expected to provide light resistance to stimulate muscle strength recovery in patients with injuries and to provide more intense strength training for healthy individuals. In this preliminary design, the maximum resistant force was designed to be 68.6 N (corresponding to a 7 kg weight dumbbell). Therefore, it was important to choose springs of suitable stiffness. In the preliminary design of the upper limb exoskeleton, interference among the different links during exercise needed to be considered. For example, the attached point B_3 was a prominent link on Link 4 that exceeded the elbow joint. In the upper limb stretching course, the motion interference of Link 4 and Link 2 would interfere if the length of the prominent link was longer than the upper arm. Therefore, l_{EB3} was designed to be 150 mm (i.e., shorter than the length of the subject's upper arm). The spring-adjustable points were limited from 4 mm to 120 mm. The adjustable lengths l_{CA1}, l_{SA2}, and l_{SA3} of Springs K_1, K_2 and K_3 were designed to be attached to Link 2, which was a reasonable and convenient location for setting the adjustment of the exoskeleton. Moreover, the length l_{B1P*} was designed to be 100 mm, which conformed to the limitations of the adjustable range. Considering the limitations and the mass properties of the linkages, together with the anthropometric parameters of humans

as expressed in Eq. (2.20), the range of spring stiffness for K_1 lies in the range

$$3.515 \text{ N/mm} \le K_1 \le 7.178 \text{ N/mm} \tag{2.39}$$

Following the same steps for shoulder flx-ext exercise, the range of spring stiffness for K_2 was derived from Eq. (2.30), and for the elbow flx-ext exercise, the range of spring stiffness for K_3 was obtained from Eq. (2.36). The ranges of spring stiffness for K_2 and K_3 were

$$1.070 \text{ N/mm} \le K_2 \le 1.789 \text{ N/mm} \tag{2.40}$$

$$1.342 \text{ N/mm} \le K_3 \le 3.184 \text{ N/mm} \tag{2.41}$$

The K_1, K_2 and K_3 springs that were available within the stiffness ranges were selected for this design. During the practical implementation of this design, we chose springs with the following stiffness from the catalog [62] of standard springs: K_1 (4.704 N/mm (0.480 kgw/mm)), K_2 (1.107 N/mm (0.113 kgw/mm)) and K_3 (1.392 N/mm (0.142 kgw/mm)).

The design parameters for the upper limb exoskeleton depended on the anthropometric parameters associated with the user's upper limb. These parameters were used to build a kinematic model of the upper limb together with the design using ADAMS software to simulate movement of the exoskeleton. ADAMS (Mechanical Dynamics Inc., U.S.) provides users with a powerful modeling and

simulation tool for virtual prototyping and motion simulation [63]. A variety of mechanical systems modeling, simulations, and analyses have been carried out using ADAMS. Renault and Ouezdou [64] presented an anthropomorphic model of a human hand, and ADAMS was used to test the design for free movement and grasping tasks. Li et al. [65] used ADAMS to simulate the movement of the human lower extremities in researching the principles of force and torque at every joint. Yin and Xu [66] presented a parallel mechanism of two platforms that were mutually connected by two RPR and two RP serial kinematic chains, and simulation using ADAMS proved the validity of the theoretical analysis. In this study, shoulder abd-add, flx-ext, and elbow flx-ext exercises were simulated with the exoskeleton to verify the validity of the theoretical analysis of this design.

Parts of the upper body, right upper arm, right forearm and the exoskeleton consisted of four links constructed using the 3D CAD software from SolidWorks, and the images were imported into ADAMS. Next, constraints and motion were added to give the parts movement. The upper body and the right upper arm parts were constrained using three revolute joints to perform shoulder int-ext, abd-add, and flx-ext motions. A revolute joint was added to connect the right upper arm and right forearm to perform elbow flx-ext motions. The Link 3 part was attached to the right upper arm part through a fixed joint, and the connection for the Link 4 and the

right forearm parts were connected in the same manner. The Link 1, 2, 3 and 4 parts were pivoted using 3 revolute joints, respectively. The Link 1 part and the ground were connected through two translational joints to allow for movement horizontally and vertically. Springs K_1, K_2 and K_3 were added, and the stiffness for each spring was determined as shown in Fig. 2.5(a). The movement of the exercises were determined by creating three splines to define the location coordinates of the upper arm. An AKISPL function for the shoulder and elbow joints drove the motions of the upper limb, and the angular velocity was set to 20 degs/s for three exercises. The shoulder abd-add, flx-ext, and elbow flx-ext exercises were run to obtain the joint torques. A simulation model of the shoulder abd-add exercise is shown in Fig. 2.5(b).

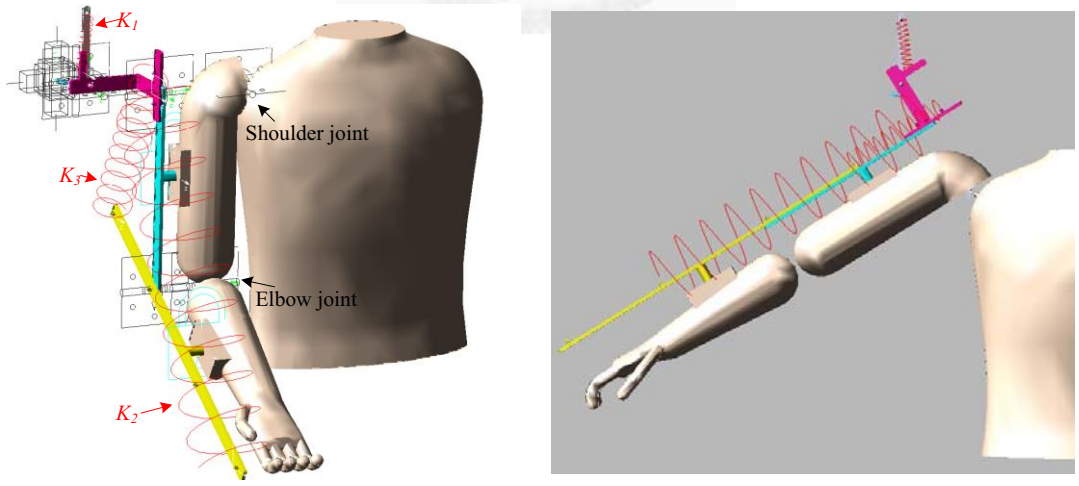

(a) The kinematic model of the upper limb and the exoskeleton

(b) Simulations of shoulder abd/add exercise were run to obtain the joint torque for the shoulder

Fig. 2.5 ADAMS simulation of the upper limb exoskeleton

2.3.3.3 Comparison between the theoretical analysis and the simulation

The preliminary exoskeleton design simulation in ADAMS was based on the spring design constrains that were derived from the objective joint torques of free-weight exercise. The objective joint toques of free-weight exercises for shoulder abd-add, flx-ext, and elbow flx-ext were described in Section 2.2.2. The theoretical values were calculated by substituting the anthropometric parameters of two healthy subjects into the equations for the objective joint torques and are listed in Table 2.5 and 2.6, for the shoulder abd-add, flx-ext, and elbow flx-ext exercises. The mass centers of the upper arm and forearm were calculated according to Clauser et al. [61].

From Table 2.5 and 2.6, the theoretical values of the joint torques appeared to be generally compatible with the data obtained from the simulation with the conceptual exoskeleton design. The results supported the preliminary design produced in ADAMS. Additionally, the difference between the theoretical and simulated joint torques was close to zero, especially for the elbow flx-ext exercise.

Table 2.5 A comparison between the theoretical and simulated data for shoulder abd-add and flx-ext exercises, and elbow flx-ext exercises (resistance=1 kgw/ 4 kgw/ 7 kgw) for a male subject.

Degrees	Male		
	$\bar{\Gamma}$	$\bar{M}_S$	$\bar{\mathrm{D}}$
Shoulder abd-add exercise			
90	0 / 0 / 0	0 / 0 / 0	0 / 0 / 0
108	5,916 / 11,658 / 17,400	5,897 / 11,638 / 17,380	0.32 / 0.17 / 0.11
126	11,253 / 22,175 / 33,096	11,236 / 22,157 / 33,079	0.15 / 0.08 / 0.05
144	15,489 / 30,521 / 45,553	15,475 / 30,507 / 45,539	0.09 / 0.05 / 0.03
162	18,208 / 35,879 / 53,551	18,199 / 35,870 / 53,542	0.05 / 0.03 / 0.02
180	19,145 / 37,726 / 56,307	19,142 / 37,723 / 56,303	0.02 / 0.01 / 0.01
Shoulder flx-ext exercise			
0	0 / 0 / 0	0 / 0 / 0	0 / 0 / 0
18	5,916 / 11,658 / 17,400	5,975 / 11,717 / 17,459	1.00 / 0.51 / 0.34
36	11,253 / 22,175 / 33,096	11,364 / 22,286 / 33,208	0.99 / 0.50 / 0.34
54	15,489 / 30,521 / 45,553	15,642 / 30,675 / 45,708	0.99 / 0.50 / 0.34
72	18,208 / 35,879 / 53,551	18,388 / 36,060 / 53,732	0.99 / 0.50 / 0.34
90	19,145 / 37,726 / 56,307	19,334 / 37,916 / 56,498	0.99 / 0.50 / 0.34
Elbow flx-ext exercise			
100	6,551 / 16,743 / 26,934	6,550 / 16,743 / 26,935	0.02 / 0.00 / 0.00
110	6,251 / 15,976 / 25,700	6,250 / 15,976 / 25,701	0.02 / 0.00 / 0.00
120	5,761 / 14,723 / 23,686	5,760 / 14,723 / 23,686	0.02 / 0.00 / 0.00
130	5,096 / 13,024 / 20,951	5,095 / 13,023 / 20,951	0.02 / 0.01 / 0.00
140	4,276 / 10,928 / 17,580	4,276 / 10,928 / 17,580	0.00 / 0.00 / 0.00
150	3,326 / 8,501 / 13,675	3,326 / 8,500 / 13,675	0.00 / 0.01 / 0.00

*$\bar{\Gamma}$: theoretical joint torques (N-mm); $\bar{M}_S$: simulated joint torques (N-mm); $\bar{\mathrm{D}}$: $|\bar{\Gamma} - \bar{M}_S|/\bar{\Gamma} \times 100\%$

Table 2.6 A comparison between the theoretical and simulated data for shoulder abd-add and flx-ext exercises, and elbow flx-ext exercises (resistance=1 kgw/ 4 kgw/ 7 kgw) for a female subject.

Degrees	Female		
	$\bar{\Gamma}$	$\bar{M}_S$	$\bar{\mathrm{D}}$
Shoulder abd-add exercise			
90	0 / 0 / 0	0 / 0 / 0	0 / 0 / 0
108	4,229 / 9,425 / 14,622	4,184 / 9,381 / 14,578	1.06 / 0.47/ 0.30
126	8,044 / 17,928 / 27,813	7,969 / 17,854 / 27,739	0.93 / 0.41 / 0.27
144	11,071 / 24,676 / 38,281	10,973 / 24,580 / 38,185	0.89 / 0.39 / 0.25
162	13,015 / 29,008 / 45,002	12,904 / 28,899 / 44,893	0.85 / 0.38 / 0.24
180	13,684 / 30,501 / 47,318	13,571 / 30,390 / 47,206	0.83 / 0.36 / 0.24
Shoulder flx-ext exercise			
0	0 / 0 / 0	0 / 0 / 0	0 / 0 / 0
18	4,229 / 9,425 / 14,622	4,282 / 9,477 / 14,674	1.25 / 0.55 / 0.36
36	8,044 / 17,928 / 27,813	8,144 / 18,026 / 27,911	1.24 / 0.55 / 0.35
54	11,071 / 24,676 / 38,281	11,210 / 24,811 / 38,416	1.26 / 0.55 / 0.35
72	13,015 / 29,008 / 45,002	13,178 / 29,167 / 45,161	1.25 / 0.55 / 0.35
90	13,684 / 30,501 / 47,318	13,856 / 30,667 / 47,485	1.26 / 0.54 / 0.35
Elbow flx-ext exercise			
100	5,007 / 13,953 / 22,900	5,007 / 13,953 / 22,900	0.00 / 0.00 / 0.00
110	4,777 / 13,314 / 21,851	4,778 / 13,314 / 21,851	0.02 / 0.00 / 0.00
120	4,403 / 12,270 / 20,138	4,403 / 12,270 / 20,138	0.00 / 0.00 / 0.00
130	3,894 / 10,854 / 17,813	3,895 / 10,854 / 17,813	0.03 / 0.00 / 0.00
140	3,268 / 9,107 / 14,947	3,268 / 9,107 / 14,947	0.00 / 0.00 / 0.00
150	2,542 / 7,084 / 11,627	2,542 / 7,084 / 11,626	0.00 / 0.00 / 0.01

*$\bar{\Gamma}$: theoretical joint torques (N-mm); $\bar{M}_S$: simulated joint torques (N-mm); $\bar{\mathrm{D}}$: $|\bar{\Gamma} - \bar{M}_S|/\bar{\Gamma} \times 100\%$

2.4 Embodiment design of the spring-loaded exoskeleton

The embodiment design was carried out using 3D CAD software, and the major materials for the links were made of aluminum alloy in this study. The resistance in the design is generated by adjusting the locations of the springs rather than changing the stiffness of the springs. This design was expected to provide different levels of resistance to stimulate muscle strength recovery in patients with injuries and to provide more intense strength training for healthy individuals. Through some basic test of zero-free-length spring concept and carefully design review, several practical considerations are found: the target value of maximum resistant force in the preliminary design was too large for our potential users; the large stiffness of the springs not only requires a higher strength of links but also increases the difficulty of operation. Therefore, in this embodiment design, the maximum resistant force was redesigned to be 49 N (corresponding to a 5 kg weight dumbbell). Therefore, it was important to choose springs of smaller stiffness and to rearrange some parameters. The spring-adjustable points were limited from 1 mm to 160 mm. The adjustable lengths l_{CA1}, l_{SA2}, and l_{SA3} of Springs K_1, K_2 and K_3 were designed to be attached to Link 2, which was a reasonable and convenient location for setting the adjustment of the exoskeleton. Moreover, the length l_{B1P*} was redesigned to be 155 mm, which conformed to the limitations of the adjustable

range. Considering the limitations and the mass properties of the linkages, together with the anthropometric parameters of humans as expressed in Eq. (2.19), the range of spring stiffness for K_1 lies in the range

$$0.95\,\text{N/mm} \le K_1 \le 1.51\,\text{N/mm} \tag{2.42}$$

Following the same steps for the shoulder flx-ext exercise, the range of spring stiffness for K_2 was derived from Eq. (2.30), and for the elbow flx-ext exercise, the range of spring stiffness for K_3 was obtained from Eq. (2.36). The ranges of spring stiffness for K_2 and K_3 were

$$0.46\,\text{N/mm} \le K_2 \le 1.36\,\text{N/mm} \tag{2.43}$$

$$0.66\,\text{N/mm} \le K_3 \le 3.27\,\text{N/mm} \tag{2.44}$$

The K_1, K_2 and K_3 springs that were available within the stiffness ranges were selected for this design. During the practical implementation of this design, we chose springs with the following stiffness from the catalog [62] of standard springs: K_1 (1.421 N/mm (0.145 kgw/mm)), K_2 (0.49 N/mm (0.05 kgw/mm)) and K_3 (0.69 N/mm (0.07 kgw/mm)). The link lengths r_u and r_f of the upper arm and forearm could be measured based on an anthropometric database. According to the anthropometric resource from the Naval Biodynamics Laboratory [67], Chandler et al. [68], and the institute of occupational safety and health in Taiwan [69], the link

lengths of upper arm and forearm, and the total body weight for small, medium, and large-sized human beings are listed in Table 2.7.

Table 2.7 Anthropometric parameters of the upper limb.

Dimension descriptions	Small	Medium	Large
Upper arm (r_u, mm)	224	255	286
Forearm (r_f, mm)	267	317	368
Total body weight (TBW, kg)	44.3	62.1	79.9

The spring design parameters of the exoskeleton were functions of the lengths of the upper arm and forearm and of the mass properties of the links. Using the values for m_u, m_f, r_u, r_f, K_1, K_2, and K_3, together with the link parameters, we calculated the range of spring-adjustable points, and these are listed in Table 2.8.

Table 2.8 Detailed spring design parameters for the exoskeleton.

Movements	Spring design parameters (mm) (Resistance:1 kg - 5 kg)			
	Spring adjustments	Small	Medium	Large
Shoulder abd-add	l_{CA1}	1-150	1-150	1-150
	l_{PB1}	155	155	155
Shoulder flx-ext	l_{SA2}	7-90	7-90	7-90
	l_{EB2}	267	317	368
	l_{SA3}	8	8	8
	l_{EB3}	0	0	0
Elbow flx-ext	l_{SA2}	0	0	0
	l_{EB2}	210	210	210
	l_{SA3}	11-160	11-160	11-160
	l_{EB3}	150	150	150
All exercises	l_{CP}	9	9	9

In the embodiment design for the device, the arrangement of three revolute joints for the 3-DOF shoulder joint is illustrated in Fig. 2.6(a). The revolute joints for Axes z_0, z_1, and z_2 were achieved using thrust bearings to decrease clearance defects. The elbow joint was accommodated using a revolute joint and selective connection positions for small, medium, and large-sized human beings to adjust the length of the upper limb for different subjects. Thrust bearings were used to achieve elbow flexion-extension motion. The length of the forearm link was also adjusted using a linear slide so that the device would fit different individuals. The CAD drawing is shown in Fig. 2.6 (b).

In this design, a standard spring with a wire and pulley construction was used to emulate a zero-free-length spring. The zero-free-length Spring K_1 was attached to Point *A1* on Link 1, and Point *A1* was attached to Link 2. An embodiment design of Spring K_1 was illustrated in Fig. 2.6 (c), and the standard Spring K_1 was fixed using a pin and connected Point *B1* and Point *A1* with wire and pulleys. The distance of Point *B1* to *A1* was not limited to the free length of the spring. The arrangements for the K_2 and K_3 springs were the same as for Spring K_1 and are shown in Fig. 2.6 (d). To increase the intensity of the exercise, the installation in Link 2 could be adjusted using three lead screws. The possibility of interference between the links and springs during exercise was carefully considered and eliminated during 3D CAD

drawing.

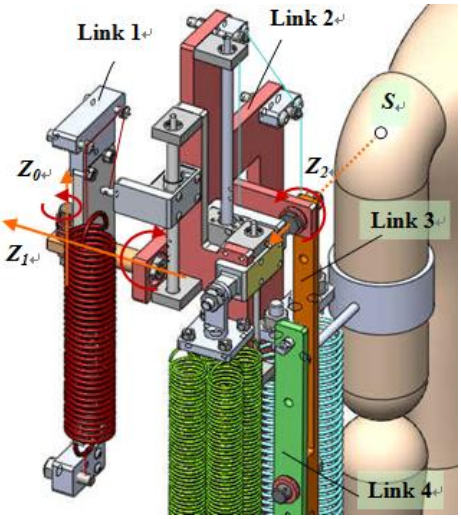

(a) The arrangement of the shoulder joint

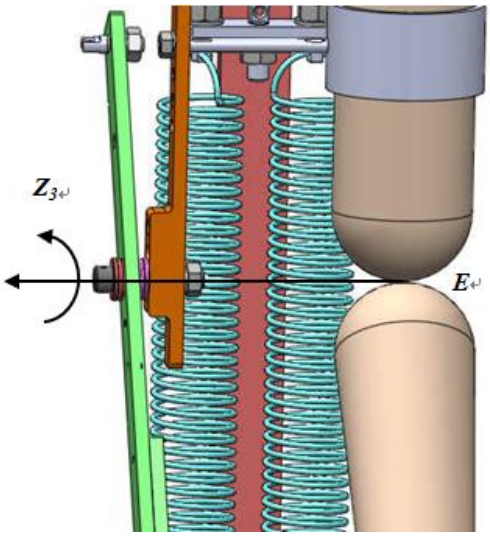

(b) The arrangement of the elbow joint

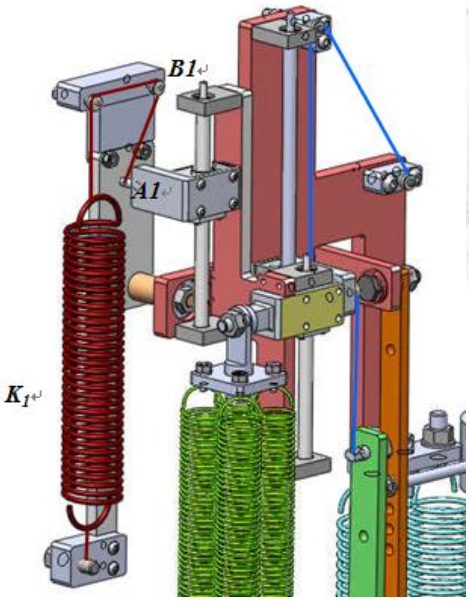

(c) The arrangement of Spring K_1

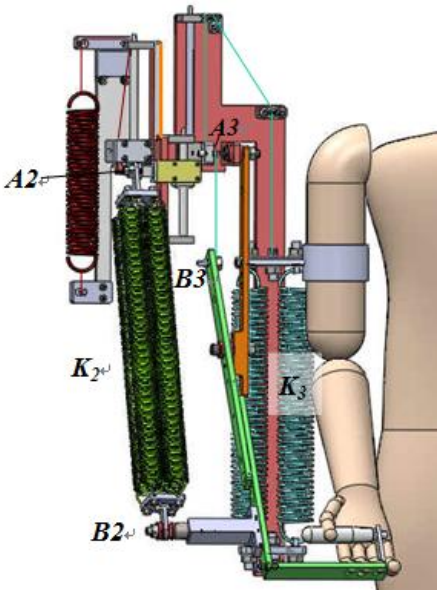

(d) The arrangement of Springs K_2 and K_3

Fig. 2.6 Embodiment design of the upper limb exoskeleton.

2.5 Summary

Several methods have been proposed for upper limb muscle training using exercise devices or machines to strengthen the muscle groups. However, most exercises control the direction of resistance to isolate specific muscle groups that need to be trained. A compact and cost-effective upper limb exoskeleton design with a 3-DOF shoulder joint and a 1-DOF elbow joint allows a patient or a healthy individual to move the limb in different planes and increases resistance through adjustments of the spring length to train more muscle groups. The exoskeleton springs were designed to equalize the joint torques for the shoulder and elbow joints with the joint torques obtained from free-weight exercises. A linear relationship was determined between the weight of the external load and the attached spring. Instead of changing the weight during the resistance exercise, the resistant force was provided by spring elements with moveable attachment points that could be adjusted to increase the intensity of muscular exercise. The upper limb exoskeleton was used to perform shoulder abd-add, flx-ext, and elbow flx-ext exercises, and the torques of the shoulder and elbow joints with the exoskeleton were expected to be equal to the objective joint torques obtained from models of free-weight exercises.

Chapter 3
Dynamic analysis

3.1 Introduction

Resistance training is a common activity for young adults, athletes, and body builders, who are healthy enough to improve muscular strength, size, athletic performance, and overall physical conditioning. It is also an effective method for developing musculoskeletal strength and is recommended by many major health organizations, such as the ACSM and the AHA [9, 11]. In fact, resistance exercise has grown in popularity for many groups, including adolescents, healthy adults, the elderly, and clinical populations. Incorporating individualized, progressive resistance training programs can reduce risk factors associated with cardiopulmonary, musculoskeletal, neuromuscular, and gerontology diseases. However, there are concerns about the negative effects and the safety of resistance exercise as a form of physical therapy when using resistance equipment or free weights [70, 71].

Free weights (e.g., barbells, dumbbells, and weighted balls) and weight machines are the most familiar forms of resistance tools for muscle training. The user's needs or patient's disability level influences the type of resistance tool

chosen. Weight machines have been considered to be safer to use and easier to manipulate, while free weights are more difficult to master and are more likely to cause injuries. New data suggest that sprains/strains account for approximately 46% of injuries, 90% of which are caused by free weights. Muscle strain typically results from overloading a passive muscle (i.e., placing too much stress on the engaged muscle fibers) or dynamically overloading an active muscle, either in concentric or eccentric action; nonurgent muscular strains and ligamentous sprains account for 46%-60% of all acute injuries in strength training. Repetitive overloading of tendons may lead to tendonitis, and although the mechanisms of muscle cramps are not fully understood, most cramps occur in a shortened muscle and are characterized by abnormal electrical activity [72-74]. Machines help stabilize the body, limit the movement around specific joints that are involved in synergy, and focus the activation to a specific set of prime movers. Conversely, free weights create a pattern of intra- and intermuscular coordination that mimics the movements of specific tasks [9].

In Chapter 2, we describe an at-home spring-loaded upper limb resistance training exoskeleton design. This exoskeleton features a 3-DOF shoulder joint and a 1-DOF elbow joint that are optimally arranged to mimic the natural upper limb movement of the GH joint: horizontal flx-ext, abd-add, flx-ext, and elbow joint

flx-ext, allowing the limb to move using single and multiple joints in different planes. Instead of increasing the external weights stepwise in free-weight exercises, this device uses zero-free-length springs, i.e., linear extension springs, in which the force is proportional to the length of the spring rather than to its elongation, allowing the resistance training exoskeleton to theoretically increase the resistance continuously by adjusting the spring length. Gradually changing the resistance allows for progressive training of more muscle groups and reduces the potential risk of injury to the upper limb skeletal muscle and joint caused by a large moment of inertia. However, only a kinematic model and the derived design constraints have been established. When designing exercise devices or rehabilitation aids, using an analytical and dynamic model of human movement helps identify the key forces, movements, and movement patterns that should be measured. This movement model provides a foundation that can serve as the basis for an experimental approach and that can be used to evaluate the efficacy of the initial experimental data. The equations of motion not only provide a critical understanding of the forces experienced by a joint and an effective model of normal joint function and injury mechanics, but they also provide an initial, theoretical understanding of the actual biodynamic system and can help determine the important dynamic properties that should be measured experimentally [75-77]. Many methods have been used to

derive the dynamic equations of motion that describe the dynamic behavior of the upper limb, such as the Lagrange-Euler method [78-79], the Newton-Euler method [80-81], the generalized D'Alembert principle [82-83], and Kane's method [84-85]. The most widely used methods for formulating the motion equations of multibody dynamic systems are based on the Lagrange-Euler and Newton-Euler methods.

Quantitative motion analyses of the upper limb have drawn significant attention in the past 20 years. This interest has been motivated by different goals. The availability and improvement in commercial human movement detection and tracking systems have enabled upper limb tracking [86-92]. Schmidt et al. [93] proposed a measurement procedure to obtain accurate joint rotation of the free wrist and elbow movement by tracking three non-collinear surface markers on each limb segment. Biryukova et al. [94] developed a method for reconstructing the kinematics of a human upper limb—consisting of the upper arm, forearm, and hand—based on the recordings of a spatial tracking system. Prokopenko et al. [95] further assessed the accuracy of the arm kinematics model proposed by Biryukova et al. for describing voluntary movement. Hingtgen et al. [96] suggested a 3-DOF shoulder joint and a 2-DOF elbow joint upper extremity kinematic model and demonstrated the effectiveness of the model by employing a Vicon motion analysis system [97] to quantify the differences between the affected and unaffected upper

extremity motion patterns in eight stroke patients. Conversely, Romilly et al. [98] attempted to assess the necessary user requirements and to determine the optimal configuration of a powered upper limb orthotic prior to prototype construction, whereas most previous studies paid more attention to the range of motion, joint angles, angular velocity/acceleration, error estimation, and the soft tissue artifacts. Most of the differences were compared between normal and impaired subjects. We conducted our experiments by measuring the shoulder and elbow joint torques during designated movements (free-weight exercise: lateral raise, front raise, and elbow curl motion; upper limb exoskeleton: shoulder abd-add, flx-ext, and elbow flx-ext) and compared them to the movements with free weights using an exoskeleton.

The objectives of this research were to develop a dynamic model to determine the required additional design constraints and the optimal configuration of a spring-loaded upper limb exoskeleton. It was hypothesized that with zero-free-length springs the spring-loaded upper limb exoskeleton was capable of reducing unfavorable lengthening of the muscles during high-intensity free-weight exercises. The motion analysis system was employed to investigate the upper limb kinematics in the given motions, which enables us to calculate kinetics and kinematics parameters during the designated movements performed with dumbbell

and with upper limb exoskeleton. Additionally, we developed proper evaluation procedures to ensure continuous and effective data collection from a larger sample of the population in the ongoing verification studies.

3.2 Dynamic model of upper limb

The Lagrange approach was used in this study to derive the equations of motion for the spring-loaded upper limb exoskeleton because it uses fewer parameters to describe a given system and to determine that these motions were mechanically analogous to the free-weight exercises.

Figure 3.1 shows the motion of an upper arm and forearm system. The upper arm segment is pictured from the GH joint *S* to the elbow joint *E*, whereas the forearm segment extends from the elbow joint *E* to the middle of the palm of the hand *H*. Several potential limitations of this study should be noted. First, the hand was assumed to be a rigid segment in the extension of the forearm, which means that wrist motion was not included in our study. The hand is usually held in a neutral position during forearm movements. Therefore, the gravitational variation due to the wrist motion is negligible, and the upper limb can be modeled as a two-link linkage. Second, this model assumes that the length of each segment remains constant, that each segment or link has a fixed mass that is concentrated at its center of mass, and that the location of each center of mass remains fixed during

the movement. Third, the joints in the model are considered to be frictionless revolute joints. Fourth, the mass moment of inertia of each segment is constant during the movement. Finally, the geometries of the upper arm and the forearm were assumed to be axially symmetric. The segmental lengths of the upper arm and the forearm are denoted as r_u and r_f, respectively. The variable g denotes the gravitational force; points G_u, G_f, and G_F identify the center of gravity of the upper arm, forearm segment, and external load, respectively; and m_{u}, m_{f}, and F_{h} denote the mass of the upper arm, forearm segment, and external load, respectively. The mass of the human hand was ignored because it is relatively light compared to the overall mass of the upper limb. The segments were connected as a revolute joint and had three axes of rotation in the shoulder joint, including the shoulder's horizontal flx-ext, abd-add, and flx-ext, and one axis of rotation in the elbow, which provided only elbow flx-ext. An orthogonal coordinate system defined by $\boldsymbol{s_1}, \boldsymbol{s_2}$, and $\boldsymbol{s_3}$ was fixed at point S and was allowed to rotate about the $\boldsymbol{s_3}$ axis so that the unit vector $\boldsymbol{s_1}$ always lies on segment SE. An orthogonal coordinate system defined by $\boldsymbol{e_1}$, $\boldsymbol{e_2}$, and $\boldsymbol{e_3}$ was defined at point E and was allowed to rotate about the $\boldsymbol{e_3}$ axis so that the unit vector $\boldsymbol{e_1}$ always lies on segment EH. θ_u and θ_f are the angles between the segment and the vertical axis (Fig. 3.1).

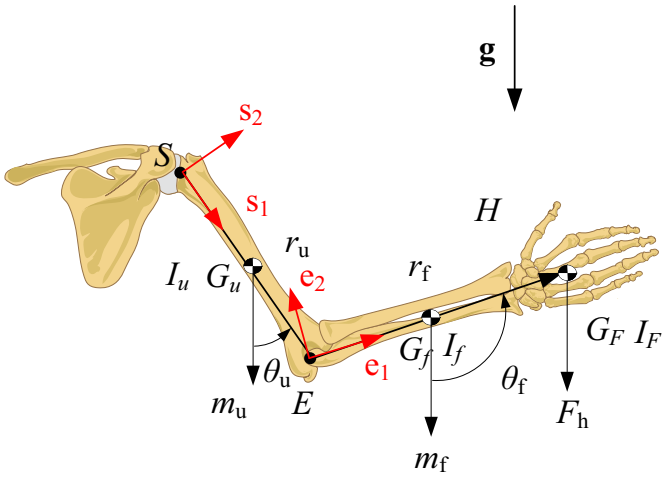

Fig. 3.1 The dynamic model and the coordinate system of the right upper limb

A system with n degrees of freedom has n generalized coordinates, denoted as q_i, where i has values from 1 to n. A generalized nonconservative force corresponding to a specific generalized coordinate is represented by Q_i and the derivative of q_i with respect to time is represented as $\dot{q}_i$. Equation (3.1) shows the general form of Lagrange's equation:

$$\frac{d}{dt}\left(\frac{\partial L}{\partial \dot{q}_i}\right) - \frac{\partial L}{\partial q_i} = Q_i \qquad i = 1, 2, \ldots n \tag{3.1}$$

The Lagrangian L is defined as the difference between the total kinetic energy T and the total potential energy V:

$$\mathrm{L} = \mathrm{T} - \mathrm{V} \tag{3.2}$$

3.3 Dynamic joint torques during free-weight exercise

The total kinetic energy T of the upper limb can be determined by summing the upper arm kinetic energy Tu, the forearm kinetic energy $T_{f,}$ and the applied load T_F, while the total potential energy *V* can be determined by summing the upper arm potential energy *V*u, the forearm potential energy V_f, and the applied load potential energy V_F. The equations of motion are then obtained by applying Lagrange's equation (3.1) and using the two generalized coordinates for the two-segment system, $q_1 = \theta_u$ and $q_2 = \theta_f$.

For the first generalized coordinate, $q_1 = \theta_u$, the equation of motion is determined to be

$$\tilde{\tau}_u = \left[I_{u,S3} + \left(m_u\zeta^2 + m_f + F_h\right)r_u^2\right]\ddot{\theta}_u + \left(m_f\xi + F_h\right)r_u r_f\ddot{\theta}_f cos\left(\theta_f - \theta_u\right)$$
$$-\left(m_f\xi + F_h\right)r_u r_f\dot{\theta}_f^2 sin\left(\theta_f - \theta_u\right) + \left(m_u\zeta r_u + m_f r_u + F_h r_u\right)gsin\theta_u \qquad (3.3)$$

For the second generalized coordinate, $q_2 = \theta_f$, the equation of motion is determined to be

$$\tilde{\tau}_f = \left[I_{f,e3} + I_{F,e3} + \left(m_f\xi^2 + F_h\right)r_f^2\right]\ddot{\theta}_f + \left(m_f\xi + F_h\right)r_u r_f\ddot{\theta}_u cos\left(\theta_f - \theta_u\right)$$
$$+\left(m_f\xi + F_h\right)r_u r_f\dot{\theta}_u^2 sin\left(\theta_f - \theta_u\right) + \left(m_f\xi r_f + F_h r_f\right)gsin\theta_f \qquad (3.4)$$

where τ_u is the moment at the upper arm and τ_f is the moment at the forearm. The first derivatives of θ_u and θ_f with respect to time are represented as $\dot{\theta}_u$ and

$\dot{\theta}_f$. The second derivatives of θ_u and θ_f with respect to time are represented as $\ddot{\theta}_u$ and $\ddot{\theta}_f$, where $I_{u,s3}$ is the $\mathbf{s_3}$ component for the mass moment of inertia about point G_u in the $\mathbf{s_1}$, $\mathbf{s_2}$, and $\mathbf{s_3}$ coordinate system. $I_{f,e3}$ and $I_{F,e3}$ are the $\mathbf{e_3}$ components for the mass moment of inertia about points G_f and G_F in the $\mathbf{e_1}$, $\mathbf{e_2}$, and $\mathbf{e_3}$ frame of reference, respectively. The variables ζ and ξ are the ratios of the longitudinal position of the center of mass for the upper arm and the forearm segments, respectively, and they are defined as percentages of the upper arm and the forearm segments length. The ratios were 0.5772 and 0.4574 for the male subject and 0.5754 and 0.4559 for the female subject [99]. ζr_u gives the length from the mass center of the upper arm to the shoulder joint; ξr_f represents the approximate length from the mass center of the forearm to the elbow joint.

3.4 Dynamic joint torques with the upper limb exoskeleton

Fig. 3-2 illustrates a spring-loaded upper limb exoskeleton. The exoskeleton is assumed to be well aligned with the upper arm and has the same motion along with the upper arm.

Therefore, the angular displacement of link 3 is determined to be the same as the upper arm, that is, θ_u equals θ_2 for the shoulder abd-add and θ_u equals θ_3 for the shoulder flx-ext. The angular displacement of link 4 is determined to be the

same as the forearm, that is, θ_f equals θ_4 for the elbow flx-ext. Link 1 remains in its position during the exoskeleton movements.

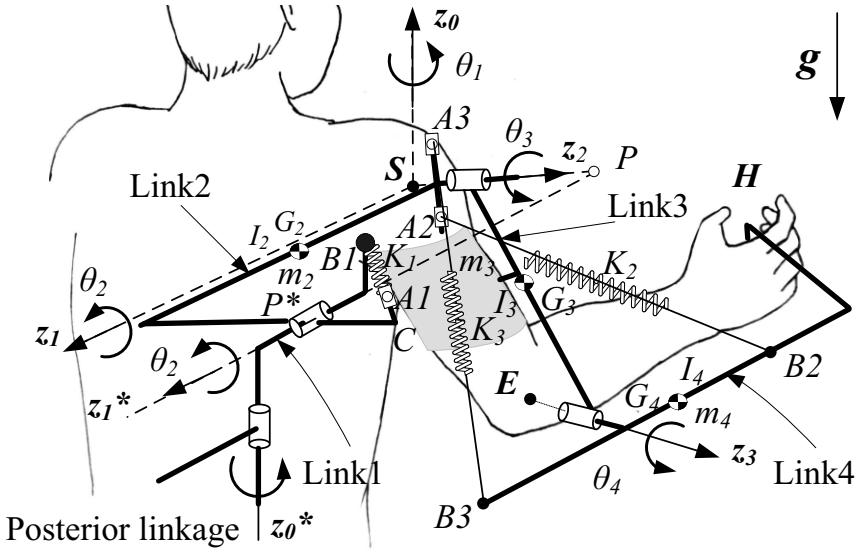

Fig. 3.2 A schematic diagram of the spring-loaded exoskeleton

The total kinetic energy of the upper limb exoskeleton can be determined by summing the upper arm kinetic energy T_u, the forearm kinetic energy T_f, the link 2 kinetic energy T_{L2}, the link 3 kinetic energy T_{L3}, and the link 4 kinetic energy T_{L4}. The total potential energy of the upper limb exoskeleton can be determined by summing the upper arm potential energy V_u, the forearm potential energy V_f, the link 2 potential energy V_{L2}, the link 3 potential energy V_{L3}, the link 4 potential energy V_{L4}, the K_1 spring potential energy V_{S1}, the K_2 spring potential energy V_{S2}, and the K_3 spring potential energy V_{S3}.

The equations of motion are then obtained by applying Lagrange's equation

(3.1) and (3.2) and by using the two generalized coordinates of the two-segment system, $q_1 = \theta_u$ and $q_2 = \theta_f$.

For the first generalized coordinate, $q_1 = \theta_u$, the equations of motion for the spring-loaded upper limb exoskeleton are determined as follows:

$$\widetilde{M}_u$$

$$= \left[I_{u,S3} + I_{G2,S3} + I_{G3,S3} + \left(m_u\zeta^2 + m_f\right)r_u^2\right.$$

$$\left. + \left(m_2 l_{2,G2/S}^2 + {}^1/_4\, m_3 l_3^2 + \ m_4 l_3^2\right)\right]\ddot{\theta}_u$$

$$+\left(m_f \xi r_u r_f + {}^1/_2\, m_4 l_3 l_4\right)\ddot{\theta}_f cos\left(\theta_f - \theta_u\right)$$

$$-\left(m_f \xi r_u r_f + \ {}^1/_2\, m_4 l_3 l_4\right)\dot{\theta}_f^2 sin\left(\theta_f - \theta_u\right)$$

$$+\left(m_u\zeta r_u + m_f r_f + m_2 l_{2,G2/S}^2 + {}^1/_2\, m_3 l_3 + m_4 l_3\right)\mathrm{g}sin\theta_u$$

$$-K_1 l_{PB1}(l_{CA1} cos\theta_u - l_{CP} sin\theta_u) + \ (K_2 l_{SA2} - K_3 l_{SA3}) r_u sin\theta_u$$

$$+(K_2 l_{EB2} l_{SA2} + K_3 l_{EB3} l_{SA3}) sin\left(\theta_u + \theta_f\right) \quad (3.5)$$

For the second generalized coordinate, $q_2 = \theta_f$, the equation of motion is determined as follows:

$$\widetilde{M}_f = \ \left[I_{f,e3} + I_{G4,e3} + m_f \xi^2 r_f^2 + {}^1/_4\, m_4 l_4^2\right]\ddot{\theta}_f$$

$$+ \left(m_f \xi r_u r_f + {}^1/_2\, m_4 l_3 l_4\right)\ddot{\theta}_u cos\left(\theta_f - \theta_u\right)$$

$$+\left[m_f \xi r_u r_f + {}^1/_2\, m_4 l_3 l_4\right]\dot{\theta}_u^2 sin\left(\theta_f - \theta_u\right) + \left(m_f \xi r_f + {}^1/_2\, m_4 l_4\right)\mathrm{g}sin\theta_f$$

$$-(K_2 l_{EB2} - K_3 l_{EB3}) r_u sin\theta_f + (K_2 l_{EB2} l_{SA2} + K_3 l_{EB3} l_{SA3}) sin\left(\theta_u + \theta_f\right) \quad (3.6)$$

where $\widetilde{M}_u$ is the moment at the upper arm (with the exoskeleton) and $\widetilde{M}_f$ is the moment at the forearm (with the exoskeleton). $I_{G2,S3}$, $I_{G3,S3}$, and $I_{G4,e3}$ are the $\mathbf{s_3}$ and $\mathbf{e_3}$ components of the mass moment of inertia about the center of mass for link 2 (point G_2) and for link 3 (point G_3) in $\mathbf{s_1}$, $\mathbf{s_2}$, and $\mathbf{s_3}$, and the center of mass for link 4 (point G_4) in the $\mathbf{e_1}$, $\mathbf{e_2}$, and $\mathbf{e_3}$ frame of reference. The variables m_2, m_3, and m_4 denote the mass of link 2, link 3, and link 4, respectively, and were assumed to be fixed and located on the center lines with respect to link 2, link 3, and link 4. $l_{2,G2/S}$ is the link length between point G_2 and shoulder joint of link 2. l_3, and l_4 represent the link lengths between two joints.

3.5 Dynamic joint torques during resistance training

3.5.1 Shoulder abd-add

A lateral raise was used as an example of the shoulder abd-add resistance exercise used to strengthen the deltoid, latissimus dorsi, pectoralis major, supraspinatus, and trapezius muscles. In the dynamic model, the angle $\theta_f = \theta_u$. Thus, the upper arm and forearm can be considered a single link; the mass moments of inertia $I_{u,S3}, I_{f,e3}$, and $I_{F,e3}$ should be replaced by $I_{u/S,S3}, I_{f/S,S3}$, and $I_{F/S,S3}$, which are the mass moments of inertia for the upper arm, forearm, and external load with respect to the shoulder joint and are determined using the parallel axis theorem. Finally, the rotation about axis z_1^* applies to θ_2 alone, and the shoulder

joint torque for θ_2 is expressed as

$$\tilde{\tau}_{2,lr}$$
$$= \left[I_{u/S,S3} + I_{f/S,S3} + I_{F/S,S3} + \left(m_u\zeta^2 + m_f + F_h\right)r_u^2 + \left(m_f\xi^2 + F_h\right)r_f^2\right.$$
$$\left. + 2\left(m_f\xi + F_h\right)r_u r_f\right]\ddot{\theta}_u$$
$$-\left(m_u\zeta r_u + m_f r_u + F_h r_u + m_f\xi r_f + F_h r_f\right)\mathrm{g}sin\theta_u \quad (3.7)$$

The joint torques for the shoulder using the exoskeleton are obtained by substituting the same angles for the lateral raising motion into Eqs. (3.5) and (3.6). The mass moments of inertia of links 2, 3, and 4—$I_{G2,S3}$, $I_{G3,S3}$, and $I_{G4,e3}$—should be replaced by the mass moments of inertia with respect to the shoulder joint—$I_{G2/S,S3}$, $I_{G3/S,S3}$, and $I_{G4/S,S3}$—using the parallel axis theorem. The potential energy of the spring depends on the movement taken because different springs are actuated depending on the movement. Only spring K_1 is actuated in the shoulder abd-add movement. The joint torque of the shoulder with the exoskeleton can be expressed as

$$\widetilde{M}_{2,lr}$$
$$= \left[I_{u/S,S3} + I_{f/S,S3} + I_{G2/S,S3} + I_{G3/S,S3} + I_{G4/S,S3} + \left(m_u\zeta^2 + m_f\right)r_u^2 + m_f\xi^2 r_f^2\right.$$
$$\left. + 2m_f\xi r_u r_f + m_2 l_{2,G2/S}^2 + {}^1/_4\, m_3 l_3^2 + m_4 l_3^2 + {}^1/_4\, m_4 l_4^2 + m_4 l_3 l_4\right]\ddot{\theta}_u$$
$$+\left(m_u\zeta r_u + m_f r_u + m_f\xi r_f + m_2 l_{2,G2/S}^2 + {}^1/_2\, m_3 l_3 + {}^1/_2\, m_4 l_4 + m_4 l_3\right)\mathrm{g}sin\theta_u$$
$$-K_1 l_{PB1}(l_{CA1}cos\theta_u - l_{CP}sin\theta_u) \quad (3.8)$$

3.5.2 Shoulder flx-ext

An example of the shoulder flx-ext resistance exercise is the frontal raise, which strengthens the deltoid, the pectoralis major, the latissimus dorsi, and the trapezius muscles. In the dynamic model, the angle $\theta_f = \theta_u$. The upper arm and forearm are considered to be a single rigid body rotating about the z_2 axis with an angle θ_3. Therefore, the mass moments of inertia $I_{u,S3}$, $I_{f,e3}$, and $I_{F,e3}$ should be replaced by $I_{u/S,S3}$, $I_{f/S,S3}$, $and\ I_{F/S,S3}$, which are the mass moment of inertia for the upper arm, forearm, and external load with respect to the shoulder joint using the parallel axis theorem. The joint torque for θ_3 can be expressed as

$$\tilde{\tau}_{3,fr}$$
$$= \left[I_{u/S,S3} + I_{f/S,S3} + I_{F/S,S3} + \left(m_u\zeta^2 + m_f + F_h\right)r_u^2 + \left(m_f\xi^2 + F_h\right)r_f^2\right.$$
$$\left. + 2\left(m_f\xi + F_h\right)r_u r_f\right]\ddot{\theta}_u$$
$$-\left(m_u\zeta r_u + m_f r_u + F_h r_u + m_f\xi r_f + F_h r_f\right)\mathrm{g}sin\theta_u \quad (3.9)$$

In the frontal raise, the shoulder and elbow joints generate torque. For the shoulder flx-ext exercise using the upper limb exoskeleton, a user would use the same movement as the free-weight frontal raise motion, and the mass moments of inertia of link 3 and link 4, $I_{G3,S3}$, $and\ I_{G4,e3}$, would be replaced by the mass moments of inertia with respect to the shoulder joint, $I_{G3/S,S3}\ and\ I_{G4/S,S3}$, by using the parallel axis theorem. Link 1 and link 2 are not involved in this motion. The

joint torque of the shoulder with the exoskeleton can be expressed as

$$\widetilde{M}_{3,fr}$$

$$= \left[I_{u/S,S3} + I_{f/S,S3} + I_{G3/S,S3} + I_{G4/S,S3} + \left(m_u\zeta^2 + m_f\right)r_u^2 + m_f\xi^2 r_f^2\right.$$

$$\left. + 2m_f\xi r_u r_f + {}^1\!/_4\, m_3 l_3^2 + m_4 l_3^2 + {}^1\!/_4\, m_4 l_4^2 + m_4 l_3 l_4\right]\ddot{\theta}_u$$

$$+\left(m_u\zeta r_u + m_f r_u + m_f\xi r_f + {}^1\!/_2\, m_3 l_3 + m_4 l_3 + {}^1\!/_2\, m_4 l_4\right)\mathrm{g}sin\theta_u$$

$$+(K_2 l_{SA2} - K_3 l_{SA3})r_u sin\theta_u - (K_2 l_{EB2} - K_3 l_{EB3})r_u sin\theta_u$$

$$+2(K_2 l_{EB2} l_{SA2} + K_3 l_{EB3} l_{SA3})sin2\theta_u \qquad (3.10)$$

3.5.3 Elbow flx-ext

An example of the elbow flx-ext resistance exercise is the dumbbell curl motion, which is used to strengthen the biceps brachii, brachialis, and brachioradialis muscles. In the dynamic model, by using an angle θ_u equal to 0 degrees, Eq. (3.4) yields the moment at the elbow. $I_{f,e3}$ and $I_{F,e3}$ should be replaced by the the mass moments of inertia with respect to the elbow joint, $I_{f/E,e3}$ and $I_{F/E,e3}$. The forearm rotates about the $\boldsymbol{e}_3$ axis with θ_f, and the elbow joint torque can be expressed as

$$\tilde{\tau}_{4,dc} = \left[I_{f/E,e3} + I_{F/E,e3} + \left(m_f\xi^2 + F_h\right)r_f^2\right]\ddot{\theta}_f + \left(m_f\xi r_f + F_h r_f\right)\mathrm{g}sin\theta_f \qquad (3.11)$$

To train the upper limb exoskeleton for the elbow flx-ext exercise, we assume

the angle θ_u equals 0 degrees, and Eq. (3.6) yields the moment at the elbow for the upper limb exoskeleton. $I_{f,e3}$ and $I_{G4,e3}$ should be replaced by the the mass moments of inertia with respect to the elbow joint, $I_{f/E,e3}$ and $I_{G4/E,e3}$. The joint torque of the elbow with the exoskeleton can be expressed as

$$\begin{aligned}\widetilde{M}_{4,dc} = &\left[I_{f/E,e3} + I_{G4/E,e3} + m_f\xi^2 r_f^2 + {}^1\!/_4\, m_4 l_4^2\right]\ddot{\theta}_f \\ &+\left(m_f\xi r_f + {}^1\!/_2\, m_4 l_4\right)\mathrm{g}sin\theta_f \; - (K_2 l_{EB2} - K_3 l_{EB3}) r_u sin\theta_f \\ &+(K_2 l_{EB2} l_{SA2} + K_3 l_{EB3} l_{SA3}) sin\theta_f \end{aligned} \quad (3.12)$$

3.6 Summary

Resistance training has been shown to be effective for developing musculoskeletal strength and is recommended by many major health organizations. Resistance training equipment design relies heavily on the analysis of human movement. Dynamic models of human movement help researchers identify key forces, movements, and movement patterns that should be measured. An at-home resistance training upper limb exoskeleton has been designed with a three DOF shoulder joint and a one DOF elbow joint to allow movement of the upper limb at single and multiple joints in different planes. The exoskeleton can continuously increase the resistance as the spring length changes to train more muscle groups and to reduce the potential risk of muscle injury to the upper limb by free weights and

training equipment. The objectives of this chapter were to develop a dynamic model of the spring-loaded upper limb exoskeleton and additional design constrains are proposed. The dynamic model suggests that the mass moment of inertia of the linkages should conform to certain constrains. For shoulder abd-add, by comparing the coefficient of the angular acceleration $\ddot{\theta}_u$ in Eqs (3.7) and (3.8) and incorporating the kinematic design constrains obtained in chapter 2, the inequality equation $I_{G2/S,S3} + I_{G3/S,S3} + I_{G4/S,S3} + m_2 l_{2,G2/S}^2 + {}^1/_4 m_3 l_3^2 + m_4 l_3^2 + {}^1/_4 m_4 l_4^2 + m_4 l_3 l_4 < I_{F/S,S3} + F_h(r_u + r_f)^2$ should be maintained to ensure that less dynamic joint torque is created by the exoskeleton movement compared with the free-weight exercise. By applying the same procedures, the inequality equations for shoulder flx-ext and elbow flx-ext can be obtained as additional design constraints for the exoskeleton design.

Chapter 4
Prototype and preliminary evaluation

4.1 The prototype

A prototype of spring-loaded upper limb exoskeleton mechanism based on the modified embodiment design described in section 2.4, which was built to evaluate the function and performance of resistance training, is shown in Fig. 4.1(a).

In this prototype, the arrangement of three revolute joints for the 3-DOF shoulder joint is illustrated in Fig. 4.1(b). The revolute joints for axes z_0, z_1, and z_2 are constructed using thrust bearings to decrease the defects of clearance. The elbow joint is accommodated through a revolute joint, which includes selective connection positions for small-, medium-, and large-sized human beings to adjust the length of the upper limb. Thrust bearings are used to achieve the elbow flexion-extension motion. The length of the forearm link can also be adjusted using selective connection positions such that the device would fit different individuals, as shown in Fig. 4.1(a).

In this design, a standard spring with a wire and pulley construction is used to emulate a zero-free-length spring. The zero-free-length spring K_1 is attached to point *B1* on link 1, and point *A1* is attached to link 2, as shown in Fig. 4.1(b). The

standard spring K_1 is fixed by a pin and connected to points *B1* and *A1* with wire and pulleys. The distance from point *B1* to *A1* is not limited to the free length of the spring. The arrangement for springs K_2 and K_3 is the same as that for spring K_1, as is shown in Fig. 4.1(a). To increase the intensity of the exercise, the spring connection locations *A1*, *A2*, and *A3*, which are separately integrated with nuts on the ball screws installed at link 2 could be adjusted using three ball screws.

The resistance in the prototype design is generated by adjusting the connecting locations (*A1*, *A2*, and *A3*) of the springs rather than changing the stiffness of the springs. This design was expected to provide low to moderate resistance to stimulate the strength of muscle recovery in patients with a variety of pathological conditions, including musculoskeletal injuries, osteoporosis, hypertension, and some chronic diseases [71]; the design was also aimed to provide more intense strength training for healthy individuals. In this study, the maximum resistant force is designed to be 49 N (corresponding to a 5-kg weight dumbbell). Therefore, it is important to choose springs with a suitable stiffness. In this prototype, l_{EB3} is designed to be 150 mm. The spring-adjustable points are limited from 1 mm to 160 mm. The adjustable lengths of l_{CA1}, l_{SA2}, and l_{SA3} of springs K_1, K_2, and K_3 are designed to be attached to link 2, which is a reasonable and convenient location at which to adjust the exoskeleton mechanism. The length of l_{B1P*} was designed to be

155 mm and conformed to the limitations of the adjustable range. Considering the limitations and the mass properties of the linkages, along with the anthropometric parameters of humans and the practical implementation of this design, we choose the springs with the following stiffnesses from a catalog [62] of standard springs: K_1 with 1.421 N/mm (0.145 kgw/mm), K_2 with 0.49 N/mm (0.05 kgw/mm) and K_3 with 0.69 N/mm (0.07 kgw/mm).

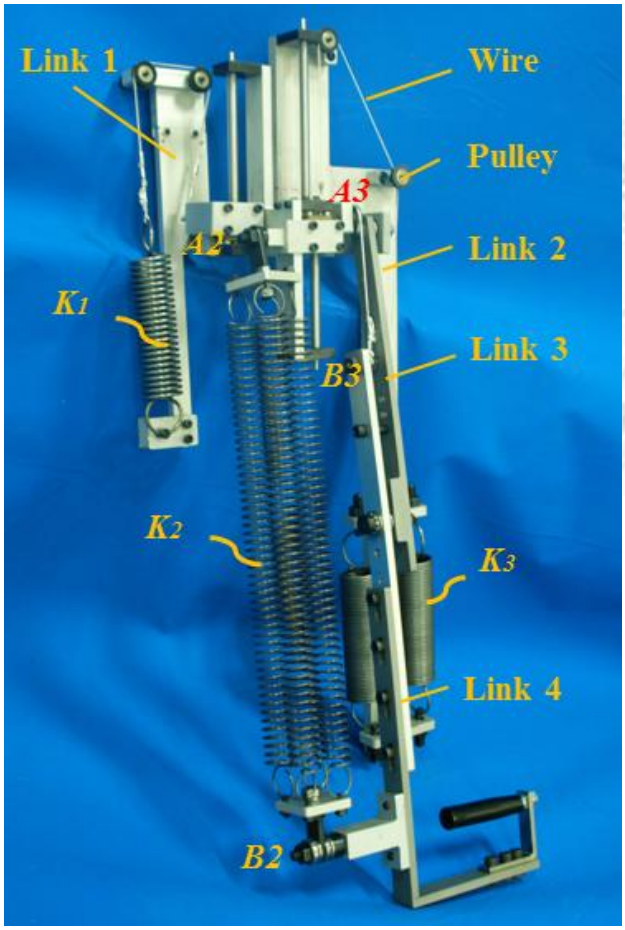

(a) The arrangement of springs K_1, K_2, and K_3

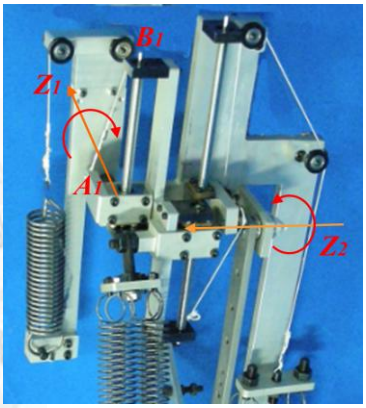

(b) The arrangement of the shoulder joint

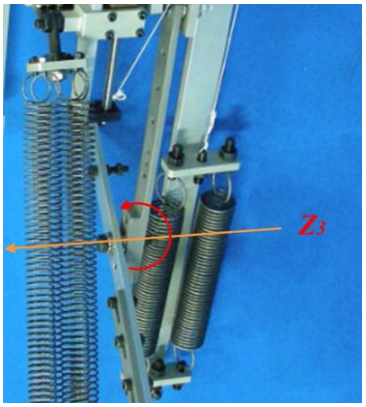

(c) The arrangement of the elbow joint

Fig. 4.1 The prototype of the upper limb exoskeleton

4.2 Experimental design

4.2.1 The subjects

One healthy male and one healthy female volunteered to participate in this preliminary evaluation. They self-reported as having no history of neural or musculoskeletal disease. Both subjects signed the informed consent forms, and the experiment was approved by ITRI's ethics committee.

4.2.2 Experimental set-up

The shoulder and elbow motions were recorded with a Vicon MX-F20 motion analysis system (Oxford Metrics Ltd., Oxford, UK), which has a 100 Hz capture rate. This system utilizes eignt synchronized high-speed infrared charge-coupled display (CCD) cameras to track eight reflective markers measuring 14 mm in diameter mounted by double-sided hypoallergenic tape on the subject. The locations of the markers were predetermined bony anatomical landmarks that were on the trunk of the subject and the upper limb of the 7th cervical vertebrae (C7), the clavicle (CLAV), the right shoulder marker (RSHO), the right lateral elbow (RLEL), the right medial elbow (RMEL), the processus styloideus radius (RMWR), the processus styloideus ulna (RLWR), and the metacarpophalangeal joints (MCPs) of the right middle finger (RFIN); these locations were used to define the anatomical coordinate system for each segment to define a set of reference axes that are

anatomical meaningful for the purposes of describing the position and orientation of motion in three-dimensional space, and were chosen for their minimal skin motion, as shown in Fig. 4-2.

(a) Front view (b) Rear view

Fig. 4.2 Marker placement on the thorax, clavicle, and right upper limb

An initial dynamic calibration followed by a static calibration of the motion capture system is performed prior to the experiment. Motion capture software (Vicon Nexus 1.3) is used to digitize the body landmarks. After the markers are properly attached, the subjects are asked to stand in object-space (or the capture volume) for the static calibration. They are then asked to move the shoulder, elbow, and wrist joint to perform the required dynamic calibration. It is necessary to ensure that each marker can be seen by at least two cameras at every instant during data recording. While the subject is performing the selected free-weight exercise and shoulder abd-add, shoulder flx-ext, and elbow flx-ext movement with the spring-loaded upper limb exoskeleton in the object-space in view of the CCD

cameras, the motion analysis system records movements of upper limb segments by tracking the 3D location of the markers.

The test of basic functions consisted of shoulder abd-add, flx-ext, and elbow flx-ext. The Vicon motion data are collected from both the male and female subjects.

The resistant force was set at two different weight levels, 1 kg and 3 kg, for the free-weight exercise. The segmental weights for the upper arms and forearms are based on those given by DeLeva [99], who proposed the body segment parameter data estimation as shown below:

$$m_u = R_u \times (\text{TBW}) \tag{4-1}$$

$$m_f = R_f \times (\text{TBW}) \tag{4-2}$$

Here, R_u and R_f are the ratios of the weights of the upper arm and the forearm segments, respectively, as percentages of the total body weight; the ratios were 0.0271 and 0.0162 for the male subject and 0.0255 and 0.0138 for the female subject. The subjects' anthropometric parameters are listed in Table 4-1.

Table 4.1 Anthropometric parameters of the subjects used in the data analysis

TBW (kg)			Longitudinal length (mm)		Segmental weight (kg)		Sagittal r (%)		Longitudinal r (%)	
M	F	Segment	M	F	M	F	M	F	M	F
77	60	Upper arm	280	263	2.09	1.53	28.5	27.8	15.8	14.8
		Forearm	352	335	1.25	0.63	27.6	26.1	12.1	9.4

TBW: Total body weight; M: Male; F: Female

Based on the anthropometric parameters of the male and female subjects, the exact values of l_{CA1}, l_{SA2}, and l_{SA3} for the 1 kg and 3 kg weight resistances applied to the upper limb exoskeleton are listed in Table 4.2. The resistance was easily changed by adjusting the position of the nut of the leading screw corresponding to the selected exercise to a new position relative to the zero position (i.e., aligned with the z_2 axis); these positions are listed Table 4.2.

Table 4.2 The adjustable spring lengths for the 1 and 3 kg weight resistances.

Subject	Resistance (kg)	Adjustments of springs for muscle strengthening exercises (mm)		
		Shoulder abd-add (l_{CA1})	Shoulder flx-ext (l_{SA2})	Elbow flx-ext (l_{SA3})
Male	1	5	9	15
	3	74	49	82
Female	1	4	10	14
	3	67	50	73

4.2.3 Protocols

Two exercise sessions (free-weight exercise and upper limb exoskeleton motion) are chosen for evaluation. Each session contains three resistance training exercises (shoulder abd-add, flx-ext, and elbow flx-ext) consisting of two sets (1 kg and 3 kg resistance) with 5 repetitions. Each movement is performed in a slow, controlled manner: lifting (1 second) and lowering (1 second) without sudden jerks and acceleration for five consecutive repetitions. The hand grip pattern of the subjects during shoulder abd-add exercise, flx-ext exercise, and elbow flx-ext exercise with exoskeleton is the same as the dumbbell lateral raise motion, the dumbbell frontal raise motion, and the dumbbell curl motion, respectively. The ranges of the movement being evaluated are shown in Fig. 4-.3. The dumbbell weights of 1 kg and 3 kg, as well as the equivalent resistance are set for free-weight exercise and the upper limb exoskeleton motion, respectively. A maximum of five minutes rest was given between each set and exercise.

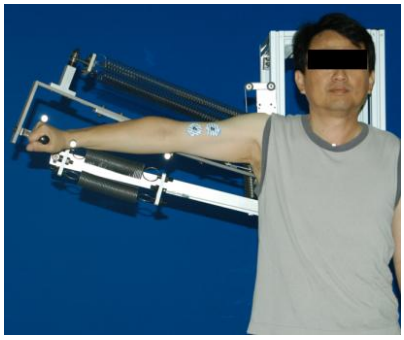

(a) Shoulder abd-add

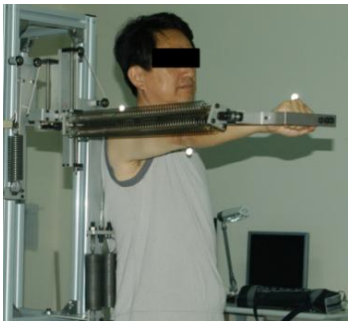

(b) Shoulder flx-ext

(c) Elbow flx-ext

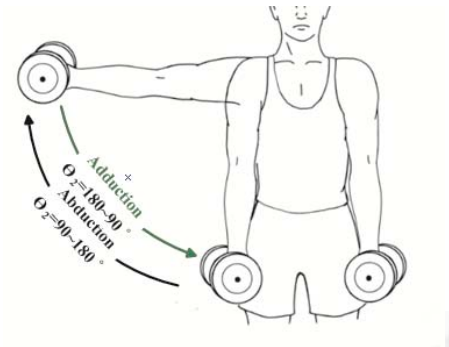

(d) Lateral raise motion

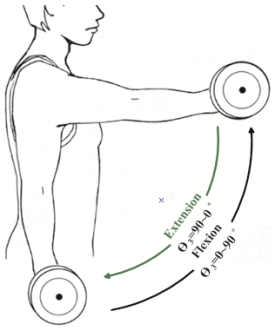

(e) Front raise motion

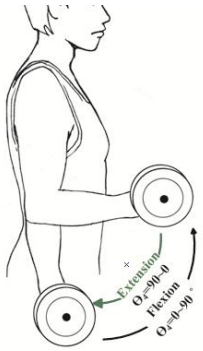

(f) Dumbbell curl motion

Fig. 4.3 Subjects performed the upper limb exoskeleton and dumbbell exercises with different movements for resistance training: (a) shoulder abd-add: the z_1^* axis is aligned with the shoulder joint, gripping the handle of the exoskeleton, and the right arm is raised laterally from the side of the body; (b) shoulder flx-ext: the z_2 axis is aligned with the shoulder joint, and the right arm is raised in a sagittal plane while keeping the elbow in a fixed position; (c) elbow flx-ext: the z_3 axis is aligned with the elbow joint, and the forearm is drawn upward in an arc from a vertical position to a horizontal position and then is moved in the reverse direction. Note that the exoskeleton is mounted on an aluminum frame; (d) dumbbell lateral raise; (e) dumbbell front raise; and (f) dumbbell curl motion and the movement range of each motion.

4.2.4 Data analysis

Detailed upper limb kinematics data are collected. The approach of inverse dynamics is the most common method used to solve for the unknown reaction force and moment. The analysis begins with the most distal segment moving upward

through the kinematic chain, and the requirements of all the external forces acting on the system are known. Joint torques are then calculated by a 3-D generic inverse dynamic method [100]. Motion analysis data from the exercises are acquired with the Vicon Nexus software and post-processed using Matlab (Mathworks Inc., Natick, MA). Analysis of the upper limb kinematics is restricted to the motion of the shoulder and elbow. The first three data points of the five repeated trials will be analyzed to obtain an average of three data results. If one of these three data points is not qualified for the data analysis, the fourth or the fifth data points will be analyzed.

(a) Shoulder abd-add exercise of the upper limb exoskeleton

(b) Shoulder flx-ext exercise of the upper limb exoskeleton

(c) Elbow flx-ext exercise of the upper limb exoskeleton

Fig. 4.4 Subjects operating the upper limb exoskeleton mechanism with difference movements for resistance training.

4.3 Results and discussion

Fig. 4.5 shows the comparisons between the joint torques of free-weight exercise and the resistance exercise using the upper limb exoskeleton (velocity and inertia were neglected). In Figs. 4.5 (a) - (d), the peak joint torques are at 180 degrees for the shoulder abd-add exercise and 90 degrees for the flx-ext exercise. The joints would generate higher torques when the upper limb straightens in the horizontal position, which is the point at which the moment arm is the furthest away from the resistant force while being perpendicular to the joint. Such an explanation can be applied to the elbow flexion-extension exercise, as shown in Figs. 4.5 (e) and (f). The peak torques of the exercise and their differences are listed in Table 4.3.

Fig. 4.6 shows the comparisons between the joint torques of free-weight exercises and the resistance exercises using the upper limb exoskeleton mechanism when considering the velocity and the effect of inertia. Generally speaking, dumbbell exercises generate a higher moment of inertia in the shoulder joint except when 1 kg of resistance is used for the dumbbell exercise and when 1 kg of resistance is used on the exoskeleton, as shown in Figs. 4.6(a) and (b). After we

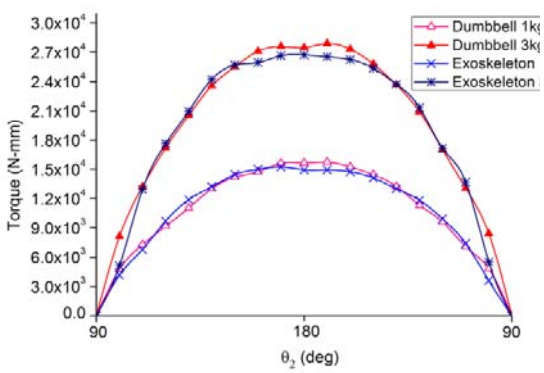

(a) Shoulder abd-add exercise (male)

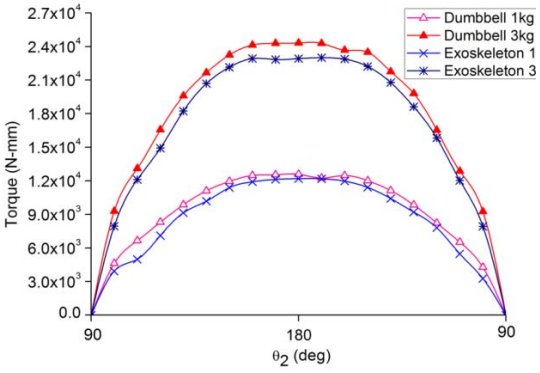

(b) Shoulder abd-add exercise (female)

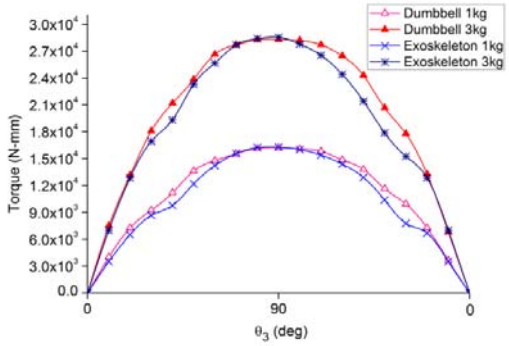

(c) Shoulder flx-ext exercise (male)

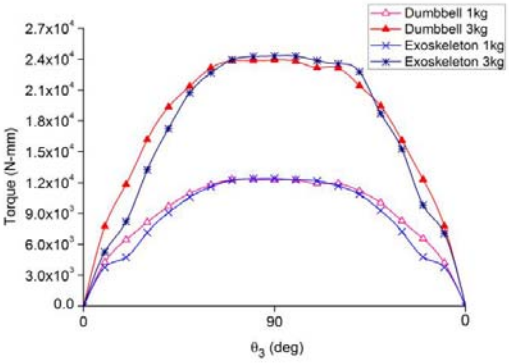

(d) Shoulder flx-ext exercise (female)

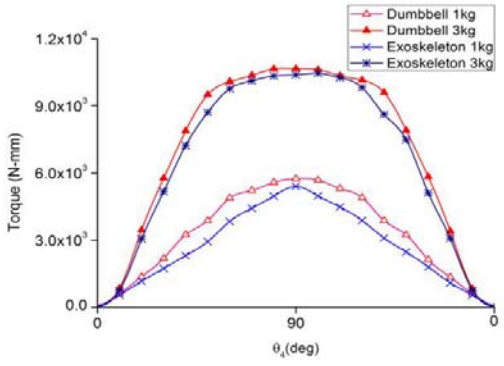

(e) Elbow flx-ext exercise (male)

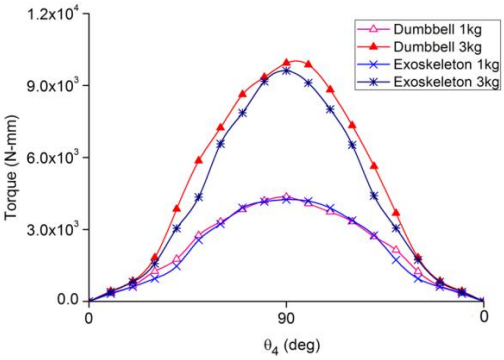

(f) Elbow flx-ext exercise (female)

Fig. 4.5 The experimental data for joint torques with 1 kg and 3 kg resistance that is provided by dumbbell and exoskeleton (without the effect of inertia)

Table 4.3 The peak torques and differences for the free-weight and upper limb exoskeleton exercises.

Subjects	Resistance (kg)	Free-weight $\bar{\tau}$ (N-mm)	Exoskeleton $\overline{M}$ (N-mm)	Difference D (%)
Shoulder abd-add exercise				
Male	1	15,743	15,247	-3.15
	3	27,937	25,946	-7.12
Female	1	12,385	12,964	4.67
	3	24,344	23,049	-5.32
Shoulder flx-ext exercise				
Male	1	16,281	16,334	0.32
	3	28,326	27,925	-1.41
Female	1	12,366	12,440	0.59
	3	23,993	24,440	1.86
Elbow flx-ext				
Male	1	5,742	5,405	-5.87
	3	10,657	10,389	-2.51
Female	1	4,354	4,246	-2.48
	3	9,934	9,618	-3.18

* $\bar{\tau}$: joint torques for the free-weight exercise; $\overline{M}$: joint torques for the exoskeleton exercise; D :$\overline{M} - \bar{\tau}/\bar{\tau} \times 100\%$

verified the calculation of the mass moment of inertia effect with respect to the dumbbells and the exoskeleton, we find that link 2 has a larger mass moment of inertia in this design compared with the 1 kg dumbbell, as shown in Fig. 4.7. Therefore, the mass of the linkage should further conform to certain additional constraints regarding the mass moment of inertia of the dumbbell and the linkage, which will be obtained from the dynamic analysis in chapter 3.

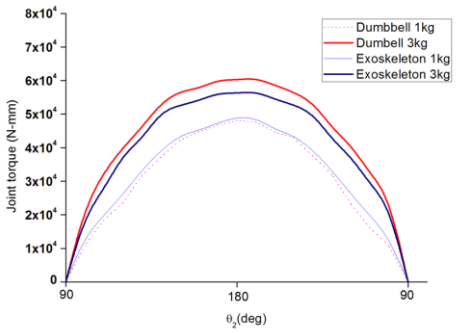

(g) Shoulder abd-add exercise (male)

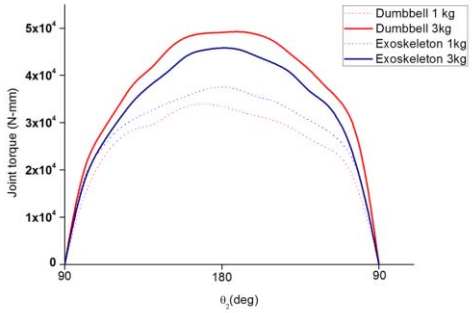

(h) Shoulder abd-add exercise (female)

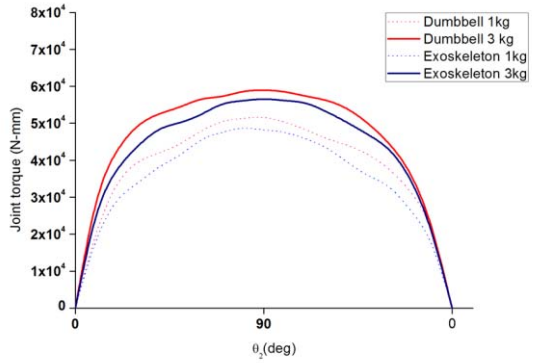

(i) Shoulder flx-ext exercise (male)

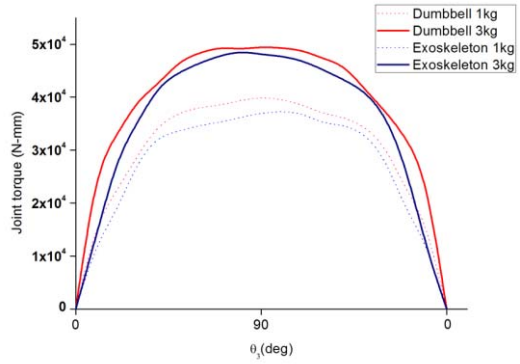

(j) Shoulder flx-ext exercise (female)

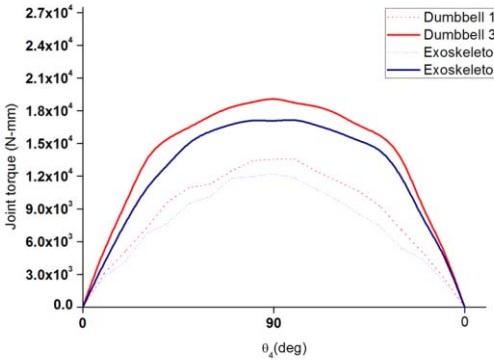

(k) Elbow flx-ext exercise (male)

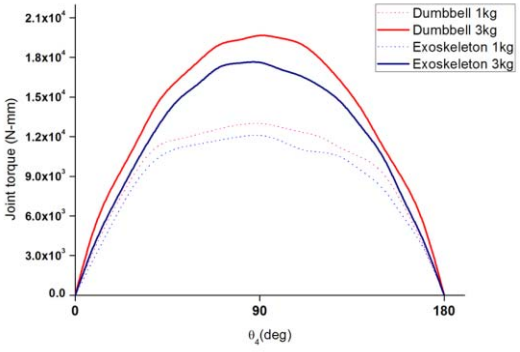

(l) Elbow flx-ext exercise (female)

Fig. 4.6 The experimental data for joint torques with 1 kg and 3 kg resistances that is provided by dumbbell and exoskeleton (with the inertia effect)

According to the data collected from the preliminary evaluation, the experimental results show that the motion tendency of shoulder abd-add, shoulder flx-ext, and elbow flx-ext for resistance exercises performed with the upper limb exoskeleton are nearly equivalent to the static joint torques obtained from the upper limb dumbbell lateral raise the dumbbell frontal raise, and dumbbell curl. However, the shoulder joint sustains a smaller moment of inertia when performing exercises with the upper limb exoskeleton.

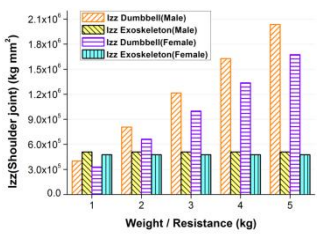

a)Shoulder abd-add movement

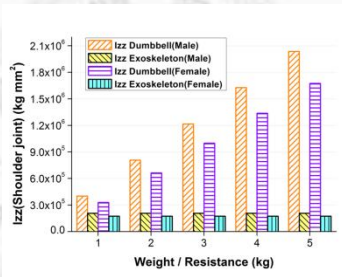

b) Shoulder flx-ext movement

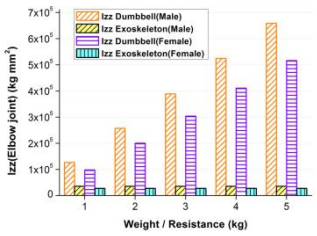

c) Elbow flx-ext movement

Fig. 4.7 Comparison of the mass moment of inertia effect caused by the dumbbell or the exoskeleton motion

4.4 Summary

In this chapter, a prototype was constructed to perform a preliminary evaluation of shoulder abd-add, shoulder flx-ext, and elbow flx-ext exercises as well. The shoulder and elbow joint torques are expected to have smaller inertial forces when using the exoskeleton compared with the joint torques obtained from free-weight exercises. The in-line motion of two subjects using free weights and the upper limb exoskeleton was recorded and analyzed. The comparisons of all of the exercises are obtained with good conformity. From the results of the preliminary evaluation, the drawbacks due to the effect of the mass moment of inertia in the free-weight exercises were obviously reduced with a small inertial spring in the design. By arranging small-inertia springs, the device is capable of reducing unfavorable lengthening of the muscles during high-intensity free-weight exercises or joint overload caused by large inertial moments. Based on the results of the evaluation, this study provides preliminary motion analysis results for the upper limb exoskeleton and determines the appropriateness of the motion analysis evaluation method and the optimal configuration of a spring-loaded upper limb exoskeleton. Further research with a broader assessment is warranted to confirm and expand on these results.

Chapter 5
Verification test: A motion analysis study

5.1 Introduction

According to the World Health Organization, by the year 2050, the number of people over 65 years old will increase by 73 percent in developed countries and by 20.7 percent worldwide [18]. This age group is particularly prone to stroke. An increasing number of elderly people and changes to their lifestyles have lead to an increase in age-related health problems other than stroke, such as chronic diseases. As a result, healthcare services and home-based rehabilitation are in high demand, and the demand for professional physical therapy is imposing an increasing burden on the healthcare system. Healthcare and rehabilitation robotic training devices have the potential to be valuable tools for rehabilitation therapy but must keep pace with both standards of care and the cost-effectiveness of today's rehabilitation trends [49].

The number of technological options for the upper limb rehabilitation training of stroke patients has dramatically increased since the upper limb rehabilitation training robot MIT-Manus was created by MIT in the 1990s for use by muscle

dystrophy patients. Numerous robotic devices that can provide different forms of mechanical input to actively assist, resist, perturb, or increase the patient's range of motion for hemiparetic upper limb training have been developed; such devices include the MIME, the ARM guide, RUPERT, ARMin, the T-Wrex, and others [24, 26, 27, 38]. A recent large multicenter randomized controlled study of robot rehabilitation that compared the MIT-Manus robot system with usual care and intensive therapist-provided therapy confirmed that the effectiveness of the robot is due to the large number of repetitions it provides; the robot's effect was similar to that of intensive therapist-provided therapy and was greater than the effect of usual care. The average cost of therapy per patient was the same for intensive therapist-provided therapy and robot therapy [101]. In contrast to the actuated upper limb robots described above, though some of them provide active mode function (i.e., the robot follows the user's arm without disturbing his/her natural motion), unpowered passive spring-loaded arm exoskeletons are less costly, safer, more compact and may be more appropriate for the return to function phase and at home use.

Comparable to the thriving development of stroke rehabilitation robotic devices, resistance training has recently been shown to also play a significant role in improving many health factors associated with the prevention of chronic diseases

including cardiovascular diseases, diabetes, hypertension, and obesity. The inclusion of resistance training as part of a physical exercise program has been endorsed by the ACSM, the AHA, and the ADA as an integral part of an overall health and fitness program. Furthermore, resistance training is recognized as a safe and effective strategy to enhance the neuromuscular systems of older adults and to improve muscle strength, power, and the ability to perform functional tasks, which may contribute to the prevention of falls and the maintenance of independence [9, 11, 52, 73, 102]. Free weights (such as dumbbells and barbells) and weight machines are the most familiar forms of resistance that may be used for muscle loading. The user's needs or patient's disability level will generally influence the type of resistance chosen. Concerns have been raised over the negative effects and the safety of resistance exercise as a physical therapy intervention and over the usage of the relevant equipment. Resistance equipment were originally designed to be used by healthy people, such as athletes or body builders, who are healthy enough to improve athletic performance or body fitness. Resistance equipment is usually used for gym- or studio-based exercise. In fact, only 23% of the U.S. population engages in leisure time resistance exercise activity at least two times a week, and participation rates are likely to be as low as 12.4% for individuals over the age of 65 [103-104]. These findings underscore the need for programs and more

appropriate exercise devices that encourage healthy people and older adults to incorporate strength training into their lives along with regular physical activity.

The purpose of this study is to investigate the joint torques exerted by the use of a spring-loaded upper limb exoskeleton or a dumbbell through the collection of experimental data and kinematics and dynamic analysis data to verify our hypothesis that, with zero-free-length springs, a spring-loaded upper limb exoskeleton is capable of reducing unfavorable lengthening of the muscles caused by inertial force during high-intensity free-weight exercises. To assess the performance of our design, we measured kinematic data by adopting a motion capture system to compare our mechanism design with free weights exercises while subjects performed designated movements. The motion capture system was adopted because it imposes less limitation on the experimental design, performance of movements, and measurement of kinematic data. The increased availability of and progress in commercial human movement detection/tracking systems have facilitated the quantitative motion analysis studies of upper limbs in a wide spectrum of applications, such as the study of movement in sport and exercise and the clinical comparison of normal movements with pathological movements. Due to widespread use, movement detection/tracking systems are well-recognized in the field of study [35, 88, 95, 98, 100, 105-106].

5.2 Methods and instrumentation

5.2.1 Spring-loaded exoskeleton

The spring-loaded exoskeleton for resistance training (SLERT) is a passive, four DOF body-powered device aimed to enable a patient or a healthy individual to move a limb at multiple joints in different planes for resistance training in a free and unconstrained environment. This design was expected to provide low to moderate resistance to enhance the muscle performance factors of strength, power, and endurance and was also intended to provide more intensive, more repetitive, and longer conditioning training for either chronic-stage patients or healthy individuals at home. The length of the upper arm and the forearm link can be adapted to fit the different body sizes of different users. The SLERT is the revised version of our previous prototype design, which was constructed to conduct a functional and performance-based evaluation of resistance training. The mechanical structure of the new prototype (Fig. 5.1) consists of four links, four revolute joints covering the basic DOF of the human arm to perform shoulder abd-add, flx-ext, int-ext, and elbow flx-ext motion, and three sets of zero-free-length springs that provide the required resistance for the designated upper limb resistance training. The design specifications of SLERT are given in Table 5.1.

The configuration of three revolute joints for the 3-DOF shoulder joint (axes z_0,

z_1 and z_2) is illustrated in Fig. 5.2(a). The revolute joints are constructed with ball bearings or thrust bearings to eliminate friction or to decrease defects of clearance. The 1-DOF elbow joint (axes z_3) is accommodated through a revolute joint, which adjusts the length of the upper limb. Thrust bearings are used to achieve the elbow flx-ext motion. The length of the forearm link can also be adjusted such that the device would fit different individuals, as shown in Fig. 5.2(b). Both shoulder and elbow joints can be locked independently to perform the designated movements. The SLERT structure is constructed primarily from aluminum alloy materials with the high stress joint sections, link 3 and link 4, fabricated in steel.

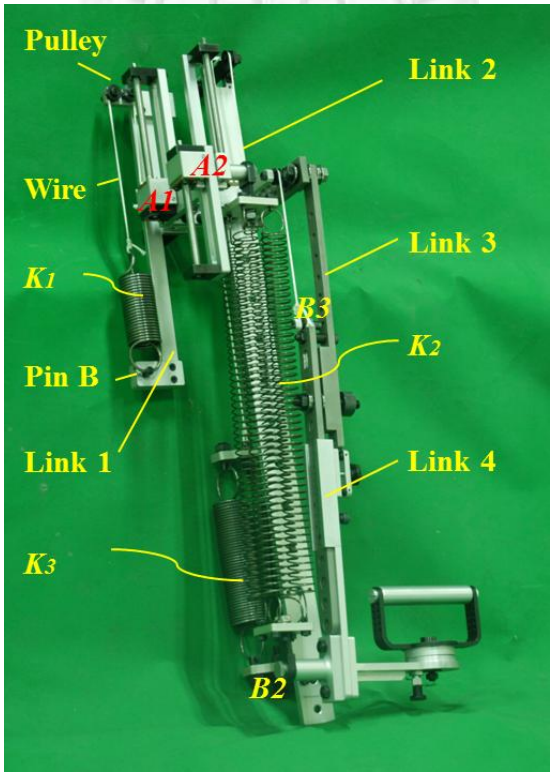

Fig. 5.1 Perspective view of SLERT.

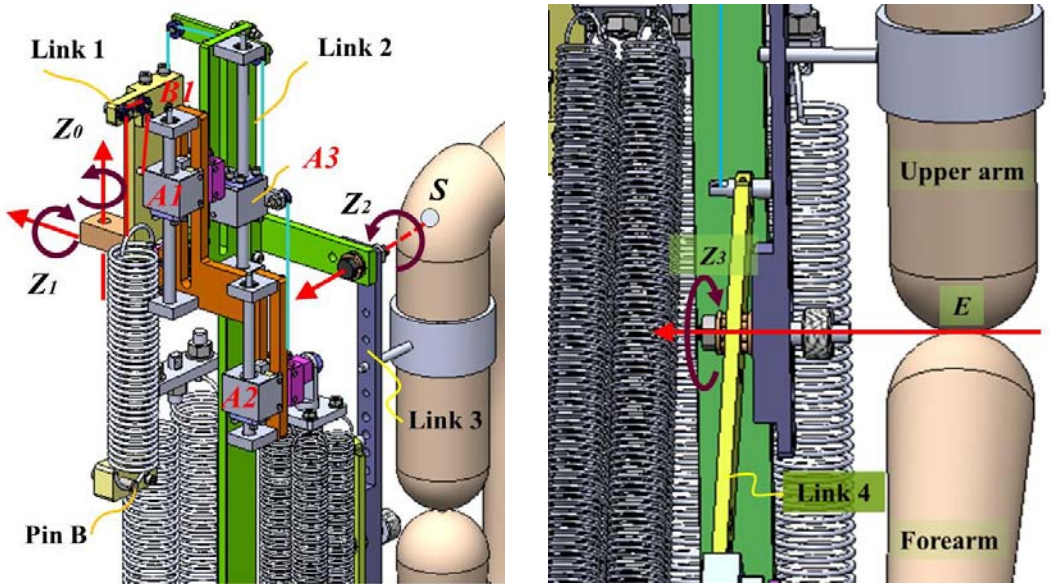

(a) The configuration of the shoulder joint (b) The configuration of the elbow joint

Fig. 5.2 The configuration CAD drawings of the shoulder and elbow joints of the upper limb exoskeleton.

A standard spring with a wire and pulley construction is used to emulate a zero-free-length spring, in which the force is proportional to the length of the spring rather than to its elongation, allowing the SLERT to increase or decrease the resistance by adjusting the spring length. All pulleys are equipped with bearings to reduce their friction and smooth their motion. The standard spring K_1 is fixed by a pin B and connected to points *B1* (on link 1) and *A1* (on link 2) with wire and pulleys, as shown in Fig. 5.2(a). The arrangement for springs K_2 and K_3 is the same as that for spring K_1, as is shown in Fig. 5.2(b). To increase the intensity of the resistance exercise, the spring connection locations *A1*, *A2*, and *A3*, which are separately integrated with nuts on the slide screws installed at link 2, can be

adjusted using three slide screws. The required resistance in our design is generated by adjusting the connecting locations (*A1*, *A2*, and *A3*) of the springs rather than by changing the stiffness of the springs. This characteristic provides more convenience and flexibility in carrying out the resistance exercise program.

Based on consideration of the target users and the purposes of their usage, the maximum resistant force of the current prototype is designed to be 49 N (corresponding to a 5-kg weight dumbbell). Based on the limitations and the mass properties of the linkages, the anthropometric parameters of humans, and the previous practical implementation experiences of this design, springs with a suitable stiffness were decided from the spring design constraints in chapter 2 and chosen from a catalog of standard springs. The design specifications are listed in Table 5.1.

Table 5.1 Design specifications of the SLERT

Property	Target value
Resistance (kg)	1-5
Upper arm length (mm)	224-286
Forearm length (mm)	267-368
Range of motion	
Shoulder abd/add (degree)	0-180
Shoulder flx/ext (degree)	0-180
Elbow flx/ext (degree)	0-145
Spring Stiffness	
K_1 (kgw/mm)	0.145
K_2 (kgw/mm)	0.05
K_3 (kgw/mm)	0.07

5.2.2 Study subjects

Six healthy subjects (three males and three females), referred to here as S1, S2, S3, S4, S5, and S6, volunteered to participate in this evaluation. Participants were required to have no previous shoulder or elbow pain or injury, and no history of neural or musculoskeletal impairments. Each participant was required to read, understand, and sign an informed consent document that had been approved by ITRI's ethics committee before instrumentation and data collection. The subjects' anthropometric parameters are listed in Table 5.2.

Table 5.2 Anthropometric parameters of the subjects (S1-S6)

Measure	All subjects	S1	S2	S3	S4	S5	S6
Number	6						
Age (year)	22.5±0.5	22	23	23	23	22	22
Gender	3M/3F	M	M	M	F	F	F
Height (cm)	164.8±6.0	171	170	163	168	162	155
Total body weight (kg)	57.6±9.2	63	62.4	68	54	56	42
Upper arm length r_u (mm)	276.6±20.9	290	295	290	280	265	240
Forearm length r_f (mm)	322.5±35.2	352	355	340	320	310	260

Results are mean ± standard deviation (SD). M: Male; F: Female

5.2.3 Instrumentation

The kinematic data of shoulder and elbow motions were acquired using a three-dimensional (3-D) passive optical motion capture system (Vicon MX, Vicon motion systems, Oxford, UK) at ITRI's research laboratory. This system consists of 8 synchronized high speed infrared charge-coupled display (CCD) cameras (Vicon

MX-F20, Vicon motion systems, Oxford, UK) operating at a frame rate of 100 Hz to track 8 reflective spherical markers measuring 14 mm in diameter and mounted by double-sided hypoallergenic tape on the subject in real-time. The locations of the markers were predetermined bony anatomical landmarks, where subcutaneous tissue was thin and relatively fixed to the underlying skeleton, that were on the trunk and the upper limb of the subject, including the 7th cervical vertebrae, the clavicle, the right shoulder marker, the right lateral elbow, the right medial elbow, the processus styloideus radius, the processus styloideus ulna, and the metacarpophalangeal joints of the right middle finger; these locations were used to define the segments that define position and orientation in three-dimensional space and were chosen for their minimal skin motion. They are listed in Table 5.3. The markers were attached to anatomical landmarks found by palpation. All the markers on all subjects were attached by the same tester to remove inter-individual variability as a source of error.

Before testing, an initial dynamic, or wand, calibration followed by a static, or calibration frame, calibration of the motion capture system was performed to ensure the mean residual error was less than 1 mm. During the two-phase calibration, the relative location of each camera with respect to the other cameras, the actual size of the recording space, and the object-space origin were determined. After the markers

Table 5.3 Marker names, locations, placement and corresponding segments

Marker	Location	Marker placement	Segment
C7	The 7th cervical vertebrae	Spinous process of the 7th cervical vertebrae	Thorax
CLAV	The clavicle	Jugular Notch where the clavicle meets the sternum	Thorax
RSHO	The right shoulder marker	Place on top of the Acromio-clavicular joint	Scapula
RLEL	The right lateral elbow	Place on lateral epicondyle approximating right elbow joint axis	Humerus
RMEL	The right medial elbow	Place on medial epicondyle approximating right elbow joint axis	Humerus
RMWR	The right wrist marker radius	The processus styloideus radius	Forearm
RLWR	The right wrist marker ulna	The processus styloideus ulna	Forearm
RFIN	The right middle finger	The metacarpophalangeal joints of the right middle finger	Hand

were properly attached, the subjects were asked to assume a neutral pose in the center of the object-space (or the capture volume) for the subject calibration. The subjects were then instructed to move their shoulder, elbow, and wrist joints to perform the required dynamic calibration. It was necessary to ensure that each marker could be detected by at least two cameras at every instant during data recording and to ensure that no other shiny reflective materials on the subjects were detected by the cameras. While the subject was performing the selected free-weight exercise and shoulder abd-add, shoulder flx-ext, and elbow flx-ext movements with the spring-loaded upper limb exoskeleton in the object-space in view of the CCD cameras, the motion analysis system recorded the movements of the upper limb

segments by tracking the 3-D position of the markers relative to a fixed lab coordinate frame. During testing, the spatial coordinates of the eight markers were captured, reconstructed, and labeled, and gaps were filled by the Nexus software (VICON Nexus 1.3, Vicon motion systems, Oxford, UK).

The verification test consisted of shoulder abd-add, flx-ext, and elbow flx-ext movements of the right upper limb. The Vicon motion data were collected from both the male and female subjects.

5.2.4 Experimental Protocols

Two exercise sessions (free-weight exercises and upper limb exoskeleton motion) were conducted for evaluation. Each session consisted of three resistance training exercises (shoulder abd-add, flx-ext, and elbow flx-ext) consisting of six sets (1 kg, 3 kg and 5 kg resistance; 1 second and 2 second motion speed) for male subjects and four sets (1 kg and 3 kg resistance; 1 second and 2 seconds motion speed) for female subjects. Each movement was performed in a slow, controlled manner: lifting (1 second and 2 seconds) and lowering (1 second and 2 seconds) without sudden jerks or acceleration for six consecutive repetitions. A metronome was employed to help the subjects maintain the tempo of their movements and a maximum of five minutes rest was given between each set and exercise. Instructions on how to perform the motion were illustrated and demonstrated to the

subjects at the beginning of the test. Subjects were also instructed to keep their left arms resting by their sides to ensure that they did not obscure or compensate for the motion of the right arm. The ranges of the movement evaluated and the grip patterns used are shown in Fig. 5.3. The designated arm motions were included in the experimental protocol (Table 5.4). The dumbbell weights of 1 kg, 3 kg and 5 kg and the equivalent resistances are set for free-weight exercise and upper limb exoskeleton motion, respectively. If the subjects were obviously out of pace (too fast or too slow) or if mistakes were made, the recordings were discarded and the measurement was restarted. Warm-up trial practices were allowed before the actual tests to reduce the number of failed trials due to inaccurate pace or movement.

(a) Dumbbell lateral raise

(b) Dumbbell frontal raise

(c) Dumbbell curl

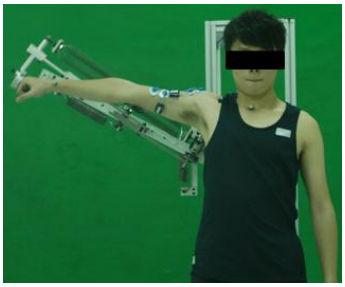

(d) Shoulder abd-add motion

(e) Shoulder flx-ext motion

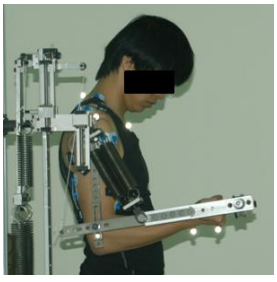

(f) Shoulder flx-ext motion

Fig. 5.3 Movement and grip patterns of the free-weight exercises and the exoskeleton motions

The starting position for the kinematic studies was defined as standing comfortably with the arms at the sides and the forearms naturally rotated in a relaxed posture (pronation). Every action and general motion started from an initial arm position in which the arm was fully extended along the body.

Table 5.4 Protocols for the dumbbell movements and the movements used with the exoskeleton.

Resistance	Movement	Description
Dumbbell	Dumbbell lateral raise	Raise the right arm laterally from the side of the body until it is in a horizontal position, while keeping the elbow in a fixed position. The palm should face the ground.
Dumbbell	Dumbbell frontal raise	Raise the right arm in a sagittal plane so that the hand ends up directly in front of the shoulder joint, while keeping the elbow locked. The palm should face the ground.
Dumbbell	Dumbbell curl	Draw the forearm upward in an arc from a vertical position to a horizontal position with the palm facing up toward the ceiling, and then reverse the movement in the opposite direction.
Exoskeleton	Shoulder abd-add	The z_1^* axis of the exoskeleton is aligned with the shoulder joint, gripping the handle of the exoskeleton, and the right arm is raised laterally from the side of the body. The palm should face the ground.
Exoskeleton	Shoulder flx-ext	The z_2 axis of the exoskeleton is aligned with the shoulder joint and the right arm is raised in a sagittal plane while keeping the elbow in a fixed position. The palm should face the ground.
Exoskeleton	Elbow flx-ext	The z_3 axis of the exoskeleton is aligned with the elbow joint and the forearm is drawn upward in an arc from a vertical position to a horizontal position with the palm facing up toward the ceiling. The movement then continues in the reverse direction.

5.2.5 Data analysis

Of the 1,040 total trials, 720 were analyzed. Analyses were performed on the subjects' right shoulders and elbows. Joint torques at the shoulder and elbow were calculated via inverse dynamics. The analysis begins with the most distal segment and continues upward through the kinematic chain, and the requirements of all the external forces acting on the system are known. The joint torques are then calculated by a 3-D generic inverse dynamic method [100]. Trial data from the exercises were captured, processed, and reviewed in the Vicon Nexus platform and post-processed offline using Matlab. To suppress noise, the collected motion data were low-pass filtered by a fourth-order Butterworth filter at a cut off frequency of 5 Hz. Trial data over the required range of motion were also truncated. The first three data points of the six repeated trials are analyzed to obtain an average of three data results. If one of these three data points is not fit for the data analysis, the fourth, or the fifth, or the sixth data points will be analyzed. The mean joint torques are then obtained from the mean value of the torques of the three male or three female subjects.

5.3 Results and discussion

Fig. 5.4 and Fig. 5.5 show the comparisons between the joint torques of free-weight exercises and the resistance exercise using the upper limb exoskeleton for male and female subjects at two different motion speeds (velocity and inertia effects were neglected). In Figs. 5.4 (a) - (d) and Figs. 5.5 (a) – (d), the peak joint torques are at 180 degrees for the shoulder abd-add exercise and 90 degrees for the flx-ext exercise. The joints would generate higher torques when the upper limb straightens in the horizontal position, which is the point at which the moment arm is the farthest away from the resistant force while being perpendicular to the joint. A similar explanation can be applied to the elbow flx-ext exercise, as shown in Figs. 5.4 (e) and (f) and Figs. 5.5 (e) and (f). The mean peak torques of the exercise at two different motion speeds, without considering the inertia effect, for male subjects, female subjects, and their differences are listed in Table 5.5 and Table 5.6.

Fig. 5.6 and Fig. 5.7 show comparisons between the joint torques of free-weight exercises and the resistance exercises using the upper limb exoskeleton mechanism at two different motion speeds when considering the velocity and the effects of inertia. Generally speaking, dumbbell exercises generate a higher moment of inertia in the shoulder joint, and the inertial effect becomes more obvious as the resistance load or the velocity increase.

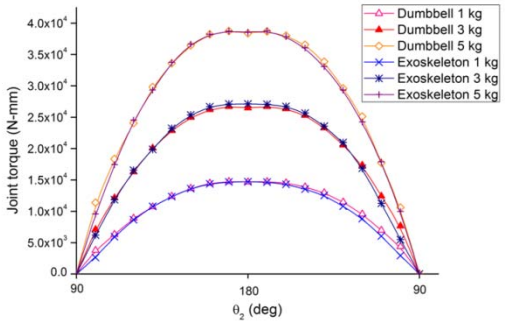

(a) Shoulder abd-add motion (male subjects)

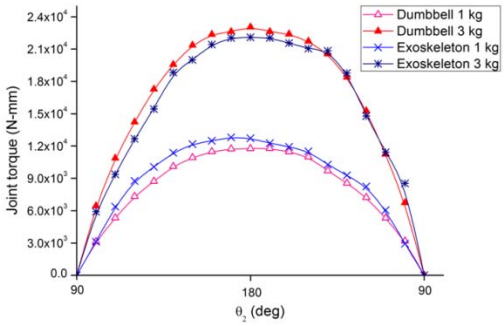

(b) Shoulder abd-add motion (female subjects)

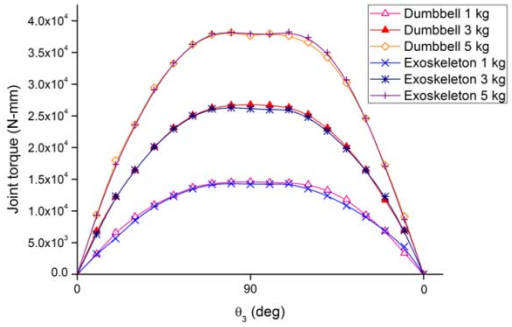

(c) Shoulder flx-ext motion (male subjects)

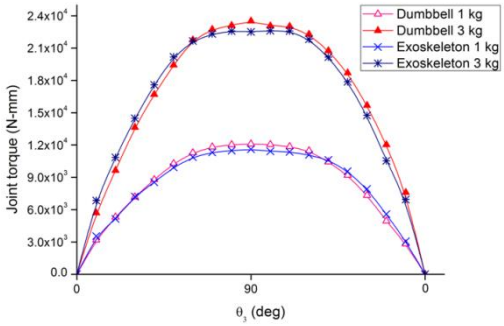

(d) Shoulder flx-ext motion (female subjects)

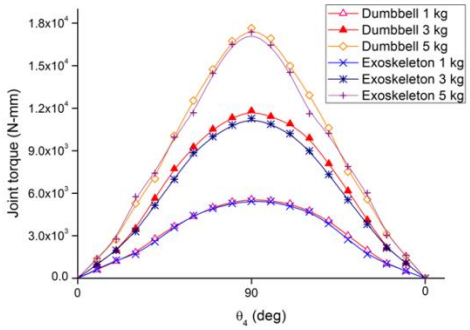

(e) Elbow flx-ext motion (male subjects)

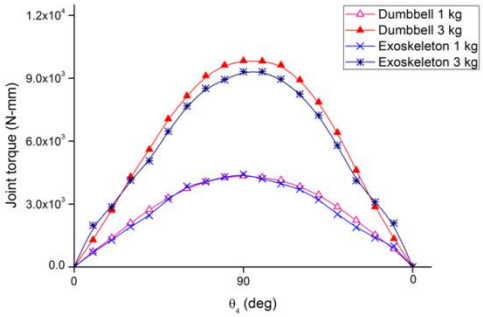

(f) Elbow flx-ext motion (female subjects)

Fig. 5.4 The experimental joint torques of the free-weight and resistance exercises using the upper limb exoskeleton without inertial effects (1 second lifting and 1 second lowering motion speed).

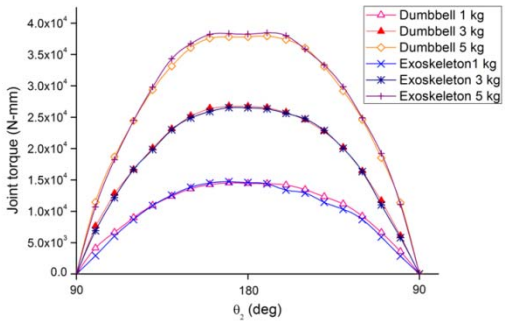

(a) Shoulder abd-add motion (male subjects)

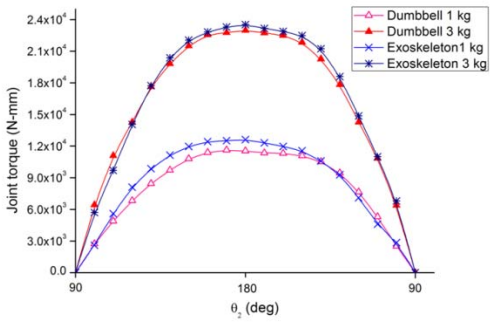

(b) Shoulder abd-add motion (female subjects)

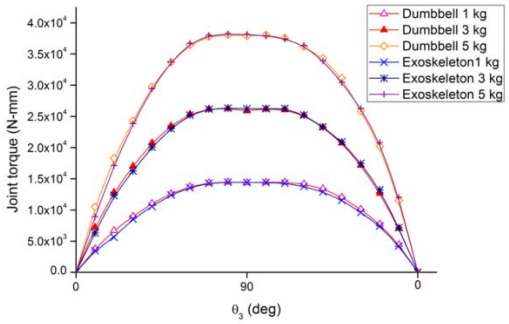

(c) Shoulder flx-ext motion (male subjects)

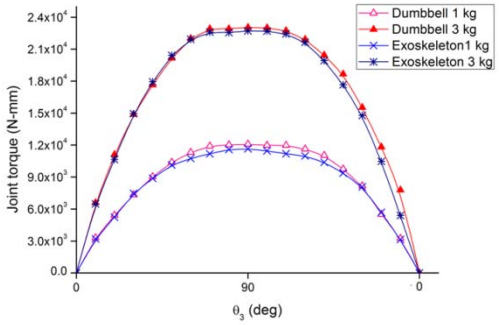

(d) Shoulder flx-ext motion (female subjects)

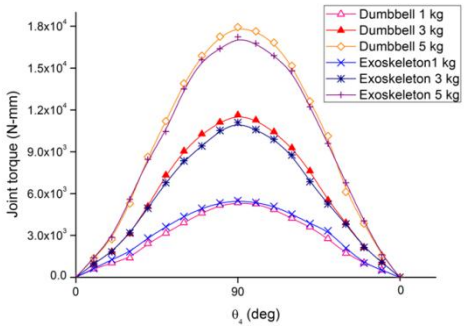

(e) Elbow flx-ext motion (male subjects)

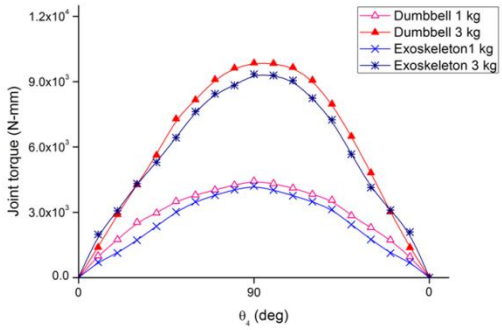

(f) Elbow flx-ext motion (female subjects)

Fig. 5.5 The experimental joint torques of the free-weight and resistance exercises using the upper limb exoskeleton without inertial effects (2 second lifting and 2 second lowering motion speed)

Table 5.5 The mean peak torques and differences for the free-weight and upper limb exoskeleton exercises at 1 second lifting and 1 second lowering motion speeds.

Subjects	Resistance (kg)	$\bar{\tau}$ (N-mm)	$\overline{M}$ (N-mm)	D (%)
Shoulder abd-add exercise				
Male	1	14,671	14,719	-0.33
	3	26,486	27,124	-2.50
	5	38,392	38,529	-0.36
Female	1	11,756	12,717	-8.17
	3	23,045	22,103	4.09
Shoulder flx-ext exercise				
Male	1	14,612	14,221	2.68
	3	26,767	26,150	2.30
	5	37,634	37,961	-0.87
Female	1	12,092	11,610	3.99
	3	23,517	22,506	4.30
Elbow flx-ext exercise				
Male	1	5,564	5,437	2.28
	3	11,814	11,273	4.58
	5	17,645	17,365	1.59
Female	1	4,344	4,423	-1.82
	3	9,832	9,312	5.29

Table 5.6 The mean peak torques and differences for the free-weight and upper limb exoskeleton exercises at 2 second lifting and 2 second lowering motion speeds.

Subjects	Resistance (kg)	$\bar{\tau}$ (N-mm)	$\overline{M}$ (N-mm)	D (%)
Shoulder abd-add exercise				
Male	1	14,455	14,583	-0.88
	3	26,741	26,502	0.89
	5	37,829	38,265	-1.15
Female	1	11,541	12,620	-4.69
	3	22,985	23,528	-2.36
Shoulder flx-ext exercise				
Male	1	14,381	14,415	-0.24
	3	25,892	26,243	-1.36
	5	37,919	38,140	-0.87
Female	1	12,081	11,657	-0.58
	3	23,043	22,719	1.41
Elbow flx-ext exercise				
Male	1	5,345	5,498	-2.86
	3	11,641	11,095	4.69
	5	17,932	17,222	3.96
Female	1	4,437	4,214	5.02
	3	9,858	9,340	5.25

Note that $\bar{\tau}$: joint torques for the free-weight exercise; $\overline{M}$: joint torques for the exoskeleton exercise; D: percentage of the difference between the free-weight and exoskeleton exercises = $\overline{M} - \bar{\tau} \big/ \bar{\tau} \times 100\%$

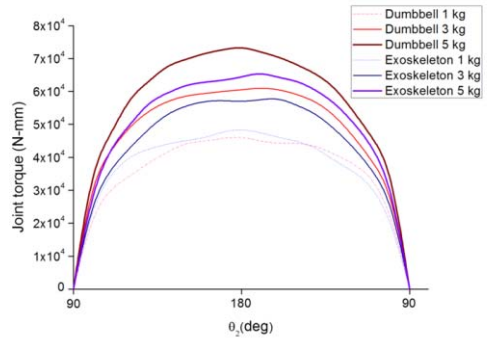

(a) Shoulder abd-add motion (male subjects)

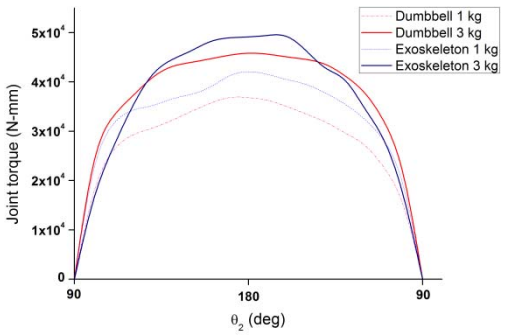

(b) Shoulder abd-add motion (female subjects)

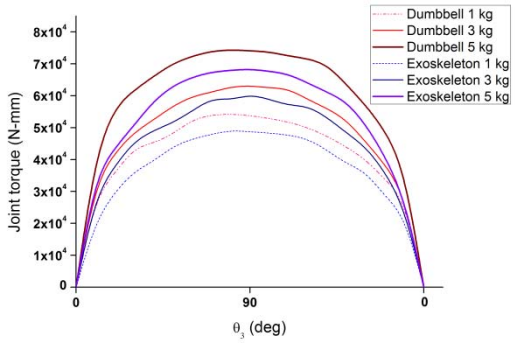

(c) Shoulder flx-ext motion (male subjects)

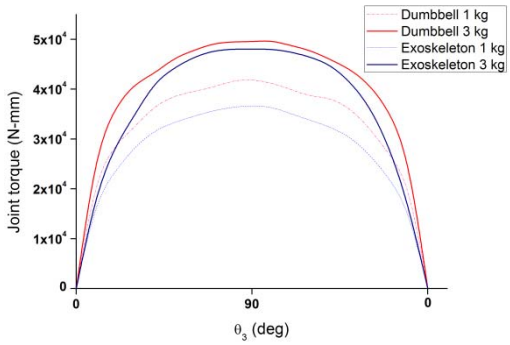

(d) Shoulder flx-ext motion (female subjects)

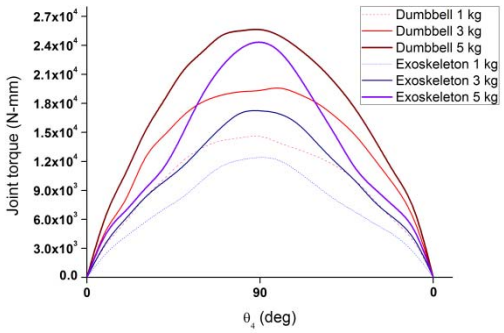

(e) Elbow flx-ext motion (male subjects)

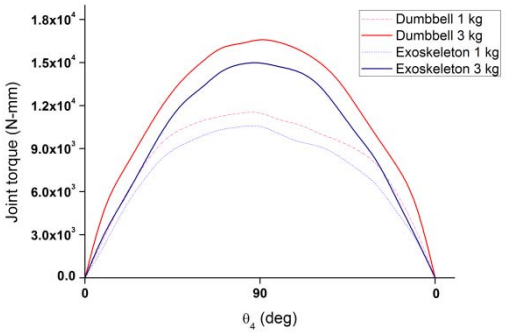

(f) Elbow flx-ext motion (female subjects)

Fig. 5.6 The experimental joint torques of the free-weight and resistance exercises using the upper limb exoskeleton with inertial effect (1 second lifting and 1 second lowering motion speed).

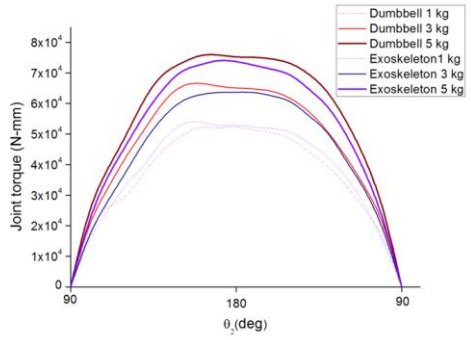

(a) Shoulder abd-add motion (male subjects)

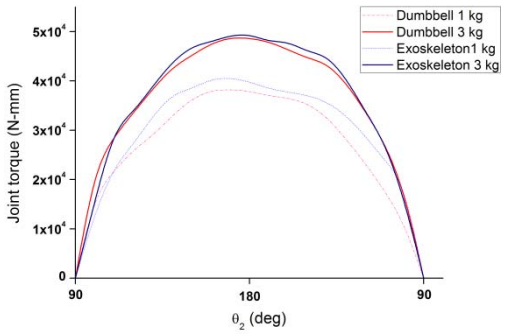

(b) Shoulder abd-add motion (female subjects)

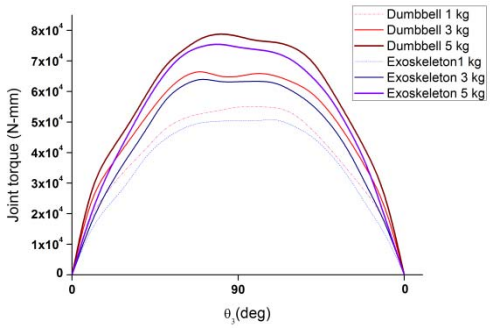

(c) Shoulder flx-ext motion (male subjects)

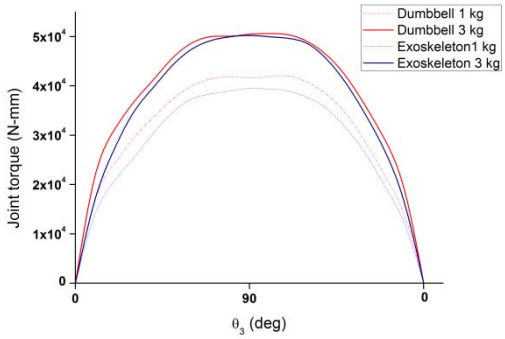

(d) Shoulder flx-ext motion (female subjects)

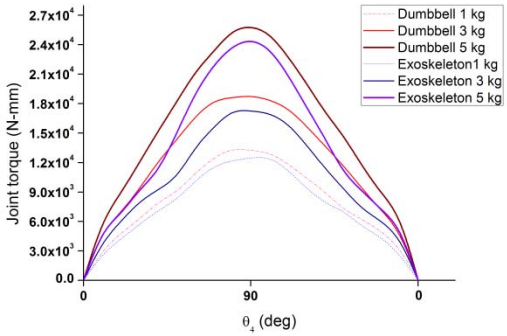

(e) Elbow flx-ext motion (male subjects)

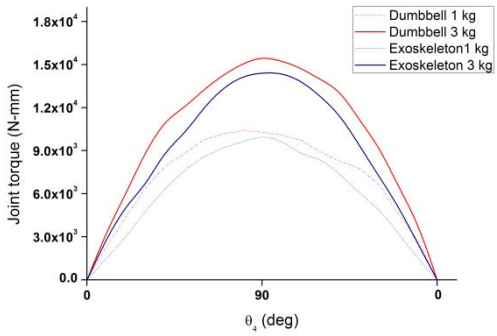

(f) Elbow flx-ext motion (female subjects)

Fig. 5.7 The experimental joint torques of the free-weight and resistance exercises using the upper limb exoskeleton with inertial effect (2 second lifting and 2 second lowering motion speed).

Fig. 5.8 compares the mass moments of inertia calculated from the 1, 3, and 5 kg fixed weight dumbbells and the exoskeleton motion of the prototype for the six subjects. The calculations show that the dumbbell held at the distal end of the upper limb has a larger inertial effect than the current upper limb exoskeleton prototype; moreover, as the weight of the dumbbell increases, the inertial effect also increases dramatically. We found that link 2 has a larger mass moment of inertia in the current exoskeleton design compared with the 1 kg dumbbell, which agrees with the experimental results, as shown in Figs. 5.8(a) and (b). Therefore, the mass of the linkage should further conform to certain additional constraints regarding the mass moment of inertia of the dumbbell and the linkage, which is obtained from the dynamic analysis in chapter 3.

The experimental results show that the motion tendency of the shoulder abd-add, shoulder flx-ext, and elbow flx-ext motions for resistance exercises performed with the upper limb exoskeleton are nearly equivalent to the joint torques obtained from the upper limb dumbbell lateral raise, the dumbbell frontal raise, and the dumbbell curl in static joint torque analysis. However, the shoulder joint sustains a smaller moment of inertia when performing exercises with the upper limb exoskeleton in dynamic joint torque analysis. From the results of the verification test, the drawbacks due to the effect of the mass moment of inertia in

the free-weight exercises were obviously reduced with a small inertial spring in the design. The collected data, along with the kinematics and dynamic analysis, may provide an integral understanding of the design requirements of a spring-loaded exoskeleton for upper limb resistance training. The design of an exoskeleton as a device should rely not only on anthropometric information about the human body but also on comprehensive information regarding human body kinematics and dynamics.

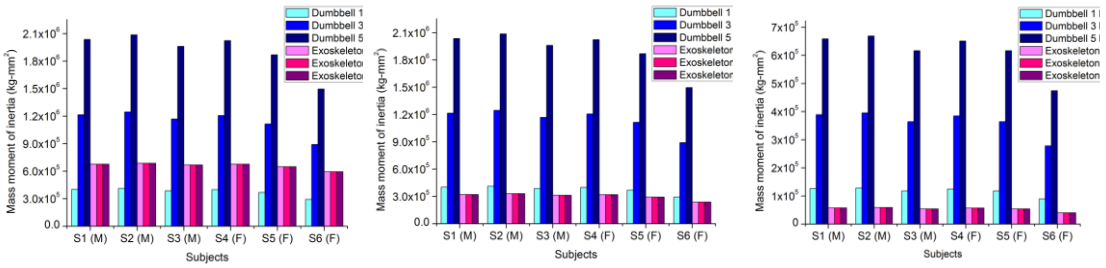

(a) Shoulder abd-add movement (b) Shoulder flx-ext movement (c) Elbow flx-ext movement

Fig. 5.8 The mass of moment of inertia effect caused by the dumbbell or the exoskeleton on the subjects.

5.4 Summary

A passive upper limb exoskeleton prototype has been modified and reconstructed in accordance with previous studies, and an analysis of on-line motion was conducted to record designated movements performed using free weights and the upper limb exoskeleton as the resistance by six subjects. The static joint torques exerted at the shoulder and elbow joints when using the exoskeleton were shown to be nearly equal to the objective static joint torques obtained from models of free-weight exercises and kinematics at lower and moderate motion speeds. The dynamic joint torques of the shoulder and elbow joints for movements performed with the exoskeleton were shown to be smaller than the objective dynamic joint torques obtained from models of free-weight exercises and kinetics, and the effect became more obvious as the resistance load and the motion velocity increased. Comparisons of all of the exercises were obtained with good conformity. We have demonstrated that the device used in this study is capable of reducing the unfavorable lengthening of muscles during high-intensity free-weight exercises or joint overload caused by large moments of inertia. Finally, this study provides verification test results for an upper limb exoskeleton and determines the appropriateness of the motion analysis evaluation method and the optimal configuration of a spring-loaded upper limb exoskeleton.

Chapter 6
Verification test: An electromyography study

6.1 Introduction

Increases in elderly populations and sedentary lifestyles have led to an increase in age-related health problems, such as decreased physical function due to diseases (particularly in developed countries). Due to a decrease in the youth and labor population, the shortage of nurses and therapists is gradually becoming a serious social problem in Taiwan. There will be a significant need for healthcare, exercise training devices and medical care devices for the elderly. Resistance training based on science has been endorsed by major national health organizations because of its potential value in functional capacity and other health-related factors [9-10, 12-13, 72]. Healthcare services and home-based rehabilitation are in demand. However, most exercise machines and devices are designed for healthy young individuals and athletes to improve their fitness and muscular performance and are usually based in gyms or studios. There are few reports concerning the development of home-based health care and exercise training devices for the upper limbs targeted for the elderly population and individuals requiring home-based

rehabilitation. We propose a spring-loaded upper limb exoskeleton for resistance training (SLERT), which is a modified version of a previously proposed prototype presented in chapter 4. The SLERT is designed to enable a patient or healthy individual to move his upper limbs at multiple joints in different resistance planes. The mechanical structure of the SLERT consists of four links and four revolute joints covering the basic DOF of the human arm to perform shoulder abd-add, flx-ext, int-ext, and elbow flx-ext motion, as well as three sets of zero-free-length springs that provide the required resistance for the designated upper limb resistance training. This device has been proven capable of reducing the unfavorable lengthening of muscles during high-intensity free-weight exercises and joint overload caused by large moments of inertia; however, the muscle activities when using the SLERT have not been investigated.

Electromyography (EMG) is a method of analyzing muscle function and has been used to evaluate muscle activity for function, control, and learning [107]. However, care must be taken in using EMG as a tool for studying human movement, including the error selection of recording electrodes, recording site, or signal acquisition specifications. Furthermore, the interpretation of the EMG signal requires a thorough knowledge of the origin of the signal, which has its physiological origins in individual groups of muscle fibers. The anatomical features

of individual muscle fibers, architectural features of whole muscle, and physiological origins of action potentials are key to understanding how to record, analyze, and interpret EMG signals [108].

Surface electromyography (sEMG) is a popular electrophysiology technique to record the physiological characteristics of muscle activities. Because sEMG recording provides a safe, easy, non-invasive, and painless measure method that allows for the objective quantification of muscle energy. sEMG offers an easy-to-handle tool for the online assessment of muscle activation and the internal load on muscles, tendons, and other tissues. sEMG has been largely applied in a wide spectrum of experimental conditions, including rehabilitation, neurology, neurophysiology, sport science, and ergonomics. sEMG allows for the investigation of both muscle activation and muscle physiological characteristics [109-111]. sEMG has been employed to investigate the activation of selected muscle groups during upper limb resistance exercises with dumbbells or elastic tubing. The test results provide scientific data for upper limb post-injury and postoperative rehabilitation or injury prevention and can be a useful aid in estimating the proper density of individual rehabilitation protocols [112-113], A combination of sEMG and fine-wire EMG has been used to reduce the invasiveness of testing for the study subjects whose muscles are being activated or for whom exercise is most effective

during the rubber-tubing exercises used by throwers during warm-ups [114]. sEMG is used for the following purposes in evaluating the neural changes induced by strength training [115]: 1) to identify normal and abnormal muscle activation patterns, which can then be related to impaired performance and function; 2) to monitor pre-treatment versus post-treatment changes in muscle activation in rehabilitation exercises; 3) to confirm muscle activity or inactivity in patients undergoing treatment; 4) to evaluate the therapeutic efficacy of robot-assisted exercise for the recovery of upper limb motor function following stroke [21, 116]; and 5) to use the EMG signal, i.e., muscle electrical activity, to trigger the assistance provided by the robot [117].

The purpose of the present study was to investigate the level of muscle activation and applied loading during upper limb resistance exercises using dumbbells compared with a spring-loaded upper limb exoskeleton. The novel spring-loaded exoskeleton enables a patient or healthy individual to move his upper limbs at multiple joints in different resistance planes. We hypothesized that the levels of muscle activation are similar when performing the same exercises using either dumbbells or a spring-loaded upper limb exoskeleton when equivalent resistance is applied. Furthermore, we hypothesized that applied loading relates to the level of muscle activation. A statistical study was conducted to test the effects of

the different settings on muscle activation.

6.2 Methods and instrumentation

6.2.1 Study subjects and preliminary sessions

Six healthy subjects (three males and three females referred to here as S1, S2, S3, S4, S5, and S6) volunteered to participate in this evaluation (age: 22.5±0.5 years; height: 164.8±6.0 cm; body weight: 57.6±9.2 kg). The participants were required to have no previous shoulder or elbow pain or injury and no history of neural or musculoskeletal impairments. The subjects were not engaged in regular athletic activities during their leisure time. We explained to each subject that before instrumentation and data collection, each participant was required to read, understand, and sign an informed consent document that had been approved by the ITRI ethics committee. The anthropometric parameters of the subjects are listed in Table 5.2 in the previous chapter.

6.2.2 Instrumentation

The EMG data of the muscle groups of interest (right shoulder and elbow motions) were acquired using sEMG. The sEMG signals were registered with an 16-channel wireless electromyography ZeroWire EMG system (ZW180/R WiFi, Aurion, Milano, Italy) used to record the muscle electrical activity resulting from contraction and relaxation while performing the designated exercises; the system

was composed of two parts: the main unit (receiver) and wearable EMG probes (34x26x19 mm in dimension, weight 0.01 kg (10 grams)). Each probe was able to collect and amplify the EMG signals and transmit the EMG data.

The skin of each subject skin was scrubbed with an isopropyl alcohol swab to minimize the contact impedance, and surface EMG conductive adhesive electrodes with a contact diameter of 22 mm were attached to the skin surface over eight upper limb muscles: the anterior deltoid (AD), middle deltoid (MD), posterior deltoid (PD), pectoralis major (PM), biceps brachii (BB), tricep brachii (TB), upper trapezius (UT), and supraspinatus (SS), as shown in Fig. 6.1. These muscles were selected for their well-known contributions to shoulder abd-add, shoulder flx-ext, and elbow flx-ext movements [60, 118]. The electrodes were positioned precisely on the midline of the muscle belly between the most distal motor point and the tendon and oriented along a line parallel to the direction of the underlying muscle fibers, as shown in Fig. 6.2 [107, 119]. Ground reference electrodes were not needed, which significantly reduced the artifact due to the movement of the wires. The absence of cables around the subject increased the comfort and freedom of movement for the subject. Each electrode was equipped with a wearable probe for signal processing and transmission and attached to the skin with double-sided tape. During the EMG studies, resistance was applied in various shoulder and elbow

positions to produce the maximum voluntary isometric contraction (MVIC) for normalization of the data for eight muscles of interest. The position was confirmed during the maximum voluntary isometric contraction tests by observing the EMG versus arm loading.

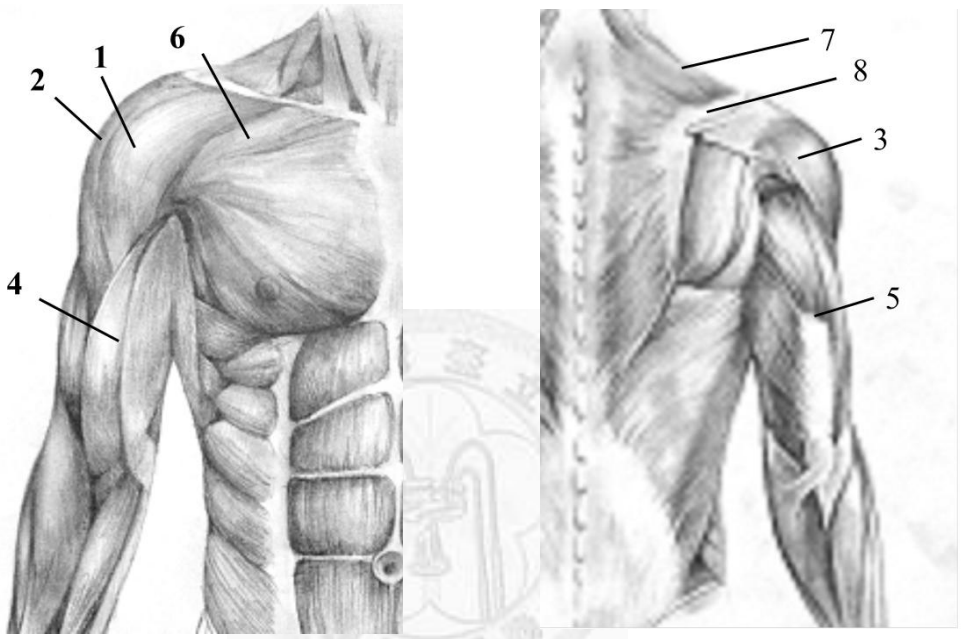

(a) Frontal (b) Posterior

Fig. 6.1 The location of the Surface EMG

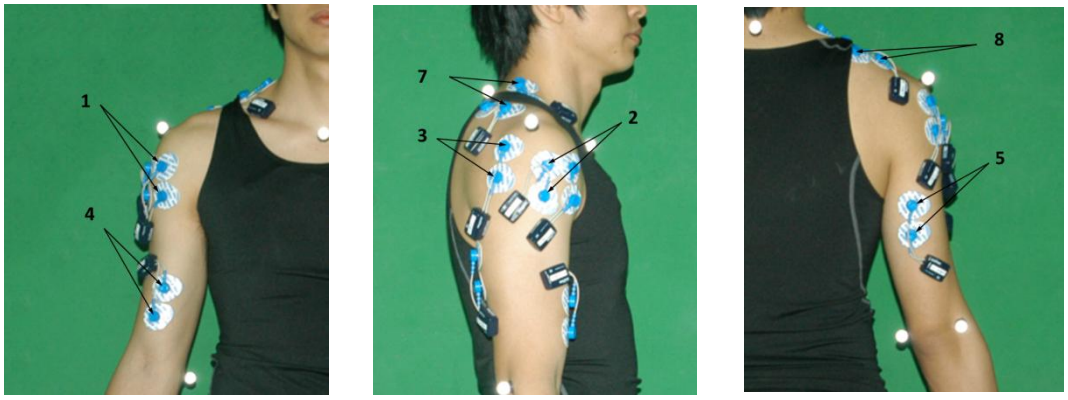

(a) Front view (b) Side view (c) Rear view

Fig. 6.2 The location of the surface EMG (note that the channel 6 for pectoralis major was covered under the cloth)

Table 6.1 The muscles tested and MVIC action used in this study.

Channel	Muscle	MVIC action
1	Anterior deltoid	Shoulder abduction in slight flexion with the humerus in slight lateral rotation against the anteromedial surface of the arm in the direction of abduction and slight extension.
2	Middle deltoid	The arm was abducted to 90° in neutral rotation (palm down) with resistance applied just proximal to the elbow in an inferior direction.
3	Posterior deltoid	Shoulder abduction in slight flexion with the humerus in slight medial rotation against the posterolateral surface of the arm above elbow in the direction of abduction and slight flexion.
4	Biceps brachii	Forearm flexion at a right angle and the forearm in supination with resistance applied against the lower forearm in the direction of extension.
5	Tricep brachii	Extension of the elbow to slightly less than full extension against the forearm in the direction of flexion.
6	Pectoralis major	Horizontal adduction of the arm with the elbow extended against the forearm in the direction of horizontal abduction
7	Upper Trapezius	Elevation the acromial end of the clavicle and scapula against the shoulder in the digression of depression.
8	Supraspinatus	The shoulder was elevated to 90° in the scapular plane, the elbow was extended, and the shoulder was in neutral rotation.

To obtain the MVIC for each muscle tested, we directed each subject to perform a series of isometric resistance contractions. The MVIC values were collected for each muscle of interest individually; the subjects performed the exercise while a qualified person held their shoulders, upper arms, and forearms and provided strong verbal encouragement (Table 6.1) [118]. For each muscle, the MVIC values were collected for approximately three seconds and used to normalize the EMG signal between 0% and 100% of each cycle. The EMG recordings and all

EMG data were sampled at 2000 Hz and stored for offline analysis.

6.2.3 Experimental protocols

Prior to the dynamic exercises described above, the subjects were asked to make approximately three maximal voluntary isometric contractions (MVICs) for the muscle group of interest. The maximal voluntary isometric contractions were performed according to the standard muscle strength testing positions that best isolate each respective muscle. Three MVICs were performed for each muscle using standard limb positions [118]. The participants were instructed to gradually increase their muscle contraction force toward maximum and then sustain the MVIC for approximately three seconds before slowly releasing the force, with 1 to 3 minutes of rest between contractions. Verbal encouragement was given during all of the trials [120-121].

At the start of each EMG recording session, all of the EMG channels were checked to ensure that strong signals were recorded with minimal noise. If signals were considered unsatisfactory, the electrodes were removed and re-positioned. The EMG data and applied weight/resistance were collected from the eight muscles of the right shoulder of each subject while the subjects performed on elbow and two shoulder movements using dumbbells and a resistance training exoskeleton.

Two exercise sessions (free-weight exercises and upper limb exoskeleton

motion) were conducted for evaluation purposes. Each session consisted of three resistance training exercises (shoulder abd-add, flx-ext, and elbow flx-ext) with four sets (1 kg and 3 kg of resistance; 1 second and 2 second motion speeds) for the male subjects and four sets (1 kg and 3 kg of resistance; 1 second and 2 seconds motion speeds) for the female subjects. Each movement was performed in a slow, controlled manner by lifting (1 second and 2 seconds) and lowering (1 second and 2 seconds) without any sudden jerks or acceleration for six consecutive repetitions. A metronome was employed to help the subjects maintain the tempo of their movements, and a maximum of five minutes rest was given between each set and exercise. Instructions on how to perform the motion were illustrated and demonstrated to the subjects at the beginning of the test. The subjects were also instructed to keep their left arms resting by their sides to ensure that they did not obscure or compensate for the motion of the right arm. The movement ranges evaluated and grip patterns used are shown in Fig. 5.3 in Chapter 5. The designated arm motions were included in the experimental protocol (Table 5.4). The dumbbell weights of 1 kg and 3 kg and equivalent resistances were set for the free-weight exercises and upper limb exoskeleton motions, respectively. If the subjects were obviously out of pace (too fast or too slow) or mistakes were made, the recordings were discarded, and the measurement was restarted. Warm-up trial practices were

allowed before the actual tests to reduce the number of failed trials due to inaccurate pacing or movement.

6.2.4 EMG analysis

All raw EMG signals, including the MVIC trials, were digitally band-pass filtered through a filter (10-200 Hz), and processed using a root mean square (RMS) algorithm with a 10-ms moving window. The equation of RMS is shown below:

$$RMS = \sqrt{\frac{1}{N}\sum_{i=1}^{N} v_i^2} \tag{6.1}$$

where v_i is the voltage value at the i th sampling and N is the number of sample in a segment. N was set to 20.

Root mean square is a technique for rectifying the raw signal and converting it into an amplitude envelope for easier viewing.

The collected data from the three MVICs for each muscle of the muscle group of interest were processed with the RMS, and the average EMG value of the maximum value of three trials was selected as the peak MVICs. All of the subsequent recordings were referenced back to the strongest effort observed and expressed as a percentage of the MVIC (% MVIC). As shown in Eq. (6.2), the raw EMG signals processed with RMS were normalized to the peak activity in the maximum isometric voluntary contraction trial and expressed as a percentage:

% MVIC=100% × (EMG value of movement / Average EMG value of the three peak MVIC) (6-2).

There are no absolute microvolt values (only a relative comparison to a maximal effort). Therefore, all muscle function can be reduced to the common feature of percentage of MVIC by normalizing the EMGs and the EMG amplitudes recorded from the same muscle on different occasions and from different muscle; thus, different individuals can be compared directly. The data were processed using Matlab (Mathworks Inc., Natick, MA).

For each exercise, we calculated the mean activation of the first three repetitions of each muscle with 1 kg and 3 kg loading at two motion speeds; if one of the three data trials was disqualified for data analysis, then the fourth, fifth, or sixth trial was substituted. All of the muscle activation data were normalized to the peak MVIC using Eq. (6.2).

6.3 Results and discussion

Tables 6.2 and 6.3 show the mean peak EMG activity and standard deviation of each muscle during the shoulder abd-add, shoulder flx-ext, and elbow flx-ext movements with 1 kg and 3 kg loading using dumbbells and a spring-loaded exoskeleton at two different motion speeds (1 second lifting and 1 second lowering; 2 second lifting and 2 second lowering). The number of acceptable subjects who

produced EMG amplitudes for each muscle test is displayed in Tables 6.2 and 6.3. When the subject inclusion criteria (for the EMG data) were applied, the data from a substantial number of subjects did not satisfy the criteria and were discarded. If the data acquired from a selected muscle of a subject during the dumbbell exercises were unqualified, the counterpart data from the subject during the spring-loaded exercises were also discarded and vice-versa.

Because of system technical problems and operation errors, the EMG data collected from S1, S4, and S6 during shoulder abd-add exercise with a spring-loaded exoskeleton (3 kg resistance) at 1 second lifting and 1 second lowering motion speed failed to be processed. The same problems were encountered for subject 6 with 1 kg resistance at 2 second lifting and 2 second lowering motion speed and subjects 2 and 6 with 3 kg resistance at 2 second lifting and 2 second lowering motion speed.

The data listed in Tables 6.2 and 6.3 show that for the shoulder abd-add, shoulder flx-ext, and elbow flx-ext exercises performed in this study with dumbbells or the spring-loaded exoskeleton, the level of muscle activation increased with the applied load, which confirms our hypothesis. The muscle groups primarily responsible for the designated exercise showed some similarities of muscle activation between the dumbbells and spring-loaded exoskeleton,

particularly in the shoulder flx-ext and elbow flx-ext exercises.

Table 6.2 The mean peak EMG activity of each muscle for the three resistance exercises expressed as a % of MVIC for peak muscle amplitude at 1 second lifting and 1 second lowering motion speed. Results are expressed as the mean (SD).

Muscles	N	DB	Exo	N	DB	Exo
		1 kg			3 kg	
Shoulder abduction-adduction						
Anterior deltoid	5	36(16)	42(11)	3	56(02)	53(20)
Middle deltoid	5	33(20)	38(19)	3	49(37)	63(17)
Posterior deltoid	5	25(17)	35(23)	3	28(23)	36(14)
Biceps brachii	5	12(15)	25(36)	3	11(08)	15(14)
Tricep brachii	5	19(36)	31(26)	3	19(19)	28(12)
Pectoralis major	5	17(15)	17(13)	3	23(18)	20(07)
Upper Trapezius	5	31(34)	38(23)	3	17(113)	32(34)
Supraspinatus	5	44(29)	54(23)	3	61(42)	69(19)
Shoulder flexion-extension						
Anterior deltoid	6	41(17)	33(10)	6	48(10)	45(13)
Middle deltoid	6	24(12)	25(15)	6	39(15)	31(18)
Posterior deltoid	6	15(08)	15(12)	6	25(22)	34(22)
Biceps brachii	5	15(21)	16(26)	5	25(23)	26(38)
Tricep brachii	6	24(33)	20(22)	6	50(55)	31(33)
Pectoralis major	6	26(17)	23(17)	6	33(21)	31(26)
Upper Trapezius	5	20(23)	17(13)	5	32(48)	57(44)
Supraspinatus	6	36(16)	39(15)	6	63(41)	73(34)
Elbow flexion-extension						
Anterior deltoid	6	10(06)	18(09)	6	19(09)	25(19)
Middle deltoid	6	6(05)	7(06)	6	20(16)	11(09)
Posterior deltoid	6	3(02)	7(05)	6	12(16)	07(03)
Biceps brachii	5	16(09)	18(04)	4	29(10)	24(04)
Tricep brachii	5	24(42)	24(35)	4	09(10)	09(09)
Pectoralis major	6	23(20)	14(9)	6	28(19)	15(10)
Upper Trapezius	6	12(21)	21(28)	6	24(40)	27(33)
Supraspinatus	6	23(14)	18(12)	6	30(18)	19(12)

N: number of subjects; DB: Dumbbell; Exo: Exoskeleton

Table 6.3 The electromyographic activity of each muscle for the three resistance exercises expressed as a % of MVIC for peak muscle amplitude at 2 second lifting and 2 second lowering motion speed. Results are expressed as the mean (SD).

Muscles	N	DB	Exo	N	DB	Exo
		1 kg			3 kg	
Shoulder abduction-adduction						
Anterior deltoid	5	37(06)	43(10)	3	59(23)	45(09)
Middle deltoid	5	43(19)	44(22)	3	62(26)	53(13)
Posterior deltoid	5	23(16)	39(25)	3	39(17)	27(10)
Biceps brachii	5	17(26)	31(52)	3	23(23)	36(43)
Tricep brachii	5	24(33)	29(30)	3	46(61)	37(33)
Pectoralis major	5	20(14)	18(12)	3	28(21)	27(20)
Upper Trapezius	5	49(55)	66(60)	3	58(62)	48(23)
Supraspinatus	5	42(17)	38(12)	3	51(18)	45(18)
Shoulder flexion-extension						
Anterior deltoid	6	33(16)	30(11)	6	44(11)	40(08)
Middle deltoid	6	27(09)	27(16)	6	39(14)	34(22)
Posterior deltoid	6	15(08)	25(13)	6	28(19)	29(15)
Biceps brachii	5	15(20)	19(33)	5	21(22)	21(26)
Tricep brachii	6	22(35)	26(25)	6	25(29)	36(16)
Pectoralis major	6	27(16)	22(14)	6	28(17)	27(08)
Upper Trapezius	5	26(26)	49(46)	5	50(31)	34(27)
Supraspinatus	6	35(23)	48(16)	6	51(25)	66(43)
Elbow flexion-extension						
Anterior deltoid	6	12(13)	23(12)	6	20(14)	18(13)
Middle deltoid	6	09(07)	10(07)	6	23(21)	08(05)
Posterior deltoid	6	06(03)	09(07)	6	08(05)	12(07)
Biceps brachii	5	14(09)	17(03)	4	25(10)	23(05)
Tricep brachii	5	37(62)	33(46)	4	22(29)	26(31)
Pectoralis major	6	31(20)	22(11)	6	26(22)	24(12)
Upper Trapezius	6	19(30)	19(16)	6	31(30)	22(20)
Supraspinatus	6	23(20)	24(20)	6	37(34)	12(08)

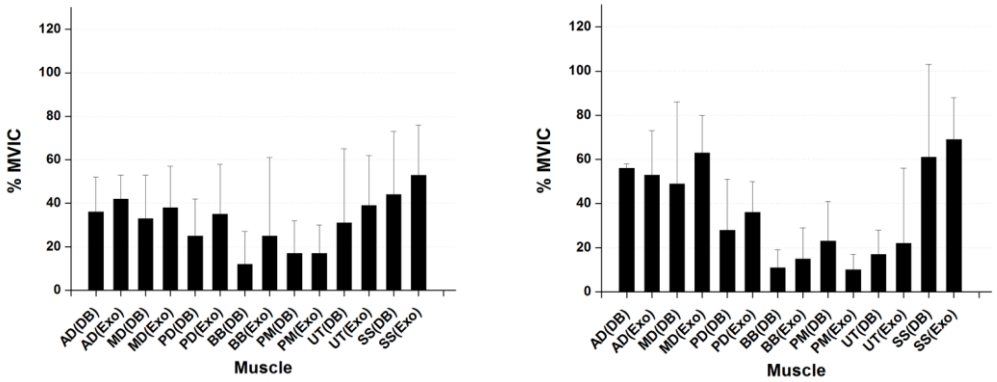

a) 1 kg load b) 3 kg load

Fig. 6.3 Muscle activation during the shoulder abduction-adduction exercise (at 1 second lifting and 1 second lowering motion speed).

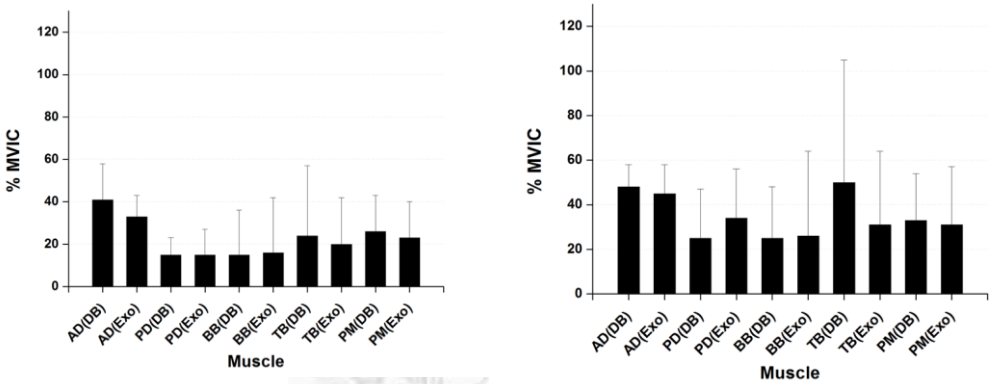

a) 1 kg loading b) 3 kg loading

Fig. 6.4 Muscle activation during the shoulder flexion-extension exercise (at 1 second lifting and 1 second lowering motion speed).

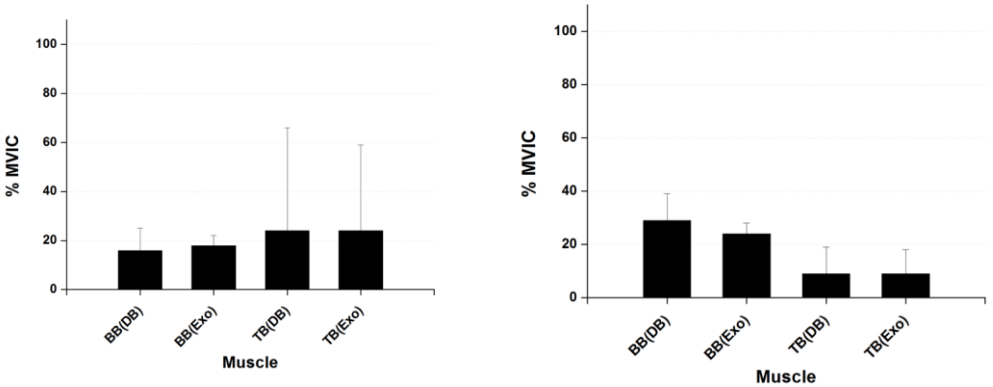

a) 1 kg loading b) 3 kg loading

Fig. 6.5 Muscle activation for during elbow flexion-extension exercise (at 1 second lifting and 1 second lowering motion speed).

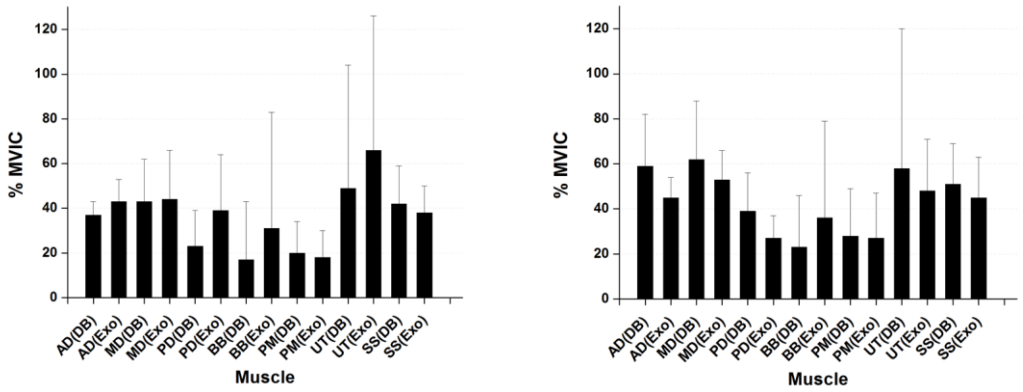

a) 1 kg loading b) 3 kg loading

Fig. 6.6 Muscle activation for during shoulder abd-add exercise (at 2 second lifting and 2 second lowering motion speed).

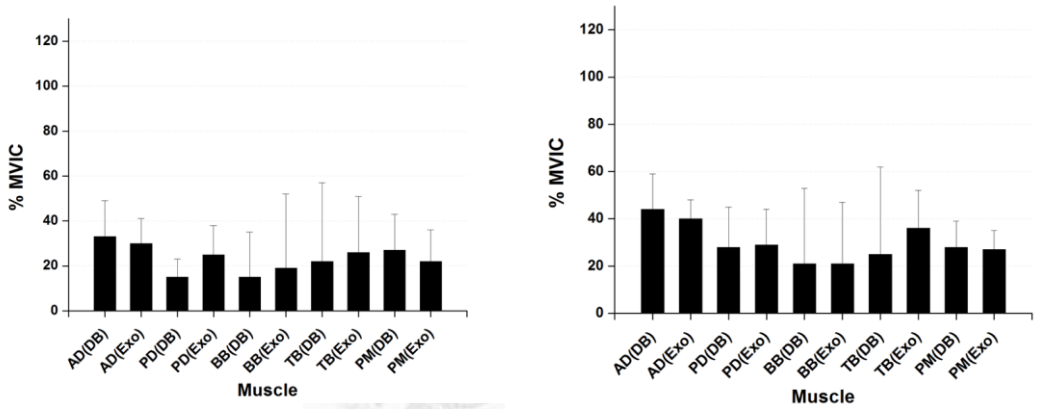

a) 1 kg loading b) 3 kg loading

Fig. 6.7 Muscle activation during the shoulder flx-ext exercise (at 2 second lifting and 2 second lowering motion speed).

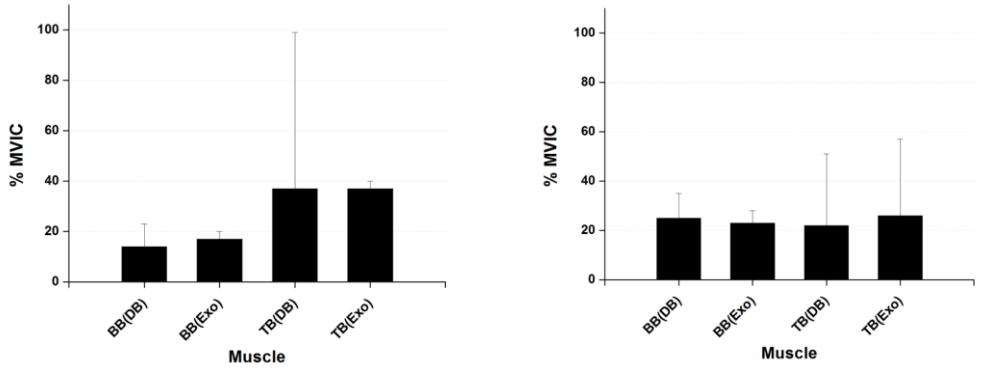

a) 1 kg loading b) 3 kg loading

Fig. 6.8 Muscle activation during the elbow flx-ext exercise (at the 2 second lifting and the 2 second lowering motion speed).

AD, MD, PD, BB, PM, UT, and SS are primarily responsible for the shoulder abd-add of the arm [113-114]. Figs. 6.3 (a) and (b) demonstrates the muscle activation during the shoulder abd-add exercise at the 1 second lifting and 1 second lowering motion speed with the 1 kg and 3 kg loading. AD, PD, BB, TB, and PM contributed the most in the shoulder flx-ext movement of the eight muscles investigated. The muscle activity of AD, PD, BB, TB and PM all showed good consistency.

Figs. 6.4 (a) and (b) demonstrate muscle activation during the shoulder flx-ext exercise with the 1 second lifting and 1 second lowering motion speed with the 1 kg and 3 kg loading; AD, PD, BB, TB, and PM contributed the most to doing shoulder flx-ext exercise in the eight muscles investigated. The muscle activity of AD, PD, BB, TB and PM showed good consistency.

Figs. 6.5 (a) and (b) demonstrate muscle activation during the elbow flx-ext exercise at the 1 second lifting and 1 second lowering motion speed with the 1 kg and 3 kg loading. Of the eight muscles investigated, BB and TB were most closely related. The muscle activity show good consistency; however, TB (DB) and TB (Exo) under the 3 kg load did not meet our expectations.

Figs. 6.6 (a) and (b) demonstrate muscle activation during the shoulder abd-add exercise at the 2 second lifting and 2 second lowering motion speed with

the 1 kg and 3 kg loading; of the eight muscles investigated, AD, MD, PD, BB, PM, and SS were most closely related. The muscle activity of AD, MD, and SS showed good consistency.

Fig. 6.7 demonstrates muscle activation during the shoulder flx-ext exercise with the 2 second lifting and 2 second lowering motion speed with the 1 kg and 3 kg loading; AD, PD, BB, TB, and PM are prime movers of the movement investigated. The muscle activity of AD, PD, BB, TB, and PM showed good consistency as the load increased from 1 kg to 3 kg .

Fig. 6.8 demonstrates the muscle activation during the elbow flx-ext exercise with the 2 second lifting and the 2 second lowering motion speed with the 1 kg and the 3 kg loading. Of the eight muscles investigated, BB and TB were the most closely related. The muscle activation was consistent during the exercises with the dumbbells and spring-loaded exoskeleton; however, TB (DB) and TB (Exo) under the 3 kg load did not meet our expectations.

Generally, the spring-loaded exoskeleton demonstrated similarity to dumbbell exercises when performing the designated movements in this study; however, inconsistencies remain in the test results that may be attributed to the experiment procedures, data processing, or precision of the spring-loaded exoskeleton. To avoid inaccuracies that could influence the subsequent values of muscle amplitude

and timing, it is necessary to ensure that the placement of the EMG electrodes is identical between all of the subjects and across test sessions. It is suggested that a standardized procedure (described in the experimental protocol) be followed strictly and that the same person be used for each collection assessment. To our knowledge, no studies have been performed that indicate which method provides the most reliable results. Despite the method used, the MVIC production depends on the subject providing maximum effort. Maximum effort can vary between individuals; therefore, one cannot always be certain that MVIC has been obtained. There are the same concerns regarding the variation of the applied resistance. Therefore, it is suggested that to maintain consistency, the positioning and resistance applied should be conducted by the same person. We recognized that our prototype is not perfect, and the small number of participants resulted in the limited strength of the statistical findings. However, this study provides evidence from another perspective to further support our previous study regarding the shoulder and elbow joint torques when performing the designated exercises with dumbbell or SLERT measured by using a motion capture system illustrated in Chapter 5.

6.4 Summary

In this experimental study, the EMG data were collected from three male and three female healthy subjects. The muscle activation and applied loads quantified in this study during the three exercises were as follows: shoulder abd-add, shoulder flx-ext, and elbow flx-ext exercises using dumbbells and a spring-loaded exoskeleton at two different motion speeds. A few muscle activations were not in accordance with our expectations. Generally, most of the results confirmed our hypothesis that the levels of muscle activation and applied loading were similar when comparing dumbbells with a spring-loaded upper limb exoskeleton. The spring-loaded exoskeleton appears to have equivalent muscle activation in terms of the peak percentage of MVIC on the muscles primarily responsible for the designated movement, which provides further evidence to support our previous joint torques study. We recognize that the glenohumeral joint is complex, with many muscles that contribute to even simple movements, and we only evaluated eight of the many muscles that can influence shoulder movement. The small sample size number the strength of the statistical findings. Nevertheless, this experimental study provided a performable test and also collected valuable data for the design improvement and continuing study of spring-loaded exoskeletons for resistance training.

Chapter 7
Conclusion and future work

Robotic device development for rehabilitation and health care applications is a quite active field of research, particularly in the after-stroke care area. There is increasing interest in extending the use of these devices to different types of diseases, ranging from the acute to the chronic phase, and these devices may be applicable during inpatient care, after discharge, and during follow-up for community outpatient rehabilitation and health care.

In fact, the AHA has suggested that robot-assisted therapy for the upper extremities (UEs) has achieved Class IIa (level of evidence A) for stroke care in the inpatient setting and Class I (level of evidence A) for stroke care in outpatient and chronic care settings. Class I is defined as “Benefit>>>Risk. Procedure/Treatment SHOULD be performed/administrated;” Class IIa is defined as “Benefit>>Risk. IT IS REASONABLE to perform procedure/administer treatment;” and Level A is defined as “Multiple populations evaluated: Data derived from multiple randomized clinical trials or meta-analyses” in the AHA 2010 guidelines for stroke care. The 2010 Veterans Administration/Department of Defense (VA/DoD) guidelines for stroke care suggest that robot-assisted movement therapy for the UEs has already

achieved strength of recommendation level B ("A recommendation that clinicians provide (the service) to eligible patients. At least fair evidence was found that the intervention improves health outcomes and concludes that benefits outweigh harm"). These endorsements came 21 years after the initial MIT-Manus program began in 1989. The use of robotic technology to assist in recovery after neurological injury has proven to be safe, feasible, and effective for the UEs for stroke populations. Notwithstanding the substantial progress in acute stroke care, the focus of research, stroke medical advances, and healthcare resources has been on acute and subacute recovery phases, with less attention given to the more chronic recovery phases, which has resulted in substantial health disparities in later phases of stroke care. These facts clearly indicate the state of the art, and there remains a need to educate the nursing staff and other members of the interdisciplinary team about the potential for recovery. There is also a need for rehabilitation robotic devices in the later or more chronic phase of stroke care and other chronic diseases. From a preventive medicine point of view, it might be more important to effectively reduce the risk of adverse health outcomes for people of all ages in advance, particularly for the elderly [122-123].

Most rehabilitation and health care robotic devices are primarily designed to actively assist patients with motions. In contrast, most exercise training devices are

body-power oriented. The users are expected to perform the motion by themselves to gain strength, power, and endurance from the exercise. This dissertation proposed a rehabilitation exercise training device from a strength exercise point of view to reduce the risk of adverse health outcomes and developed a general design scheme for spring-loaded upper limb exoskeletons for resistance training: the equivalence concept, a kinematic model, a dynamic model, motion analysis, and an EMG evaluation were utilized. Efforts have been made through these investigations to better understand the physical significance of using a spring-loaded exoskeleton for upper limb resistance training. As a result, alternative designs, inventions, and new applications can be developed more easily, systematically, and efficiently for the benefit of society.

7.1 Lessons have been learned

A general challenge of the application of exoskeletons is their proper adjustment to the anatomical constraints of the different types of joints. The adaptation to different body sizes is more difficult than in end-effector-based systems. A quickly adjustable joint design for easier use is essential for easier clinical and at-home use.

Engineers always struggle with the stiffness, weight, shape, and dimension of mechanical component designs, not to mention the cost. In practice, many

standardized components, such as bearings, springs and slide screws, are commercially available; therefore, compromises in dimensions, weight, and cost are made in the selection of these components, and limitations regarding the shape, size, weight, and material properties are imposed on the designer. For example, in our first and second prototype, the slide screws and nuts for adjusting the length of the zero-free-length spring along with the K_2 and K_3 spring are installed in link 2; the total weight and inertia of link 2 are inevitably increased, and the shoulder abd-add motion is subsequently affected.

Spring installation often involves counterbalances among the springs and attached links or attached components. As a result, large internal forces on the spring struts may cause bending of the attached link, and increased contact friction on the kinematic parts will affect the smoothness of the motion or the joint adjustment of the exoskeleton. Placing all of the spring attachments as close to the center of the links and components as possible or counterbalancing the moment also improves the link bending problem. Equipping the kinematic components with bearings will reduce the contact friction; however, it will not only increase the complexity of the design, manufacture, and assembly, it will also increase the weight, cost, and dimensions of the device.

Valuable time and resources are consumed in the iterative design process and

while waiting for the prototype to be built and for components to be reworked. “Doing the right thing” and “doing the thing right” are both important yet difficult to achieve, particularly when there are many uncertainties in the design and manufacturing process. Detailed design reviews and cross-team communication are helpful in reducing mistakes.

Currently, there is no clear design target available for rehabilitation-focused robotic exercise training devices or any reliable standard against which to measure their performance and effectiveness. Slow and painstaking experimental trials and the accumulation of evidence are also necessary to demonstrate progress. The function test is not focused only on the mechanism of the system like the conventional machine test is; subjects also play an important role in the biomechanical evaluation test. Having the correct equipment is a fundamental consideration for the development of a successful experiment, and appropriate technical skills to operate the system are required for successful high-quality data collection. All of these considerations make the coordination of the experiment more complex and usually time-consuming. Therefore, scientific training to use the tools and a well-planned experiment are essential to further our knowledge of the field of study.

7.2 Summary of contributions

The contributions made by this research are summarized below:

1. A spring-loaded upper limb exoskeleton is proposed to provide adjustable resistance for the elderly and clinical populations for resistance training at the shoulder and elbow joints in different planes. The exoskeleton is capable of reducing the unfavorable lengthening of muscles during high-intensity free-weight exercises and joint overload caused by large moments of inertia.
2. To formulate the kinematic and dynamic models necessary to develop the required design criteria for the spring-loaded exoskeleton for resistance training, an equivalent concept is introduced that is mechanically analogous to free-weight exercises.
3. The configuration and constructed mechanical components of a spring-loaded upper limb exoskeleton prototype were designed using the zero-free-length spring concept and the developed design criteria.
4. A motion capture and EMG experimental design appropriate for performing the required mechanical and biomechanical assessment of the upper limb exoskeleton resistance training devices was established.
5. The device was evaluated through the established experimental design with three male and three female healthy young subjects and a biomechanical

analysis: joint torques and the muscle activities of eight major upper limb muscles were determined while performing the designated resistance training.

7.3 Recommendations for future work

It is recommended that the following changes be made to the spring-loaded exoskeleton for resistance training in continuing research.

1. A more dexterous shoulder joint design is needed to provide a wider range of motion in 3-D space. It is desirable that the resistance training exoskeleton not compromise the natural upper limb motion and workspace of the users.
2. Current exoskeleton designs tend to exercise only the proximal arm, and thus they provide movement training at the shoulder and partially at the elbow but not at the wrist and hand; consequently, exoskeletons that train the shoulder and partially train the elbow are limited in their ability to improve the completion of upper limb resistance exercises.
3. Equipping the exoskeleton with sensors to record simultaneous kinematic and force data could provide researchers, patients, and therapists with immediate measures of training performance, and this may offer new opportunities for designing better devices and therapeutic programs, ultimately increasing the efficiency of rehabilitation training.
4. Developing an intuitive user interface for self-operation of the device by the

users.

5. Developing a more compact design for the device so that it is more cost effective and portable.

It is recommended that more cross-disciplinary focus groups be conducted to evaluate further devices, especially focus groups with therapeutic exercise professionals and additional focus groups involving the elderly and their caregivers.

A full biomechanical study of the prototype should be performed in different configurations with more subjects, particularly for targeted special interest groups. In addition, clinical trials of the device would be necessary to determine its clinical efficacy.

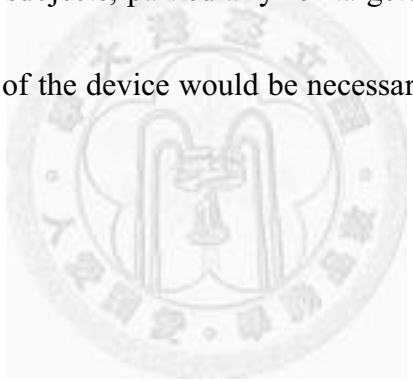

References

〔1〕 World Health Organization, *Global Strategy on Diet, Physical Activity and Health*, Geneva, WHO, May, 2004.

〔2〕 European Commission, *EU physical activity guidelines. Recommended policy actions in support of health-enhancing physical activity*. Brussels: EU Working Group - Sport and Health, 2008.

〔3〕 U. S. Department of Health and Human Services, *Physical Activity Guidelines for Americans*, October, 2008.

〔4〕 Caspersen C. J., Powell K. E., Chritenson G. M., Physical activity, exercise, and physical fitness, *Public Health Report* 1985;100:125-131.

〔5〕 Department of Health and Human Services. *Physical Activity Fundamental to Preventing Disease*, June 20, 2002.

〔6〕 Warburton D. E. R., Nicol C. W., and Bredin S. S. D., Health benefits of physical activity: the evidence, *Canadian Medical Association Journal* 2006; 174(6): 801-809.

〔7〕 Kruk J., Physical activity and health, *Asian Pacific Journal of Cancer Prevention* 2009; 10: 721-728.

〔8〕 Haskell W. L., Lee, I. M., Pate, R. R., Powell, K. E., Blair, S. N., Franklin, B. A., Macera, C. A., Heath, G. W., Thompson, P. D., and Bauman, A., Physical activity and public health: updated recommendation for adults from the ACSM and AHA, *Circulation* 2007;116:1081-1093.

〔9〕 American College of Sports Medicine, Position stand: progression models in resistance training for healthy adults, *Medicine & Science in Sports & Exercise* 2002;34:364-380.

〔10〕 Faigenbaum A. D., Kraemer W. J., Blimkie C. J. R., Jeffreys I., Micheli L. J., Nitka M., and Rowland T. W., Youth resistance training: Updated position statement paper from the National Strength and Conditioning Association, *Journal of Strength & Conditioning Research* 2009;23(5):S60–S79.

〔11〕 Williams M. A., Haskell, W. L., Ades, P. A., Amsterdam, E. A., Bittner, V., Franklin, B. A., Gulanick, M., Laing, S. T., and Stewart, K. J., Resistance Exercise in Individuals With and Without Cardiovascular Disease: 2007 update, *Circulation* 2007;116:572-584.

〔12〕 Ries A. L., Bauldoff G. S., Carlin B. W., Casaburi, R., Emery C. F., Mahler D. A., Make B., Rochester C. L., ZuWallack R., and Herrerias C., Pulmonary Rehabilitation: Joint ACCP/AACVPR Evidence-Based

Clinical Practice Guidelines, *Chest* 2007;131:4S-42S.

〔13〕 Sigal R. J., Kenny G. P., Wasserman, D. H., Castaneda-Sceppa C., and White R. D., Physical Activity/Exercise and Type 2 Diabetes: A consensus statement from the American Diabetes Association, *Diabetes Care* 2006;29(6): 1433-1438.

〔14〕 Pollock M. L. and Vincent K. R., Resistance training for health, *Presidents Council Physical Fitness Sports Research Digest* 1996;2(8):1-9.

〔15〕 Stone M., Plisk S., and Collin D., Training principles: evaluation of modes and methods of resistance training--a coaching perspective, *Sports Biomechanics* 2002;1(1):79-103.

〔16〕 United Nations Department of Economic and Social Affair, Population Division, *World Population Prospects: The 2010 Revision*, New York, 2011.

〔17〕 http://esa.un.org/unpd/wpp/unpp/panel_population.htm.

〔18〕 Mackay J. and Mensah G. A., *The atlas of heart disease and stroke*, Geneva (Switzerland): World Health Organization, 2004.

〔19〕 Roger V. L. et al., Heart Disease and Stroke Statistics—2012 Update: A Report From the American Heart Association, *Circulation* 2012;125: e2-e220.

〔20〕 Krebs H. I., Hogan N., Aisen M. L., and Volpe B. T., Robot-aided neurorehabilitation, *IEEE Transactions on Rehabilitation. Engineering* 1998;6: 75-87.

〔21〕 Burgar C. G., Lum P. S., Shor P. C., and Machiel H. F. Van der Loos, Development of Robots for Rehabilitation Therapy: The Palo Alto VA/Stanford experience, *Journal of Rehabilitation Research and Development* 2000; 37(6): 663-673.

〔22〕 Loureiro R. , Amirabdollahian F. , Topping M., Driessen B., and Harwin W., Upper Limb Robot Mediated Stroke Therapy—GENTLE/s Approach, *Autonomous Robots* 2003; 15(1): 35-51.

〔23〕 Reinkensmeyer D. J., Kahn L. E., Averbuch M., Mckenna-Cole A., Schmit B. D., and Rymer W. Z., Understanding and Treating Arm Movement Impairment after Chronic Brain Injury: Progress with the ARM guide, *Journal of Rehabilitation Research and Development* 2000; 37(6): 653-662.

〔24〕 Riener R., Nef T., and Colombo G., Robot-aided neurorehabilitation of the upper extremities, *Medical and Biological Engineering and Computing*, 2005; 43: 2-10.

〔25〕 Prange G. B., Jannink M. J. A., Groothuis-Oudshoorn C. G. M., Hermens

H. J., and IJzerman M. J., Systematic review of the effect of robot-aided therapy on recovery of the hemiparetic arm after stroke, *Journal of Rehabilitation Research and Development* 2006; 43(2): 171-184.

〔26〕 Kwakkei G., Kollen B. J., and Krebs H. I., Effects of robot-assisted therapy on upper limb recovery after stroke: a systematic review, *Neurorehabilitation and Neural Repair* 2008; 22(2): 111-121.

〔27〕 Lo H. S. and Xie S. Q., Exoskeleton robots for upper-limb rehabilitation: State of the art and future prospects, *Medical Engineering and Physics* 2012; 34: 261-268.

〔28〕 Zoss A. B., Kazerooni H., and Chu A., Biomechanical design of the Berkeley Lower Extremity Exoskeleton (BLEEX), *IEEE/ASME Trans. Mechatronics* 2006; 11(2): 128–138.

〔29〕 Kawamoto H. and Sankai Y., Power assist system HAL-3 for gait disorder person, in *Proc. Int. Conf. Comput. Helping People Special Needs (ICCHP)* (Lecture Notes on Computer Science), vol. 2398, Berlin, Germany: Springer-Verlag, 2002.

〔30〕 Housman S. J., Rahman V. L.T., Sanchez R. J. Jr., and Reinkensmeyer D. J., Arm-Training with T-WREX After Chronic Stroke: Preliminary Results of a Randomized Controlled Trial, Rehabilitation Robotics, ICORR 2007. IEEE 10th International Conference: 562-568.

〔31〕 Sanchez, R. J., Wolbrecht, E. T., Smith R., Liu J., Rao S., Cramer S., Rahman T., Bobrow J. E., and Reinkensmeyer D. J., A pneumatic robot for re-training arm movement after stroke: Rationale and mechanical design, in Rehabilitation Robotics, 2005, ICCOR 2005, 9th International Conference, 2005: 500-504.

〔32〕 Nef T., Guidali M., and Riener R., ARMin III-arm therapy exoskeleton with an ergonomic shoulder actuation, *Applied Bionics and Biomechanics* 2009; 6: 127-142.

〔33〕 Balasubramanian S., Wei R., Perez M., Shepard B., Koeneman E., Koeneman J., and He J., RUPERT: An Exoskeleton Robot for Assisting Rehabilitation of Arm Functions, *Virtual Rehabilitation*, 2008: 163-167.

〔34〕 Perry J. C., Rosen J., and Burns S., Upper-limb powered exoskeleton design, *IEEE/ASME Transactions on mechatronics* 2007; 12(4): 408-417.

〔35〕 Klein J., Spencer S. J., Allington J., Minakata K., Wolbrecht E. T., Smith R., Bobrow J. E., and Reinkensmeyer D. J., Biomimetric Orthosis for the Neurorehabilitation of the Elbow and Shoulder (BONES), Proceedings of the 2nd Biennial IEEE/RAS-EMBS internal Conference on Biomedical Robotics and Biomechronics, Scottsdale, AZ, USA, Oct., 2008: 535-541.

〔36〕 Tsagarakis N. G., and Caldwell D. G., Development and Control of a 'Soft-Actuated' Exoskeleton for Use in Physiotherapy and Training, *Autonomous Robots* 2003; 15: 21–33.

〔37〕 Arno H. A. Stienen , Edsko E. G. Hekman, Alfred C. Schouten, Frans C. T. van der Helm, and Herman van der Kooij Suitability of hydraulic disk brakes for passive actuation of upper-extremity rehabilitation exoskeleton, Applied Bionics and Biomechanics 2009; 6(2): 103-114.

〔38〕 Gijbels D., Lamers L., Kerkhofs L., Alders G., Knippenberg E., and Feys P., The Armeo Spring as training tool to improve upper limb functionality in multiple sclerosis: a pilot study, *Journal of NeuroEngineering and Rehabilitation* 2011; 8(1): 5.

〔39〕 Rocon E., Belda-Lois J. M., Ruiz A. F., Manto M., Moreno J. C., and Pons J. L., Design and Validation of a Rehabilitation Robotic Exoskeleton for Tremor Assessment and Suppression, IEEE Transactions on Neural Systems and Rehabilitation Engineering 2007; 15(3): 367-378.

〔40〕 Mikołajewska E., and Mikołajewski D., Exoskeletons in Neurological Diseases– Current and Potential Future Applications, Adv Clin Exp Med 2011; 20(2): 227–233.

〔41〕 Voris H. C., Handle and Exercise Arm Assembly for Use with Exercise Machine, U. S. Patent 6,394,937, May 28, 2002.

〔42〕 Webber R. T., Hockridge B., and Meredith J. O., Rigid Arm Pull Down Exercise Machine, U. S. Patent, 7601187 B2, Oct. 13, 2009.

〔43〕 Webber R. T., Hockridge B., and Meredith J. O., Chest Press Exercise Machine with Self-Aligning Pivoting Upper Support, U. S. Patent 7670269 B2, Mar. 2, 2010.

〔44〕 Liao C. S., Arm Exerciser, U. S. Patent 7,235,038 B2, June 26, 2007.

〔45〕 Laudone J. A., Jointed Bar for an Exercise Machine, U. S. Patent, 5613928, Mar. 25, 1997.

〔46〕 Howell L. L. and Magleby S. P., Substantially Constant-Force Exercise Machine, U. S. Patent 7,060,012, Jun. 13, 2006.

〔47〕 Lu E. C., Wang R. H., Heebert D., Boger J., Galea M. P., and Mihailidis A., The development of an upper limb stroke rehabilitation robot: identification of clinical practices and design requirements through a survey of therapists, Disability and Rehabilitation, *Assistive Technology* 2011; 6(5): 420-431.

〔48〕 Garcia N., Sabater-Navarro J. M., Gugliemeli E., and Casala A., Trends in rehabilitation robotics, *Medical Biological Engineering & Computing* 2011; 49: 1089-1091.

〔49〕 Brochard S., Robertson J., Me´de´e B., and Re´my-Ne´ris O., What's new in new technologies for upper extremity rehabilitation?, *Current Opinion in Neurology* 2010; 23: 683–687.

〔50〕 Oatis C. A., *Kinesiology: The Mechanics & Pathomechanics of Human Movement*, second ed., Lippincott Williams & Wilkins, Baltimore, 2009.

〔51〕 Hisamoto S., and Higuchi M., *Age-related Changes in Muscle Strength of Healthy Japanese*, Standardization Center, NITE, Osaka, Japan, Human and Welfare Technology Division, 2007.

〔52〕 Hass C. J., Feigenbaum M. S., and Franklin B. A., Prescription of Resistance Training for Healthy Populations, *Sports Medicine.* 2001; 31(14): 953-964.

〔53〕 Teixeira-Salmela L. F., Olney S., Nadeau J. S., and Brouwer B., Muscle Strengthening and Physical Conditioning to Reduce Impairment and Disability in Chronic Stroke Survivors, *Archives Physical Medicine and Rehabilitation* 1999; 80(10): 1211-1218.

〔54〕 Scarborough D. M., Krebs D. E., and Harris B. A., Quadriceps Muscle Strength and Dynamic Stability in Elderly Persons, *Gait & Posture* 1999; 10(1): 10-20.

〔55〕 Denavit J. and Hartenberg R. S., Kinematic notation for lower pair mechanisms based on matrices, ASME Journal of Applied Mechanics 1955; 77: 215-221.

〔56〕 Baechle T. R. and Earle R., *Essentials of Strength Training and Conditioning*, Human Kinetics, National Strength & Conditioning Association, U.S., 2000.

〔57〕 Klopcar N., and Lenarcic J., Kinematic Model for Determination of Human Arm Reachable Workspace, *Meccanica* 2005; 40(2): 203-219.

〔58〕 Banala S. K., Agrawal S. Fattah K., Krishnamoorthy A., V., Hsu W. L., Scholz J., and Rudlph K., Gravity-Balancing Leg Orthosis and Its Performance Evaluation, *IEEE Trans on Rob* 2006; 22(6): 1228-1239.

〔59〕 Barents R., Schenk M., Van Dorsser W. D., Wisse B.M., and Herder J. L., Spring-to-spring Balancing as Energy-free Adjustment Method in Gravity Equilibrators, Proc. ASME Int Des Eng Tech Conf Comput Inf Eng Inf. Eng. Conf. DETC **7** (part B) 2009; 689-700.

〔60〕 Hamill J. and Knutzen K. M., *Biomechanical Basis of Human Movement*, third ed., Lippincott Williams & Wilkins, Baltimore, 2009.

〔61〕 Clauser C. E., McConville J. T., and Young J. W., *Weight, volume, and center of mass of segments of the human body*, Aerospace Medical Research Laboratories, Wright-Patterson Air Force Base, Dayton, Ohio,

AMRL-TR-69-70, 1969.

〔62〕 The Stock Precision Engineered Components (SPEC), Associated Spring , [Online].Available:http://springming.so-buy.com/ezfiles/springming/img/img/61161/SPEC-04E.pdf.

〔63〕 Li Z. and Kota S., Virtual Prototyping and Motion Simulation with ADAMS, *Journal of Computing and Information Science in Engineering* 2001; 1(3): 276-279.

〔64〕 Renault M. and Ouezdou F. B., Dynamic simulation of hand-forearm system, IEEE International Workshop on Robot and Human Interactive Communication 2001: 20-25.

〔65〕 Li J.,Cheng Q., Liang H., and Guo Z., The Motion Simulation of Human Lower Extremity Based on Dynamics, 7th Asian-pacific Conference on Medical and Biological Engineering IFMBE Proceedings 2008; 19 (part 5): 151-154.

〔66〕 Yin X. and Xu Y., Design and Simulation of Chinese Massage Robot Based on Parallel Mechanism, International Conference on Mechanic Automation and Control Engineering (MACE) 2010: 2512-2515.

〔67〕 Naval Biodynamics Laboratory, *Anthropometry and Mass Distribution for Human Analogues, Volume I: Military Male Aviators*, Naval Medical Research and Development Command Bethesda, New Orleans, LA. 1988.

〔68〕 Chandler R. F., Clauser C. E., McConville J. T., Reynolds H. M., and Young J. W., *Investigation of Inertial Properties of the Human Body*, Aerospace Medical Research Laboratory, Wright-Patterson AFB, Ohio, AFAMRL-TR-74-137, 1974.

〔69〕 Institute of Occupational Safety & Health, 2008, [Online]. Available: http://www.iosh.gov.tw/Publish.aspx?cnid=26&P=812

〔70〕 Kraemer, W.J. and Ratamess, N.A., Fundamentals of resistance training: progression and exercise prescription, *Medicine and Science in Sports and Exercise*. 2004; 36(4): 674-688.

〔71〕 Taylor, N.F., Dodd, K.J., and Damiano, D. L., Progressive resistance exercise in physical therapy: A summary of systematic reviews, *Physical. Therapy*. 2005; 5(11): 1208-1223.

〔72〕 Risser W. L., Weight-training injuries in children and adolescents, *Amercian Family Physician*. 1991; 44: 2104-2110.

〔73〕 Kerr, Z. Y., Collins C. L., and Comstock R. D., Epidemiology of weight training-related injuries presenting to United States emergency departments, 1990 to 2007, *The American Journal of Sports Medicine*, Apr. 2010; 38(4): 765-771.

〔74〕 Lavallee M. E. and Balam T., An overview of strength training injuries: acute and chronic, *Current sports Medicine Report* 2010; 9(5): 307-313.

〔75〕 Buckley, M. A., Yardley, A., Johnson, G. R., and Carus, D. A., Dynamics of the upper limb during performance of the tasks of everyday living-a review of the current knowledge base," *Proceedings of the Institution of Mechanical Engineers*, *Part H: Journal of Engineering in Medicine* 1996; 210: 241-247.

〔76〕 Myer, K., *Biomedical Engineering and Design Handbook*, 2nd ed., McGraw-Hill, New York, 2009.

〔77〕 Hollerbach, J. M. and Flash, T, Dynamic interactions between limb segments during planar arm movement, *Biological Cybernetics* 1982; 44(1): 67-77.

〔78〕 Nef, T., Mihelj, M., and Riener, R., ARMin: a robot for patient-cooperative arm therapy, *Medical and Biological Engineering and Computing* 2007; 45: 887-900.

〔79〕 Nagarsheth H. J., Savsani P. V., and Patel M. A., Modeling and Dynamics of Human Arm, *4th IEEE* Conference on *Automation. Science and Engineering*, *Washington* 2008; 924-928.

〔80〕 Apkarian J. Naumann S., and Cairns B., A three-dimensional kinematic and dynamic model of the lower limb, *Journal of Biomechanics* 1989;22(2): 143-155.

〔81〕 Requejo P. S., Wahl D. P., Bontrager E. L., Newsam C. J., Gronley J. K., Mulroy S. J., and Perry, J., Upper extremity kinetics during Lofstrand crutch-assisted gait, *Medical Engineering and Physics.* 2005; 27: 19-29.

〔82〕 Thomas J. S., Corcos D. M., and Hasan Z., Kinematic and kinetic constraints on arm, trunk, and leg segments in target-reaching movement, *Journal of Neurophysiology.* 2005; 93: 352-364.

〔83〕 Shemmell J.,Corcos D.M., and Hasan Z., Kinetic and kinematic adaptation to anisotropic load, *Experimental Brain Research* 2009;192:1-8.

〔84〕 Nagano A., Yoshioka S., Komura T., Himeno R., and Fukashiro, S., A three-dimensional linked segment model of the whole human body, *International Journal of Sport and Health Science* 2005; 3: 311-325.

〔85〕 AbdulRahman S. A., Rambely A. S., and Ahmad R. R., A biomechanical model via Kane's equation─solving trunk motion with load carriage, *American Journal of Scientific and Industrial Research* 2011; 2(4): 678-685.

〔86〕 Anglin C and Wyss U.P., Review of arm motion analyses, *Proceedings of the Institution of Mechanical Engineers; Part H: Journal of Engineering*

in Medicine 2000; 214(5): 541-555.

〔87〕 Richards J.G., The measurement of human motion: A comparison of commercially available system, *Human. Movement. Science.* 1999; 18: 589-602.

〔88〕 Zhou H. and Hu H., Human motion tracking for rehabilitation-A survey, Biomed. *Signal Process Control* 2008; 3: 1-18.

〔89〕 Cappozzo A., Croce U.D., Leardini A., and Chiari L., Human movement analysis using sterophotogrammetry, Part 1: theoretical background, *Gait and Posture* 2005; 21: 186-196.

〔90〕 Chiari L., Croce U.D., Leardini A., and Cappozzo, A., Human movement analysis using sterophotogrammetry, Part 2: Instrumental errors, *Gait and Posture* 2005; 21: 197-211.

〔91〕 Leardini A., Chiari L., Croce U.D., and Cappozzo A., Human movement analysis using sterophotogrammetry, Part 3: Soft tissue artifact assessment and compensation, *Gait and Posture* 2005; 21: 212-225.

〔92〕 Croce U.D., Leardini A., Chiari L., and Cappozzo A., Human movement analysis using sterophotogrammetry, Part 4: assessment of anatomical landmark misplacement and its effects on joint kinematics, *Gait and Posture* 2005; 21: 226-237.

〔93〕 Schmidt R., Disselhorst-Klug C., Silny J., and Rau G., A marker-based measurement procedure for unconstrained wrist and elbow motions, *Journal of Biomechanics* 1999; 32: 615-621.

〔94〕 Biryukova E.V., Roby-Brami A., Frolov A.A., and Mokhtari M., Kinematics of human arm reconstructed from spatial tracking system recordings, *Journal of Biomechanics* 2000; 33: 985-995.

〔95〕 Prokopenko R.A., Biryukova E.V., Roby-Brami A., and Frolov A. A., Assement of the accuracy of a human arm model with seven degrees of freedom, *Journal of Biomechanics* 2001; 34: 177-185.

〔96〕 Hingtgen B., McGuire J.R., Wang, M., and Harris G.F., An upper extremity kinematic model for evaluation of hemiparetic stroke, *Journal of Biomechanics* 2006; 39: 681-688.

〔97〕 http://www.vicon.com/

〔98〕 Romilly D.P., Anglin C., Gosine R.G., Hershler C., and Raschke, S.U., A functional task analysis and motion simulation for the development of a powered upper-limb orthosis, *IEEE Trans. on Rehabilitation Engineering* 1994; 2(3): 119-129.

〔99〕 DeLeva P., Adjustments to Zatsiorsky-Seluyanov's Segment inertia parameters, *Journal of Biomechanics* 1996; 29(9): 1223-1230.

〔100〕Dumas R., Aissaoui R., and De Guise J. A., A 3D generic inverse dynamic method using wrench notation and quaternion algebra, *Computer methods in Biomedical Engineering*, 2004; 7(3): 159-166.

〔101〕Lo A. C., Guarino P. D., Richards, L. G., et al., Robot-assisted therapy for long-term upper-limb impairment after stroke, *The New England Journal of Medicine* 2010; 362: 1772-1783.

〔102〕Peterson M. D., Rhea M. R., Sen A., and Gordon P. M., Resistance exercise for muscular strength in older adults: a meta-analysis, *Ageing Research Review* 2010; 9: 226-237.

〔103〕Center of Disease Control, QuickStats: Percentage of Adults Aged >=18 Years Who Engaged in Leisure-Time Strengthening Activities at Least Twice a Week,* by Race/Ethnicity and Sex --- National Health Interview Survey, United States, 2009, *MMMR Morbidity and Mortality Weekly Report* 2011; 60(41): 1429.

〔104〕Center of Disease Control, Trends in strength Training---United States, 1998-2004, *MMMR Morbidity and Mortality Weekly Report* 2006; 55(28): 770-792.

〔105〕Henmi S., Yonenobu K., and Masatomi T., A biomechanical study of activities of daily living using neck and upper limbs with an optical three-dimensional motion analysis system, *Modern rheumatology* 2006; 16: 289-293.

〔106〕Chiu L. Z. F. and Salem G. J., Comparison of joint kinetics during free weight and flywheel resistance exercise, *Journal of Strength and Conditioning Research* 2006; 20(3): 555–562.

〔107〕Soderberg G. L. and Knutson L. M., A guide for use and interpretation of kinesiologic electromyographic data, *Physical Therapy* 2000; 80(5): 485-498.

〔108〕Karmen G. and Gabriel D. A., *Essential of Electromyography*, Human Kinetics, Champaign, IL, 2010.

〔109〕Criswell E., *Cram's Introduction to Surface Electromyography*, Jones and Bartlett, Sudbury, MA, 2011.

〔110〕Merletti R. and Parker P. A., *Electromyography: physiology, engineering, and noninvasive applications*, John Wiley and Sons, Hoboken, NJ, 2004.

〔111〕Felici F., Neuromuscular responses to exercise investigated through surface EMG, *Journal of Electromyography and kinesiology* 2006; 16: 578-585.

〔112〕Hintermeister R. A., Lange G. W., Schultheis J. M., Bey M.J., and Hawkins R. J., Electromyographic activity and applied load during

shoulder rehabilitation exercises using elastic resistance, *The American Journal of Sports Medicine* 1998; 26(2): 210-220.

〔113〕 Anderson L. L., Anderson C. H., Mortensen O. S., Poulsen O. M., Bjornlund I. B., and Zebis M. K., Muscle activation and perceived loading during rehabilitation exercises: comparison of dumbbells and elastic resistance, *Physical Therapy* 2010; 90(4): 538-549.

〔114〕 Myers J. B., Pasquale M. R., Laudner K. G., Sell T. C., Bradley J. P., and Lephart S. M., On-the-field resistance-tubing exercises for throwers: An electromyographic analysis, *Journal of Atheletic Training* 2005; 40(1): 15-22.

〔115〕 Gabriel D. A., Karmen G., and Frost G., Neural adaptions to resistive exercise: mechanisms and recommendations for training practices, *Sport Medicine* 2006; 36(2): 133-149.

〔116〕 Lum P. S., Burger C. G., and Shor P. C., Evidence for improved muscle activation patterns after retraining of reaching movements with the MIMI robotic system in subjects with post-stroke hemiparesis, *IEEE Transactions on Neural System on Neuro Ssystem and Rehabilitation Engineering* 2004; 12(2): 186-256.

〔117〕 Hughes A. M., Freeman C. T., Burridge J. H., Chapell P. H., Lewin P. L., and Rogers E., Shoulder and elbow muscle activity during fully supported trajectory tracking in people who have had a stroke, *Journal of Electromyography and Kinesilology* 2010; 20: 465-476.

〔118〕 Kendall F. P., and McCreary E. K., PGP. *Muscle: testing and function*, 5th ed., Baltimore: Williams & Wilkins; 2005.

〔119〕 De Luca C. J., The use of surface electromyography in biomechanics, *Journal of Applied Biomechanics* 1997; 13: 135-163.

〔120〕 Knutson L. M., Soderberg G. L., Ballantyne B. T., and Clarke W. R., A study of various normalization procedures for within day electromyographic data, *Journal of Electromyography and kinesiology* 1994; 4(1): 47-59.

〔121〕 Ekstrom R. A., Soderberg G. L., and Donatelli R. A., Normalization procedures using maximum voluntary isometric contractions for the serratus anterior and trapezius muscles during surface EMG analysis, *Journal of Electromyography and kinesiology* 2005; 15: 418-428.

〔122〕 Miller E. L., Murray L., Richards L., Zorowitz R. D., Bakas T., Clark P., and Bollinger S. A., The comprehensive overview of Nursing and interdisciplinary rehabilitation care of the stroke patients: a scientific statement from the American Heart Association, *Stroke* 2010; 41:

2402-2448.
〔123〕Department of Veterans Affairs and Department Defense, *VA/DoD clinical practice guideline for the management of stroke rehabilitation*. Washington, DC: The Office of Quality and Performance, VA & Quality Management Division, United States Army MEDCOM; 2010.